Doctral Dissertation

Characterization and Isomerization of (all-*E*)-Lycopene Derived from Natural Origin

Masaki Honda

Research & Development Division, Kagome Co., Ltd.,

Nishitomiyama, Nasushiobara, Japan

February 2016

Graphica abstract

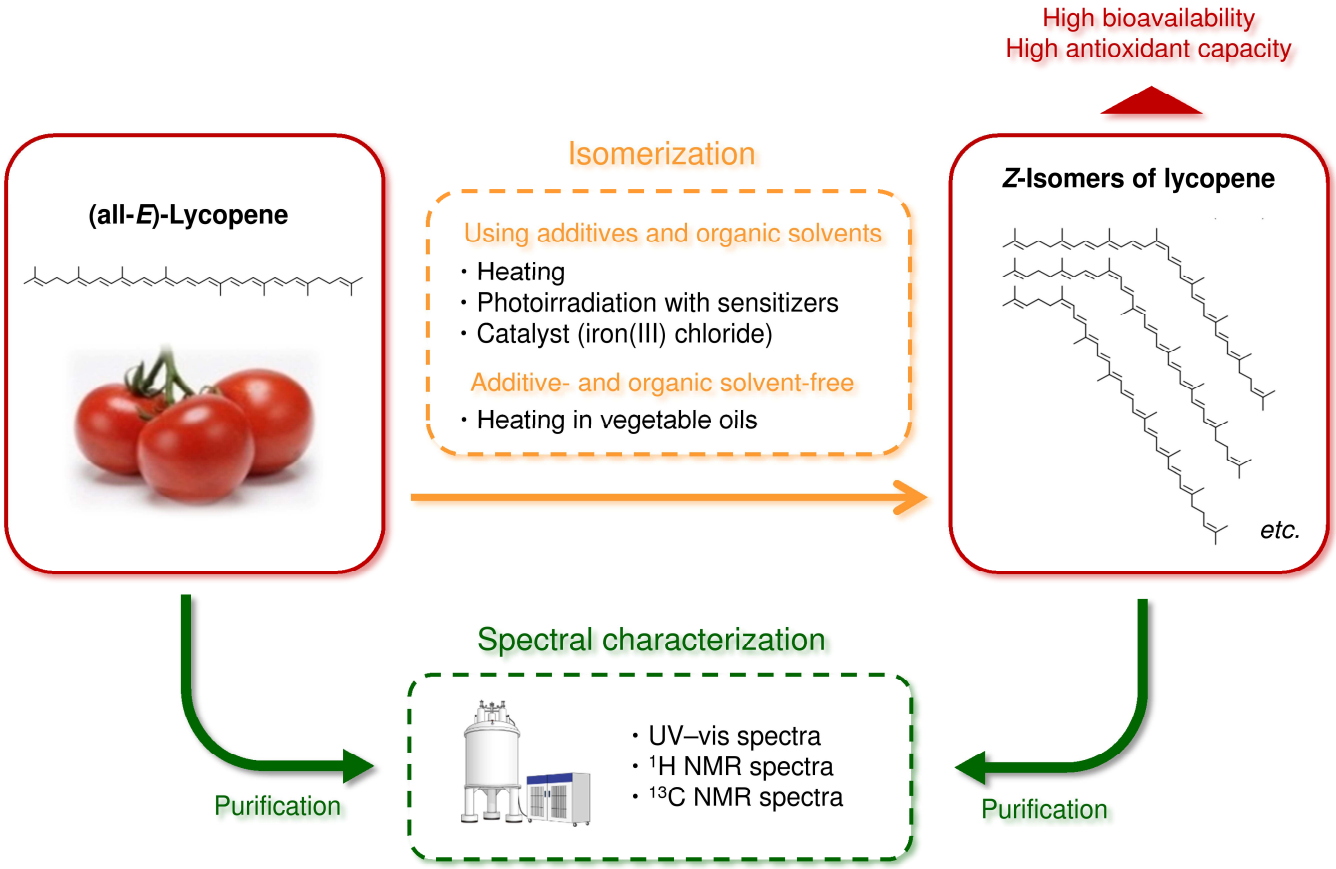

Abstract

Characterization of (all-*E*)- and (15*Z*)-lycopene purified from natural origin, and isomerization of (all-*E*)-lycopene to *Z*-isomers by heating, photoirradiation, and catalyst were demonstrated.

A large amount of (all-*E*)-lycopene was successfully purified from tomato paste using an improved method that included a procedure to wash crystalline powder with acetone. The melting point of (all-*E*)-lycopene was determined to be 173.2 °C by differential scanning calorimetry (DSC) measurements. Bathochromic shifts were observed in the absorption maxima of all solvents tested (at most a 36 nm shift for $\lambda 2$ in carbon disulfide, as was observed in hexane) and were accompanied by absorbance decreases, namely, a hypochromic effect, showing a higher correlation between the position and the intensity of the main absorption bands. This bathochromic shift was dependent upon the polarizability of the solvent rather than its polarity. The structure of (all-*E*)-lycopene in $CDCl_3$ and C_6D_6 was identified on the basis of one- and two-dimensional nuclear magnetic resonance (NMR) spectra, including ^{1}H and ^{13}C NMR, homonuclear correlation spectroscopy (^{1}H-^{1}H COSY), heteronuclear multiple-quantum coherence (HMQC), and heteronuclear multiplebond connectivity (HMBC).

(15*Z*)-Lycopene was prepared by thermal isomerization of (all-*E*)-lycopene derived from tomatoes, and isolated by using a series of chromatographies. The fine red crystalline powder of (15*Z*)-lycopene was obtained from 556 mg of (all-*E*)-lycopene with a yield of 0.6 mg (purity: reversed-phase HPLC, 97.2%; normal-phase HPLC, ≥99.9%), and ^{1}H and ^{13}C NMR spectra of the isomer were fully assigned. Moreover, the occurrence and availability of the 15*Z*-isomer were discussed on the basis of the calculation method.

Thermal isomerization of (all-*E*)-lycopene was investigated in various organic solvents. Isomerization ratios to the *Z*-isomers of lycopene in CH_2Cl_2 and $CHCl_3$ over 24 h were calculated to be 19.7% and 11.4% at 4 °C and 77.8% and 48.4% at 50 °C, respectively. In CH_2Br_2, more than 60% was attained in the first several hours, independent of temperature. The predominant *Z*-isomers obtained thermally, (9*Z*)- and (13*Z*)-lycopene, were purified and their absorption maxima and molar extinction coefficients in hexane were determined for the first time. Absorption values at 460 nm were also measured for both *Z*-isomers along with (all-*E*)-lycopene to accurately evaluate their concentrations by HPLC analysis. This approach successfully revealed that (13*Z*)-lycopene formed predominantly in benzene or $CHCl_3$ at 50 °C; in contrast, the 5*Z*-isomer was preferentially obtained in CH_2Cl_2 or CH_2Br_2.

Photoisomerization of (all-*E*)-lycopene to the corresponding *Z*-isomers was investigated under visible to middle-infrared light irradiation in the presence of several sensitizers, including edible ones. Highly purified (all-*E*)-lycopene from tomato paste was isomerized to *Z*-isomers to the extent of 46.4–57.4% after irradiation with the sensitizers for 60 min in acetone, in which a thermodynamically-stable isomer of (5*Z*)-lycopene was predominantly generated, while kinetically-preferable (9*Z*)- and (13*Z*)-lycopene were dominant without sensitizer. Examination of the time course of photoisomerization demonstrated that the highest isomerization efficiency (80.4%) was attained using erythrosine as the sensitizer under 480–600 nm light irradiation in hexane for 60 min, a protocol which successfully suppressed the decomposition of lycopene. (5*Z*)-Lycopene, reported as a more bioavailable isomer, was again predominantly produced with erythrosine and rose bengal in each solvent.

Catalytic isomerization of (all-*E*)-lycopene to *Z*-isomers using iron(III) chloride was investigated and optimized under various conditions of solvents, concentrations of iron(III) chloride, and reaction temperatures. The total contents of *Z*-isomers converted were higher in the order of CH_2Cl_2 (78.4%) > benzene (61.4%) > acetone (51.5%) > ethyl acetate (50.8%) at 20 °C for 3 h using 1.0×10^{-3} mg/mL iron(III) chloride for 0.1 mg/mL (all-*E*)-lycopene. However, the decomposition of lycopene was markedly

accelerated in CH_2Cl_2. As the concentration of catalyst increased in acetone, the *Z*-isomerization ratio of lycopene increased to more than 80%, followed by rapid decomposition of lycopene to undetectable levels using > 4.0×10^{-3} mg/mL iron(III) chloride with the above concentration of (all-*E*)-lycopene. Finally, greater isomerization (79.9%) was attained at 60 °C in acetone for 3 h in the presence of 1.0×10^{-3} mg/mL iron(III) chloride, largely without decomposition of lycopene (remaining ratio of total amount of lycopene isomers after the reaction, 96.5%).

As a method without use of organic solvents and food additives, thermal isomerization of (all-*E*)-lycopene in edible vegetable oils (perilla, linseed, grape seed, soybean, corn, sesame, rapeseed, rice bran, safflower seed, olive, and sunflower seed oil) was also investigated. Purified (all-*E*)-lycopene from tomatoes was converted to *Z*-isomers in the range of 44.8 to 58.8% content, and the remaining ratio of total amount of lycopene isomers without decomposition were ranged from 38.8 to 79.6% after heating at 100 °C for 1 h in the vegetable oils. Both of the values were exceedingly high in sesame oil; 58.8% of total *Z*-isomers content and 78.3% of remaining lycopene. In particular, (5*Z*)-lycopene which has higher bioavailability and antioxidant capacity as well as greater storage stability among the *Z*-isomers was notably increased in that oil; approximately threefold higher than the average of the other vegetable oils.

Contents

Abbreviations

B3LYP: Becke-3-Lee-Yang-Parr

CCl_4: tetrachloride

C_6D_6: benzene-d_6

$CDCl_3$: chloroform-*d*

CH_2Br_2: dibromomethane

CH_2Cl_2: dichloromethane

$CHCl_3$: chloroform

DFT: density-functional theory

DIPEA: *N*,*N*-diisopropylethylamine

DSC: differential scanning calorimetry

Erythrosine: erythrosine B

FA: fatty acid

FAB: fast-atom bombardment

FTIR: fourier transform infrared

^1H-^1H COSY: homonuclear correlation spectroscopy

HMBC: heteronuclear multiplebond connectivity

HMHU: (3*E*,5*E*,7*E*,9*E*,11*E*,13*E*,15*E*,17*E*,19*E*,21*E*,23*E*)-3,7,11,16,20,24-hexamethylhexacosa-3,5,7,9,11,13,15,17,19,21,23-undecaene

HMQC: heteronuclear multiple-quantum coherence

HPLC: high-performance liquid chromatography

HRMS: high-resolution mass spectrum

IV: iodine value

MB: methylene blue

MTBE: methyl *tert*-butyl ether

ND: not detected

NMR: nuclear magnetic resonance

NOE: nuclear Overhauser effect

PTFE: polytetrafluoroethylene

RB: rose bengal

SD: standard deviation

SV: saponification value

SE: standard error

TMS: tetramethylsilane

TMTU: (2*Z*,4*E*,6*E*,8*E*,10*E*,12*E*,14*E*,16*E*,18*E*,20*E*,22*Z*)-6,10,15,19-tetramethytetracosa-

2,4,6,8,10,12,14,16,18,20,22-undecaene

TS: transition state

UV–vis: ultraviolet–visible

UZ: unidentified *Z*-isomer of lycopene

Chapter 1

General introduction

1.1. Background

Lycopene is a well-known carotenoid found abundantly in vegetables and fruits with a red color such as tomatoes, red carrots [1], watermelons, and gac (*Momordica cochinchinensis*) [2] as well as in microorganisms such as *Dunaliella salina* [3], *Chlorella* spp. [4,5], and *Blakeslea trispora* [6,7]. Lycopene, like other carotenoids, is responsible for the characteristic bright color of these organisms and plays a protective role against oxidative stress [8–10]. The natural benefits of lycopene have been applied not only to food and dietary supplements as edible colorants and antioxidants, but also to medical approaches to cancer and arteriosclerosis prevention [11–13], taking advantage of its physiological properties and biocompatibility. These useful functions of lycopene, the molecular formula of which is $C_{40}H_{56}$, have been attributed to its chemical structure containing many unsaturated bonds in which eleven double bonds are conjugated and more effectively allow the absorption of relatively long-wavelength light and quench singlet oxygen. Therefore, many researchers have studied this useful pigment, and published excellent reports from the middle of the 20th century [14–19]. However, these studies were performed with lycopene prepared from different origins and with different purification degrees, which could lead to a misunderstanding due to different values for basic physicochemical properties. Under these circumstances, first

of all, we performed an extraction of (all-*E*)-lycopene (Figure 1A) with higher purity from a tomato paste, and determined its physical and chemical properties including some spectrophotometric measurements.

The structural assignments and UV–vis spectral features of (5*Z*)-, (9*Z*)- and (13*Z*)-lycopene (Figure 1B–D), the predominant *Z*-isomers contained in processed tomato products [20], were demonstrated through the successful acquisition of highly purified preparations of the isomers by using a series of chromatographies [21].

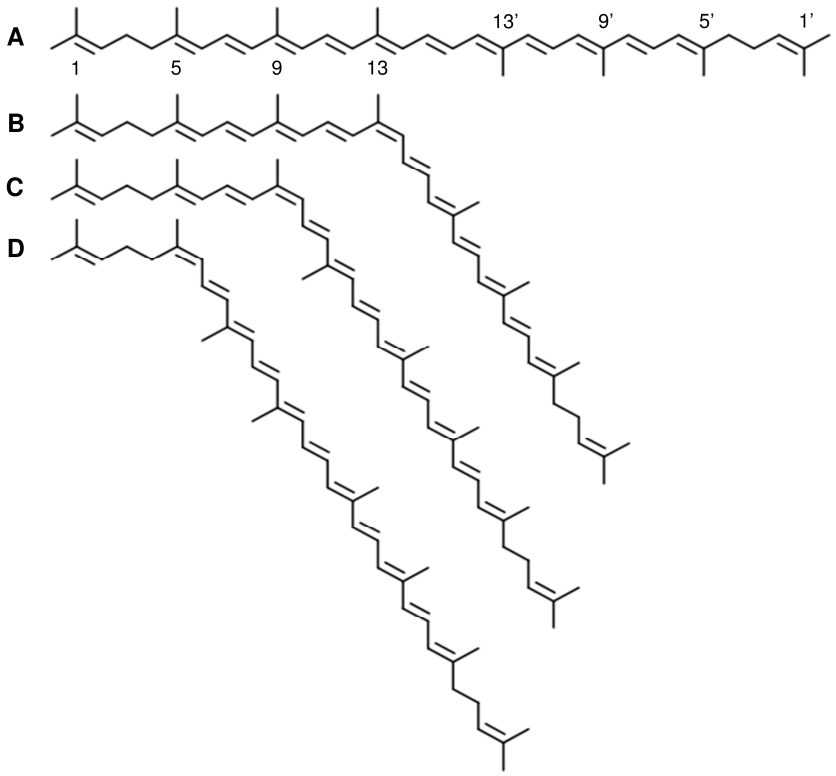

Figure 1. Chemical structures of the predominant isomers of lycopene contained in processed tomato products: (A) (all-*E*)-lycopene; (B) (13*Z*)-lycopene; (C) (9*Z*)-lycopene; (D) (5Z)-lycopene.

On the other hand, (15*Z*)-lycopene (Figure 2) which would be generated from (all-*E*)-lycopene by geometric isomerization was considered to be a putative isomer for more than half a century, whereas a possible (15*Z*)-lycopene was synthesized via a Wittig reaction [22,23]. In the present study, we revealed, for the first time, the occurrence of (15Z)-lycopene from natural sources during a heat treatment by isolating and identifying the isomer on the basis of more sophisticated chromatographic and spectroscopic methods, respectively. These characterization of (all-*E*)-lycopene and the *Z*-isomers is considered important to attain depth the discussions about isomerization of lycopene.

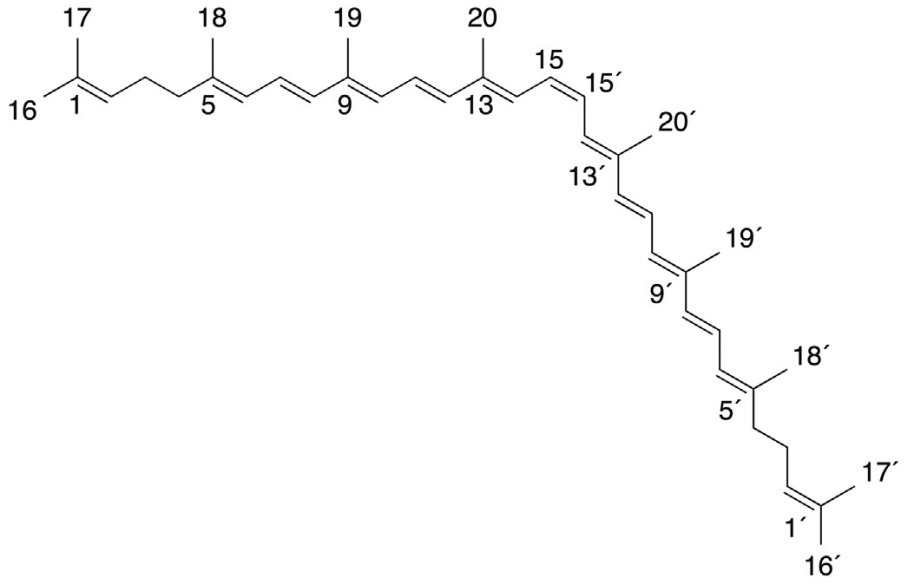

Figure 2. Chemical structure of (15*Z*)-lycopene. (15*Z*)-Lycopene in this study was purified from a mixture of lycopene isomers, which was prepared by heating (all-*E*)-lycopene of a tomato origin.

Although lycopene has a large number of geometric isomers caused by *E*/*Z* isomerization at arbitrary sites within the 11 conjugated double bonds (Figure 1), most lycopene is present in the all-*E*-configuration (Figure1A) in plants, representing about 80–97% of total lycopene in tomatoes and related products [20]. However, in the human body, such as blood and prostate tissue, more than 50% of total lycopene exists in the *Z*-form (Figure 1B–D) [20,24–29]. This suggests that *Z*-isomers of lycopene are more bioavailable than the all-*E*-configuration. In fact, according to experiments using a Caco-2 human intestinal cell model [30] and lymph cannulated ferrets [29], the bioavailability of *Z*-isomers of lycopene was shown to be significantly greater than that of the all-*E*-configuration. Also in humans, the intake of tomato sauce rich in *Z*-form lycopene brought about a marked increase of plasma lycopene concentration, compared with one rich in all-*E*-isomer [31]. In addition, *Z*-isomers of lycopene have been reported to show a higher antioxidant capacity than the all-*E* configuration [32–34]. As such, it is conceivable that intake of *Z*-isomers of lycopene could be preferable for health reasons because of their good bioavailability and functionality, and it is therefore important to gain a better understanding of the isomerization of (all-*E*)-lycopene to *Z*-isomers and to develop the efficient methods for this reaction. Since global trend is toward natural and additive-free for foods and drinks, and it is required to produce more

safely and accurately lycopene preparations rich in *Z*-forms without those chemical agents, we developed not only the isomerization methods using additives and organic solvents putting importance on efficiency but also additive- and organic solvent-free isomerization method. Namely, we demonstrated the isomerization of (all-*E*)-lycopene by heating, photoirradiation, and catalyst in organic solvent putting importance on efficiency, and heating in edible vegetable oils putting importance on natural, respectively, in this study.

1.2. Research objectives

This study focuses on characterization of (all-*E*)- and (15*Z*)-lycopene purified from natural origin, and isomerization of (all-*E*)-lycopene to *Z*-isomers. First of all we aimed to establish a purification method of (all-*E*)-lycopene from tomato paste, and acquired its chemical and physical properties to deepen the understanding of the *E*/*Z* isomerization reaction of lycopene in Chapter 2. In the same way, (15*Z*)-lycopene which has never identified from natural origin was purified and characterized in Chapter 3. Then we aimed to establish isomerization methods of (all-*E*)-lycopene to *Z*-isomers, which were focused on both efficiency (Chapter 4–6) and natural (Chapter 7). Detailed objectives of this study as follows:

♦ To examine the fundamental data such as the melting point, UV–vis, IR, and NMR spectra of purified (all-*E*)-lycopene from tomato paste (Chapter 2).

♦ To characterize (15*Z*)-lycopene which has never identified from natural origin by spectral methods such as UV–vis, ^{1}H, and ^{13}C NMR spectroscopy (Chapter 3).

♦ To develop the efficient isomerization method of (all-*E*)-lycopene to *Z*-isomers by heating, photoirradiation, and catalyst in organic solvent (Chapter 4–6).

♦ To develop the additive- and organic solvent-free isomerization method of (all-*E*)-lycopene to *Z*-isomers by heating in edible vegetable oils (Chapter 7).

1.3. References

[1] Horvitz, M. A., Simon, P. W., Tanumihardjo, S. A. Lycopene and *β*-carotene are bioavailable from lycopene 'red' carrots in humans. *Eur. J. Clin. Nutr.* **2004**, *58*, 803–811.

[2] Aoki, H., Kieu, N. T., Kuze, N., Tomisaka, K., Van Chuyen, N. Carotenoid pigments in GAC fruit (*Momordica cochinchinensis* SPRENG). *Biosci. Biotechnol. Biochem.* **2002**, *66*, 2479–2482.

[3] Orset, S. C., Young, A. J. Exposure to low irradiances favors the synthesis of 9-*cis* *β*, *β*-carotene in *Dunaliella salina* (Teod.). *Plant Physiol.* **2000**, *122*, 609–618.

[4] Ishikawa, E., Abe, H. Lycopene accumulation and cyclic carotenoid deficiency in heterotrophic *Chlorella* treated with nicotine. *J. Ind. Microbiol. Biotechnol.* **2004**, *31*, 585–589.

[5] Renju, G. L., Muraleedhara Kurup, G., Saritha Kumari, C. H. Anti-inflammatory activity of lycopene isolated from *Chlorella marina* on type II collagen induced arthritis in *Sprague Dawley* rats. *Immunopharmacol. Immunotoxicol.* **2013**, *35*, 282–291.

[6] Estrella, A., López-Ortiz, J. F., Cabri, W., Rodríguez-Otero, C., Fraile, N., Erbes, A. J., Espartero, J. L., Carmona-Cuenca, I, Chaves, E., Muñoz-Ruiz, A. Natural lycopene from *Blakeslea trispora*: all-trans lycopene themochemical and structural properties.

Thermochim. Acta **2004**, *417*, 157–161.

[7] López-Nieto, M. J., Costa, J., Peiro, E., Méndez, E., Rodríguez-Sáiz, M., de la Fuente, J. L., Cabri, W., Barredo, J. L. Biotechnological lycopene production by mated fermentation of *Blakeslea trispora*. *Appl. Microbiol. Biotechnol.* **2004**, *66*, 153–159.

[8] Di Mascio, P., Kaiser, S., Sies, H. Lycopene as the most efficient biological carotenoid singlet oxygen quencher. *Arch. Biochem. Biophys.* **1989**, *274*, 532–538.

[9] Stahl, W., Sies, H. Antioxidant activity of carotenoids. *Mol. Aspects Med.* **2003**, *24*, 345–351.

[10] Cantrell, A., McGarvey, D. J., Truscott, T. G., Rancan, F., Böhm, F. Singlet oxygen quenching by dietary carotenoids in a model membrane environment. *Arch. Biochem. Biophys.* **2003**, *412*, 47–54.

[11] Dahan, K., Fennal, M., Kumar, N. B. Lycopene in the prevention of prostate cancer. *J. Soc. Integr. Oncol.* **2008**, *6*, 29–36.

[12] Gann, P. H., Ma, J., Giovannucci, E., Willett, W., Sacks, F. M., Hennekens, C. H., Stampfer, M. J. Lower prostate cancer risk in men with elevated plasma lycopene levels: results of a prospective analysis. *Cancer Res.* **1999**, *59*, 1225–1230.

[13] Palozza, P., Parrone, N., Simone, R. E., Catalano, A. Lycopene in atherosclerosis prevention: an integrated scheme of the potential mechanisms of action from cell

culture studies. *Arch. Biochem. Biophys.* **2010**, *504*, 26–33.

[14] Zechmeister, L., LeRosen, A. L., Schroeder, W. A., Polgár, A., Pauling, L. Spectral characteristics and configuration of some stereoisomeric carotenoids including prolycopene and pro-γ-carotene. *J. Am. Chem. Soc.* **1943**, *65*, 1940–1951.

[15] Davis, W. B. Preparation of lycopene from tomato paste for use as a spectrophotometric standard. *Anal. Chem.* **1949**, *21*, 1226–1228.

[16] Karrer, P., Jucker, E. *Carotenoids*, Elsevier: New York and Amsterdam, **1950**.

[17] Surmatis, J. D., Ofner, A. Total synthesis of spirilloxanthin, dehydrolycopene, and 1,1'-dihydroxy-1,2,1',2'-tetrahydrolycopene. *J. Org. Chem.* **1963**, *28*, 2735–2739.

[18] Manchand, P. S., Rüegg, R., Schwieter, U., Siddons, P. T., Weedon, B. C. L. Carotenoids and related compounds. Part XI. Syntheses of δ-carotene and ε-carotene. *J. Chem. Soc.* **1965**, 2019–2026.

[19] Davis, B. H. Carotenoid. In *Chemistry and Biochemistry of Plant Pigments*; Goodwin, T. W., Ed.; Academic Press: London, **1976**; pp 38–165.

[20] Schierle, J., Bretzel, W., Bühler, I., Faccin, N., Hess, D., Steiner, K., Schüep, W. Content and isomeric ratio of lycopene in food and human blood plasma. *Food Chem.* **1997**, *59*, 459–465.

[21] Honda, M., Takahashi, N., Kuwa, T., Takehara, M., Inoue, Y., Kumagai, T.

Spectral characterization of *Z*-isomers of lycopene formed during heat treatment and solvent effects on the *E*/*Z* isomerization process. *Food Chem.* **2015**, *171*, 323–329.

[22] Hengartner, U., Bernhard, K., Meyer, K., Englert, G., Glinz, E. Synthesis, isolation, and NMR-spectroscopic characterization of fourteen (*Z*)-isomers of lycopene and of some acetylenic didehydro- and tetradehydrolycopenes. *Helv. Chim. Acta* **1992**, *75*, 1848–1865.

[23] Isler, O., Gutmann, H., Lindlar, H., Montavon, M., Rüegg, R., Ryser, G., Zeller, P. Synthesen in der Carotinoid-Reihe. 6. Mitteilung. Synthese von Crocetindialdehyd und Lycopin. *Helv. Chim. Acta* **1956**, *39*, 463–473.

[24] Schieber, A., Carle, R. Occurrence of carotenoid *cis*-isomers in food: technological, analytical, and nutritional implications. *Trends Food Sci. Technol.* **2005**, *16*, 416–422.

[25] Stahl, W., Schwarz, W., Sundquist, A. R., Sies, H. *cis–trans* Isomers of lycopene and *β*-carotene in human serum and tissues. *Arch. Biochem. Biophys*. **1992**, *294*, 173–177.

[26] Clinton, S. K., Emenhiser, C., Schwartz, S. J., Bostwick, D. G., Williams, A. W., Moore, B. J., Erdman, J. W., Jr. *cis-trans* Lycopene isomers, carotenoids, and retinol in the human prostate. *Cancer Epidemiol. Biomarkers Prev*. **1996**, *5*, 823–833.

[27] Richelle, M., Sanchez, B., Tavazzi, I., Lambelet, P., Bortlik, K., Williamson, G. Lycopene isomerisation takes place within enterocytes during absorption in human subjects. *Br. J. Nutr*. **2010**, *103*, 1800–1807.

[28] Richelle, M., Lambelet, P., Rytz, A., Tavazzi, I., Mermoud, A.-F., Juhel, C., Borel, P., Bortlik, K. The proportion of lycopene isomers in human plasma is modulated by lycopene isomer profile in the meal but not by lycopene preparation. *Br. J. Nutr*. **2012**, *107*, 1482–1488.

[29] Boileau, A. C., Merchen, N. R., Wasson, K., Atkinson, C. A., Erdman, J. W., Jr. *cis*-Lycopene is more bioavailable than *trans*-lycopene in vitro and in vivo in lymph-cannulated ferrets. *J. Nutr*. **1999**, *129*, 1176–1181.

[30] Failla, M. L., Chitchumroonchokchai, C., Ishida, B. K. In vitro micellarization and intestinal cell uptake of *cis* isomers of lycopene exceed those of all-*trans* lycopene. *J. Nutr*. **2008**, *138*, 482–486.

[31] Unlu, N. Z., Bohn, T., Francis, D. M., Nagaraja, H. N., Clinton, S. K., Schwartz, S. J. Lycopene from heat-induced *cis*-isomer-rich tomato sauce is more bioavailable than from all-*trans*-rich tomato sauce in human subjects. *Br. J. Nutr*. **2007**, *98*, 140–146.

[32] Schieber, A., Carle, R. Occurrence of carotenoid *cis*-isomers in food: technological, analytical, and nutritional implications. *Trends Food Sci. Technol.* **2005**, *16*, 416–422.

[33] Böhm, V., Puspitasari-Nienaber, N. L., Ferruzzi, M. G., Schwartz, S. J. Trolox equivalent antioxidant capacity of different geometrical isomers of α-carotene, β-carotene, lycopene, and zeaxanthin. *J. Agric. Food Chem.* **2002**, *50*, 221–226.

[34] Müller, L., Goupy, P., Fröhlich, K., Dangles, O., Caris-Veyrat, C., Böhm, V. Comparative study on antioxidant activity of lycopene (*Z*)-isomers in different assays. *J. Agric. Food Chem.* **2011**, *59*, 4504–4511.

Chapter 2

Purification and characterization of (all-E)-lycopene from tomato paste

2.1. Table of contents

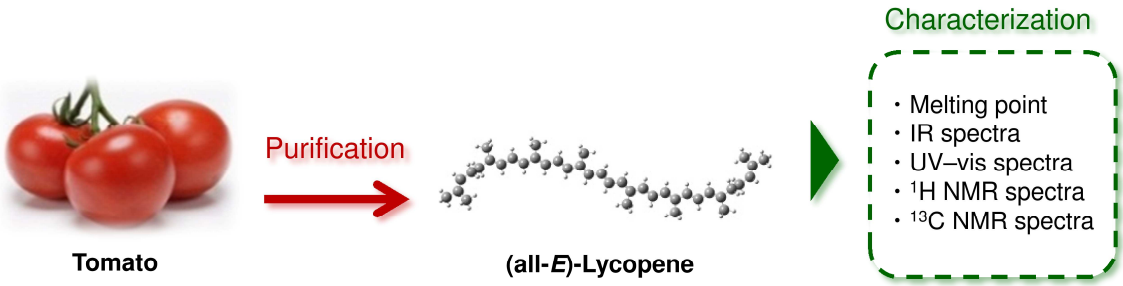

2.2. Introduction

Many researchers have studied lycopene and published excellent reports from the middle of the 20th century [1−6]. However, these studies were performed with lycopene prepared from different origins and with different purification degrees, which could lead to a misunderstanding because of different values for basic physicochemical properties. Under these circumstances, we performed an extraction of (all-*E*)-lycopene (Figure 1) with higher purity from a tomato paste and determined its physical and chemical properties, including some spectrophotometric measurements. The results of our study give new criteria for the identification of lycopene and contribute to the fundamental chemistry of this carotenoid in the food science and technology field.

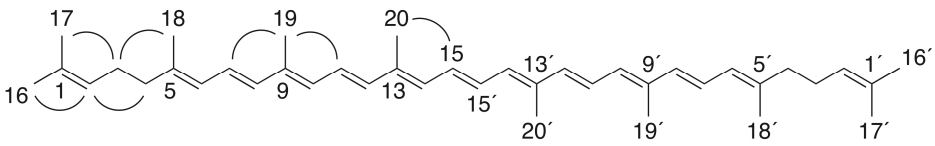

Figure 1. Chemical structure of (all-*E*)-lycopene. The NOE correlations observed in the two-dimensional NMR measurements are shown as curved lines in one half-side of the symmetrical structure of the lycopene.

2.3. Materials and methods

2.3.1. Chemicals

All reagents and solvents used in this study were summarized in Table 1.

Table 1 Summery of reagents and solvents used in this study

regents	grade	supplier
acetic ether[a]	extra pure	Nakaraitesuku Co., Ltd.
acetone	specially prepared	Nakaraitesuku Co., Ltd.
acetonitrile	specially prepared	Wako Pure Chemical Industries, Ltd.
anisole	extra pure	Kishida Chemical Co., Ltd.
benzene	extra pure	Nakaraitesuku Co., Ltd.
benzonitrile	special	Wako Pure Chemical Industries, Ltd.
t-butyl methyl ether	extra pure	Nakaraitesuku Co., Ltd.
carbon bisulfide	special	Wako Pure Chemical Industries, Ltd.
$CDCl_3$	99.8%	Sceti Co., Ltd.
$CHCl_3$	extra pure	Wako Pure Chemical Industries, Ltd.
CH_2Cl_2	extra pure	Nakaraitesuku Co., Ltd.
cyclohexane	specially prepared	Wako Pure Chemical Industries, Ltd.
N,*N*-dimethylaniline	special	Wako Pure Chemical Industries, Ltd.
dimethyl phthalate	special	Nakaraitesuku Co., Ltd.
ethanol	extra pure	Nakaraitesuku Co., Ltd.
hexane[a]	extra pure	Wako Pure Chemical Industries, Ltd.
methanol	HPLC	Sigma-Aldrich Co.
pyridine	special	Nakaraitesuku Co., Ltd.
tetrahydrofuran[a]	extra pure	Wako Pure Chemical Industries, Ltd.

[a]Used after distilling.

2.3.2. Extraction and purification of (all-*E*)-lycopene from tomato paste

All procedures were performed at room temperature, unless otherwise indicated. A total of 500 mL of CH_2Cl_2 was added to 50 g of tomato paste (Kagome Co., Ltd., Tokyo,

Japan; lycopene content, 8–12 g/kg) in an Erlenmeyer flask, and the mixture was stirred for 60 min in darkness. The organic layer was separated with a separatory funnel, and repetitive extraction was performed on the resulting suspension by the same volume of CH_2Cl_2. The solvent was evaporated on a rotary evaporator under a vacuum (170 mmHg) at 25 °C for 30 min. The crude extract (345 mg) containing lycopene was dissolved in 15 mL of benzene at 60 °C within ten minutes, and recrystallized at 4 °C for 4 h under shading. The resulting crystals were collected by suction filtration on a Kiriyama funnel (No. 5B filter paper), rinsed with 100 mL of acetone, and dried *in vacuo*: 188 mg of fine red crystalline powder, M.p. 173.2 °C (DSC). HPLC: ≥ 99.3%. UV–vis: Table 1. IR (KBr): Table 2. NMR: Table3. HRMS–FAB (*m/z*): $[M + H]^+$ calcd for $C_{40}H_{57}$, 537.4460; found, 537.4418.

2.3.3. UV−vis, FTIR, mass, and NMR spectroscopic analyses

UV–vis spectra of the purified lycopene were measured in organic solvents over a scanning range of 200–600 nm, and the λ maxima of the compounds were determined. Spectra were recorded with a Hitachi U-2910 spectrophotometer (Tokyo, Japan).

IR spectrum of (all-*E*)-lycopene was obtained by JASCO FT/IR 4100 (Tokyo) using the KBr disc in the range of 4000–400 cm^{-1}.

The HRMS of (all-*E*)-lycopene was recorded in the positive-ion mode by FAB+ on a JOEL JMS-700T instrument (Tokyo), using 3-nitrobenzyl alcohol as the matrix.

NMR spectra of (all-*E*)-lycopene were recorded using a JEOL JMN-LA400 FT 400 NMR spectrometer at 400 MHz (^{1}H) and 100 MHz (^{13}C). Chemical shifts were recorded as the δ value (ppm) using TMS as an internal standard. Spectra were observed on $CDCl_3$ and C_6D_6.

2.3.4. DSC analysis

The melting point of purified (all-*E*)-lycopene was determined by DSC using a DSC-60A system (Shimadzu, Kyoto, Japan). DSC measurements were performed with aluminum sample pans and empty reference pans. Both the sample and reference were scanned at a heating rate of 5 K/min from 303 to 473 K under a nitrogen atmosphere with a flow rate of 50 mL/min. The mass of the sample was 7 mg. All measurements were performed in triplicate.

2.3.5. HPLC analysis

Reversed-phase HPLC analysis with a photodiode array detector (SPD-M10AVP, Shimadzu, Kyoto, Japan) was performed under the following conditions: column, YMC

Carotenoid (250 × 4.6 mm i.d., 5 μm particles, YMC, Kyoto); solvent A, methanol/MTBE/ H_2O (75:15:10, v/v/v); solvent B, methanol/MTBE/H_2O (7:90:3, v/v/v); gradient, started with 100% eluent A and ended with 100% eluent B over a period of 35 min; flow rate 3.0 mL/min; column temperature, 22 °C. A typical chromatogram of the lycopene isomers was obtained with a retention time of and absorption maxima at: (13*Z*)-lycopene (24.6 min; 440.0, 465.0, 496.5 nm; (*Z*)-peak [7] at 361 nm with relative intensity of 59.2% D_B/D_{II}), (9*Z*)-lycopene (27.6 min; 441.0, 467.0, 497.5 nm; (*Z*)-peak at 361 nm with 13.7% D_B/D_{II}), (all-*E*)-lycopene (31.9 min; 445.0, 472.5, 503.5 nm), and (5*Z*)-lycopene (32.6 min; 445.0, 472.0, 503.5 nm). The quantification of all lycopene was performed by peak area integration at 470 nm, showing a reliable approximation for the analysis of isomers [8,9].

2.3.6. Computational analysis

In order to evaluate the validity of the experimental value, *Ab initio* and DFT calculations on the infrared spectrum of (all-*E*)-lycopene were performed with Gaussian 03 software using the B3LYP functional and 6-31G(*d*) basis set.

2.4. Results and discussion

2.4.1. Physical Properties of (all-*E*)-Lycopene

In this study, a large amount of (all-*E*)-lycopene was successfully purified from tomato samples without laborious chromatographic procedures [10,11]. This improved method included a procedure to wash crystalline powder with acetone, in which the solubility of (all-*E*)-lycopene was low (ca. 0.75 mg/mL) [12]. The total yield of the pure (all-*E*) form (purity ≥ 99.3% by HPLC) was at least 30% when the lycopene content of the tomato paste was considered. The DSC curve for the purified lycopene showed in Figure 2. The melting point was determined from the onset point of the DSC curve [13], which was scanned at a heating rate of 5 K/min: two possible melting points of 163.8 °C and 173.2 °C were observed. The lower value would be attributed to the lycopene (*Z*)-isomers arose from the (all-*E*) form because of the heating process. The content of the (all-*E*) form was reduced to 61.6% by reversed-phase HPLC for lycopene samples after the DSC measurement. The melting point of (all-*E*)-lycopene was then determined to be 173.2 °C, which was consistent with the value obtained by Manchand et al [5].

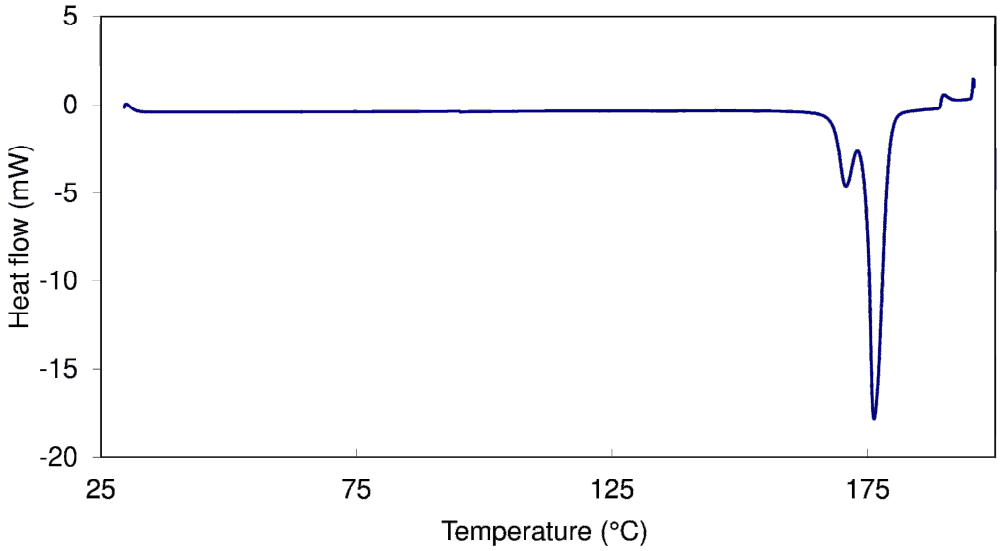

Figure 2. DSC curve of the purified (all-*E*)-lycopene.

Lycopene has an electron spectrum characterized by eleven conjugated double bonds, which geometrically impose a linear and highly planar structure. The UV spectra and summery of absorption maxima and molecular extinction coefficient of the purified (all-*E*)-lycopene in thirteen organic solvents were showed in Figure 3 and Table 2, respectively. In hexane, (all-*E*)-lycopene showed strong absorption maxima at 502.5, 471.0, and 444.0 nm with molar extinction coefficients estimated as 168 × 10^3, 182 × 10^3, and 118 × 10^3, corresponding to vibrational transition energies of 0–0, 0–1, and 0–2, respectively. The peak at approximately 360 nm, the so-called *Z*-peak [7,14], was not observed in this sample. Furthermore, absorption maxima and molar extinction coefficients with (all-*E*)-lycopene were measured in various organic solvents to

investigate the solvent effect on the electronic spectrum of the molecule. All values for the maxima (λ_2) of the fine structure in this study were also consistent with the calculated values according to an empirical rule [15–17]. The values (λ_1, λ_2, and λ_3) listed in this table were plotted as a function of wavelength in Figure 4A. From these results, bathochromic shifts in the absorption maxima were observed in all solvents tested (at most a 36 nm shift for λ_2 in carbon disulfide, as was observed in hexane), and were accompanied by absorbance decreases, namely a hypochromic effect, showing a higher correlation between the position and the intensity of the main absorption bands. Although many studies suggested that the bathochromic shift had been independently reported previously [18,19], the highly purified (all-*E*)-lycopene had first enabled a discussion of the solvent effect on this carotenoid. This bathochromic shift depends on the polarizability of the solvent because of high correlation between them (Figure 4B) [20], rather than on its polarity (data not shown). We revealed the solvent effect on the electron spectra of (all-*E*)-lycopene for the first time. It has been difficult to evaluate the solvent effect for (all-*E*)-lycopene because of its different purification grade with different origins. This finding contributes to the fundamental chemistry of carotenoids, and will be a new criterion for the identification and evaluation of lycopene in agriculture, food, and medical fields.

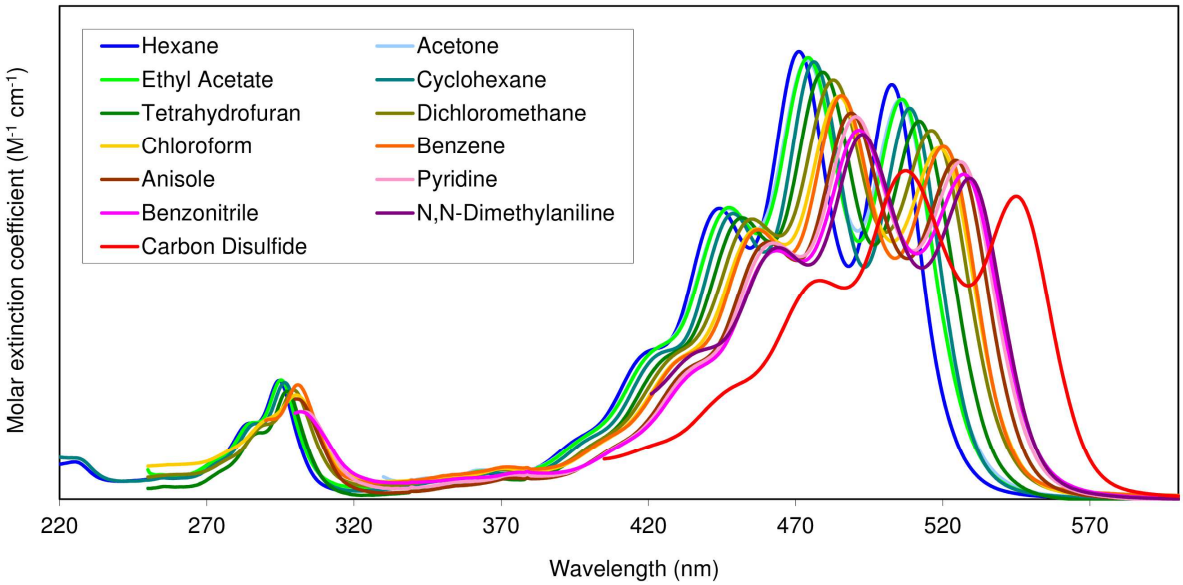

Figure 3. Ultraviolet (UV) spectra of the purified (all-*E*)-lycopene in thirteen organic solvents.

Table 2. Absorption maxima and molar extinction coefficients of (all-*E*)-lycopene from tomato[a]

solvent	λ_1		λ_2		λ_3		λ_{max} calcd[b]
methanol	444.0	ND[c]	469.5	ND	501.5	ND	486.5
hexane	444.0	(118)	471.0	(182)	502.5	(168)	470.5
hexane/chloroform (98:2)[d]	443	(123)	470	(187)	502	(172)	ND
MTBE[e]	445.5	(120)	472.0	(180)	503.5	(164)	ND
ethanol	446.0	ND	472.5	ND	504.0	ND	473.0
acetonitrile	446.0	ND	472.5	ND	504.0	ND	ND
acetone	447.0	(118)	474.0	(178)	505.5	(162)	ND
ethyl acetate	447.5	(118)	474.0	(179)	506.0	(162)	ND
cyclohexane	448.5	(116)	476.0	(177)	508.5	(159)	478.0
tetrahydrofuran	452.0	(114)	479.0	(173)	512.0	(153)	ND
dichloromethane	455.0	(113)	482.5	(170)	515.5	(150)	ND
chloroform	456.5	(110)	484.5	(164)	518.0	(143)	483.5
toluene	456.5	(110)	485.0	(165)	519.5	(144)	ND
benzene	457.5	(110)	485.5	(164)	520.0	(144)	487.5
anisole	460.5	(104)	489.0	(157)	524.5	(137)	ND
dimethyl phthalate	461.5	ND	489.5	ND	525.0	ND	ND
pyridine	462.5	(104)	490.5	(155)	526.0	(137)	490.0
benzonitrile	463.5	(101)	491.5	(150)	527.0	(132)	ND
N,*N*-dimethylaniline	464.0	(102)	492.5	(148)	529.0	(130)	ND
carbon disulfide	478.0	(89)	507.0	(133)	544.5	(123)	505.5

[a] λ_{1-3} in nm; values in parentheses, $\varepsilon \times 10^{-3}$. [b] Calculated according to the literatures [13–16]. [c] Not determined. [d] Synthetic (all-*E*)-lycopene [21]. [e] Methyl *tert*-butyl ether, containing 0.1% dichloromethane.

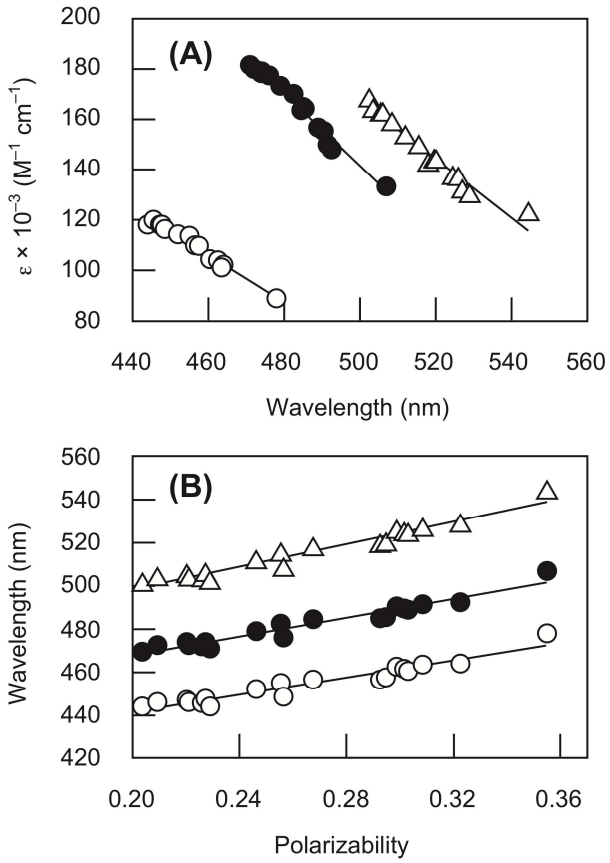

Figure 4. Relationships between the absorption maxima and molar extinction coefficients of (all-*E*)-lycopene in various solvents (A), and between the polarizabilities of the solvents and the absorption maxima (B). The values of λ_1 (○), λ_2 (●), and λ_3 (△) are from Table 1. Polarizability of the solvent is calculated as follows: $(n^2-1)/(n^2+2)$, where n is the refractive index of the solvent [22].

The IR spectrum of (all-*E*)-lycopene was measured (Figure 5) and characteristic absorptions are shown in Table 2, along with those calculated by the Gaussian program. Observed and calculated values from C−H and C=C stretches, and C−H out-of-plane attributed to the alkene as well as other origins, were consistent with each other. This

computational estimation with high fidelity would depend on the restriction of the molecular motion of lycopene caused by the eleven conjugated double bonds. Therefore, these observations will facilitate an evaluation of the relative free energy of lycopene (*Z*)-isomer contained in foods or originate from heat-induced isomerization.

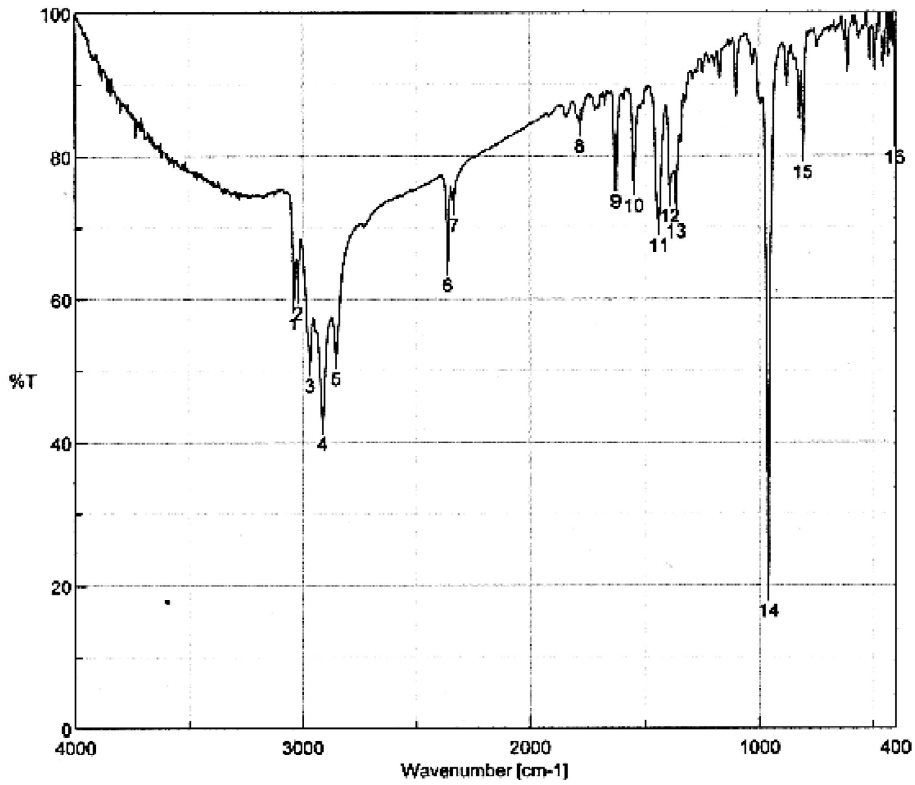

Figure 5. Infrared (IR) spectrum of the purified (all-*E*)-lycopene.

Table 3. Infrared absorption bands of (all-*E*)-lycopene extracted and purified from tomato paste and their calculated values

origin	frequency (cm^{-1})	
	found	calcd[a]
C−H stretch, alkene	3038, 3020 m	3072−3055, 3033−3007 m
C−H stretch, methylene/methyl	2968, 2912, 2854 s	2981−2962, 2926−2894, 2894 m to s
C=C stretch	1627, 1552 w	1636, 1558 m
C−H deformation, methylene/methyl	1441 m	1460−1444 m
C−H deformation, methyl	1391, 1364 m	1399−1375, 1364−1350 m
C−H out-of-plane, (*E*) disubstituted double bond	960 s	976−946 s

[a]Calculated by the Gaussian program.

2.4.2. NMR assignment of (all-*E*)-lycopene

The structure of (all-*E*)-lycopene has been identified on the basis of one- and two-dimensional NMR spectra including ^{1}H- (Figure 6) and ^{13}C-NMR, ^{1}H-^{1}H-COSY (homonuclear correlation spectroscopy), HMQC (heteronuclear multiple-quantum coherence), and HMBC (hetero-nuclear multiple-bond connectivity). Chemical shifts for proton and carbon signals of the (all-*E*)-lycopene in this work were good accordance with those of the synthetic (all-*E*)-lycopene [20] (Table 3). Spectral data on (all-*E*)-lycopene in $CDCl_3$ were also independently reported by different literatures [22–

25]; however, some values reported were not consistent among the previous studies, e.g. for the coupling constants of protons H−C(11), H−C(11´) and the chemical shift value of carbon atoms C(14), C(14´). In our study with thoroughly purified lycopene, the coupling constant values between H−C(11), H−C(11´) and H−C(10), H−C(10´), and between H−C(11), H−C(11´) and H−C(12), H−C(12´) were measured as 11.4 and 14.9 Hz, respectively. The chemical shift for C(14), C(14´) could be assigned to the signal observed at 132.64 ppm by the HMQC experiment, and refinement of the NMR signal assignment of (all-*E*)-lycopene was then achieved in $CDCl_3$.

Measurements were subsequently performed in another solvent, C_6D_6 in expectation of NMR signal charts distinct from those obtained in $CDCl_3$ because of differences in their physical properties such as polarity, resonancy, and viscosity. Proton and ^{13}C signals in C_6D_6 were preliminarily assigned by the results obtained in $CDCl_3$, and ascertained by ^{1}H homonuclear decoupling and the NOE difference experiments in addition to the above two-dimensional measurements (Figure 1). As shown in Table 3, chemical shifts in methyl protons between H−C(19), H−C(19´) and H−C(20), H−C(20´) were discriminated in C_6D_6 at 1.925 and 1.876 ppm respectively (Table 3), whereas these signals appeared as a singlet at 1.968 ppm in $CDCl_3$ (this study and the references [23,24]). Furthermore, the coupling system between H−C(14), H−C(14´) and H−C(15),

H−C(15´) could be analyzed in C_6D_6, whereas their corresponding signals in $CDCl_3$ overlapped with H−C(8), H−C(8´), and H−C(11), H−C(11´), respectively and were assigned to a multiplet. The observed spin signal occurred in the AA´BB´ type system, to which similar coupling was assigned in some carotenoids such as prolycopene and (9Z,9´Z)-7,8,7´,8´-tetrahydrolycopene [21,26], and the full assignment of ^{1}H and ^{13}C signals was then given in Table 3. The unambiguous determination attained in this study will also help to analyze the (*Z*)-isomers occurring in natural sources and those generated from the isomerization of (all-*E*)-lycopene by a heating process.

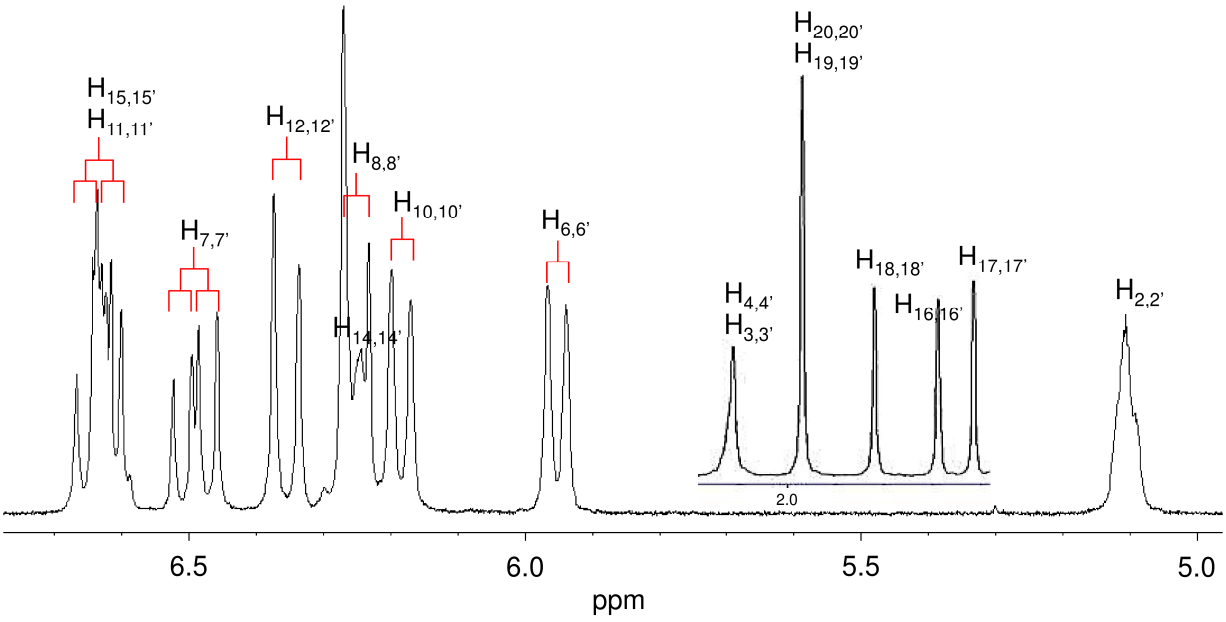

Figure 6. ^{1}H NMR spectrum of the purified (all-*E*)-lycopene. (400 MHz, $CDCl_3$).

Table 4. Refinement of ^{1}H and ^{13}C NMR assignments of (all-*E*)-lycopene from tomato[a]

proton	*d* in ppm (multiplicity, coupling constant in Hz)		carbon	*d* in ppm	
	in $CDCl_3$ [synthetic lycopene] [20]	in C_6D_6		in $CDCl_3$ [synthetic]	in C_6D_6
			C(1), C(1´)	131.72 [131.64]	131.58
H–C(2), H–C(2´)	5.11 (m) [5.11]	5.23 (m)	C(2), C(2´)	123.96 [124.12]	124.50
2H–C(3), 2H–C(3´)	2.11 (m) [*ca.* 2.11]	2.18 (m)	C(3), C(3´)	26.70 [26.83]	27.10
2H–C(4), 2H–C(4´)	2.11 (m) [*ca.* 2.11]	2.18 (m)	C(4), C(4´)	40.23 [40.30]	40.62
			C(5), C(5´)	139.47 [139.30]	138.95
H–C(6), H–C(6´)	5.95 (d, *J* = 11.0) [5.95]	6.16 (d, *J* = 11.0)	C(6), C(6´)	125.74 [125.94]	126.77
H–C(7), H–C(7´)	6.49 (dd, *J* = 11.0, 15.0) [6.49]	6.67 (dd, *J* = 11.0, 15.1)	C(7), C(7´)	124.79 [124.87]	125.31
H–C(8), H–C(8´)	6.25 (d, *J* = 15.0) [6.25]	6.44 (d, *J* = 15.1)	C(8), C(8´)	135.40 [135.54]	136.17
			C(9), C(9´)	136.15 [136.15]	136.37
H–C(10), H–C(10´)	6.18 (d, *J* = 11.4) [6.18]	6.36 (d, *J* = 11.6)	C(10), C(10´)	131.55 [131.64]	132.39
H–C(11), H–C(11´)	6.64 (dd, *J* = 11.4, 14.9) [6.64]	6.77 (dd, *J* = 11.6, 15.0)	C(11), C(11´)	125.15 [125.21]	125.66
H–C(12), H–C(12´)	6.35 (d, *J* = 14.9) [6.35]	6.49 (d, *J* = 15.0)	C(12), C(12´)	137.35 [137.46]	138.00
			C(13), C(13´)	136.56 [136.54]	136.83
H–C(14), H–C(14´)	6.24 (m) [6.25]	6.34 (AA´of AA´BB´ system)	C(14), C(14´)	132.64 [132.71]	133.39
H–C(15), H–C(15´)	6.62 (m) [6.62]	6.70 (BB´of AA´BB´ system)	C(15), C(15´)	130.07 [130.17]	130.70
3H–C(16), 3H–C(16´)	1.687 (s) [1.688]	1.674 (s)	C(16), C(16´)	25.68 [25.66]	25.84
3H–C(17), 3H–C(17´)	1.614 (s) [1.612]	1.568 (s)	C(17), C(17´)	17.70 [17.70]	17.73
3H–C(18), 3H–C(18´)	1.818 (s) [1.818]	1.749 (s)	C(18), C(18´)	16.99 [16.97]	16.90
3H–C(19), 3H–C(19´)	1.968 (s) [1.968]	1.925 (s)	C(19), C(19´)	12.90 [12.90]	12.98
3H–C(20), 3H–C(20´)	1.968 (s) [1.968]	1.876 (s)	C(20), C(20´)	12.79 [12.81]	12.86

[a] ^{1}H and ^{13}C NMR were recorded at 400 and 100 MHz, respectively. s = singlet, d = doublet, dd = doublet of doublet, m = multiplet.

2.5. Reference

[1] Zechmeister, L., LeRosen, A. L., Schroeder, W. A., Polgár, A., Pauling, L. Spectral characteristics and configuration of some stereoisomeric carotenoids including prolycopene and pro-γ-carotene. *J. Am. Chem. Soc.* **1943**, *65*, 1940–1951.

[2] Davis, W. B. Preparation of lycopene from tomato paste for use as a spectrophotometric standard. *Anal. Chem.* **1949**, *21*, 1226–1228.

[3] Karrer, P., Jucker, E. Carotenoids; Elsevier: Amsterdam, Netherlands, **1950**.

[4] Surmatis, J. D., Ofner, A. Total synthesis of spirilloxanthin, dehydrolycopene, and 1,1′-dihydroxy-1,2,1′,2′-tetrahydrolycopene. *J. Org. Chem.* **1963**, *28*, 2735–2739.

[5] Manchand, P. S., Rüegg, R., Schwieter, U., Siddons, P. T., Weedon, B. C. L. Carotenoids and related compounds. Part XI. Syntheses of δ-carotene and ε-carotene. *J. Chem. Soc.* **1965**, 2019–2026.

[6] Davis, B. H. Carotenoid. In Chemistry and Biochemistry of Plant Pigments; Goodwin, T. W., Ed.; Academic Press: London, U.K., **1976**; pp 38–165.

[7] Britton, G. UV/visible spectroscopy. In *Carotenoids Volume 1B: Spectroscopy*; Britton, G.; Liaaen-Jensen, S.; Pfander, H., Eds.; Birkhäuser Verlag: Basel, **1995**; pp 13–62.

[8] Schierle, J., Bretzel, W., Bühler, I., Faccin, N., Hess, D., Steiner, K., Schüep, W.

Content and isomeric ratio of lycopene in food and human blood plasma. *Food Chem.* **1997**, *59*, 459–465.

[9] Ishida, B. K., Ma, J., Chan, B. A simple, rapid method for HPLC analysis of lycopene isomers. *Phytochem. Anal.* **2001**, *12*, 194–198.

[10] Zhang, J.-P., Chen, C.-H., Koyama, Y. Vibrational relaxation and redistribution in the $2Ag^-$ state of *all-trans*-lycopene as revealed by picosecond time-resolved absorption spectroscopy. *J. Phys. Chem. B* **1998**, *102*, 1632–1640.

[11] Choksi, P. M., Joshi, V. Y. A review on lycopene−extraction, purification, stability and applications. *Int. J. Food Prop.* **2007**, *10*, 289–298.

[12] Craft, N. E., Soares, J. H., Jr. Relative solubility, stability, and absorptivity of lutein and *β*-carotene in organic solvents. *J. Agric. Food Chem.* **1992**, *40*, 431–434.

[13] Estrella, A., López-Ortiz, J. F., Cabri, W., Rodríguez-Otero, C., Fraile, N., Erbes, A. J., Espartero, J. L., Carmona-Cuenca, I, Chaves, E., Muñoz-Ruiz, A. Natural lycopene from *Blakeslea trispora*: all-trans lycopene themochemical and structural properties. *Thermochim. Acta* **2004**, *417*, 157–161.

[14] Zechmeister, L., Polgár, A. *cis–trans* Isomerization and spectral characteristics of carotenoids and some related compounds. *J. Am. Chem. Soc.* **1943**, *65*, 1522–1528.

[15] Hirayama, K. Relation between chemical structure and visible and ultra-violet

spectra. I-II. II. Polyenes and alkylated polyenes. *Nippon Kagaku Zassi* **1954**, *75*, 29–35.

[16] Hirayama, K. Relation between chemical structure and visible and ultra-violet spectra. III. Solvents effects on absorption of polyenes. *Nippon Kagaku Zassi* **1954**, *75*, 667–674.

[17] Hirayama, K. Relation between chemical structure and visible and ultra-violet spectra. IV. Effects of substituents and special structures. *Nippon Kagaku Zassi* **1954**, *75*, 674–678.

[18] Naviglio, D., Pizzolongo, F., Ferrara, L., Naviglio, B., Aragòn, A., Santini, A. Extraction of pure lycopene from industrial tomato waste in water using the extractor Naviglio®. *Afr. J. Food Sci.* **2008**, *2*, 37–44.

[19] Hertzberg, S., Liaaren-Jensen, S. Bacterial carotenoids: the carotenoids of *Mycobacterium phlei* strain Vera. 2. The Structure on the phlei-xanthophylls−two novel tertiary glycoside. *Acta Chem. Scand.* **1967**, *21*, 15–41.

[20] Mimuro, M., Nagashima, U., Nagaoka, S., Nishimura, Y., Takaichi, S., Katoh, T., Yamazaki, I. Quantitative analysis of the solvent effect on the relaxation processes of carotenoids showing dual emissive characteristics. *Chem. Phys. Lett.* **1992**, *191*, 219–224.

[21] Hengartner, U., Bernhard, K., Meyer, K., Englert, G., Glinz, E. Synthesis, isolation, and NMR-spectroscopic characterization of fourteen (*Z*)-isomers of lycopene and of some acetylenic didehydro- and tetradehydrolycopenes. *Helv. Chim. Acta* **1992**, *75*, 1848–1865.

[22] Budavari, S., O'Neil, M. J., Smith, A., Heckelman, P. E. The Merck Index, 13th ed.; Merck: Rahway, N. J., **2001**.

[23] Tiziani, S., Schwartz, S. J., Vodovotz, Y. Profiling of carotenoids in tomato juice by one- and two-dimensional NMR. *J. Agric. Food Chem.* **2006**, *54*, 6094–6100.

[24] Fröhlich, K., Conrad, J., Schmid, A., Breithaupt, D. E., Böhm, V. Isolation and structural elucidation of different geometrical isomers of lycopene. *Int. J. Vitam. Nutr. Res.* **2007**, *77*, 369–375.

[25] Kishimoto, S., Maoka, T., Sumitomo, K., Ohmiya A. Analysis of carotenoid composition in petals of calendula (*Calendula officinalis* L.). *Biosci. Biotechnol. Biochem.* **2005**, *69*, 2122–2128.

[26] Englert, G. NMR spectroscopy. In *Carotenoids Volume 1B: Spectroscopy*; Britton, G., Liaaen-Jensen, S., Pfander, H., Eds.; Birkhäuser Verlag: Basel, **1995**; pp 147–260.

Chapter 3

Isolation and characterization of (15Z)-lycopene thermally generated from a natural source

3.1. Table of contents

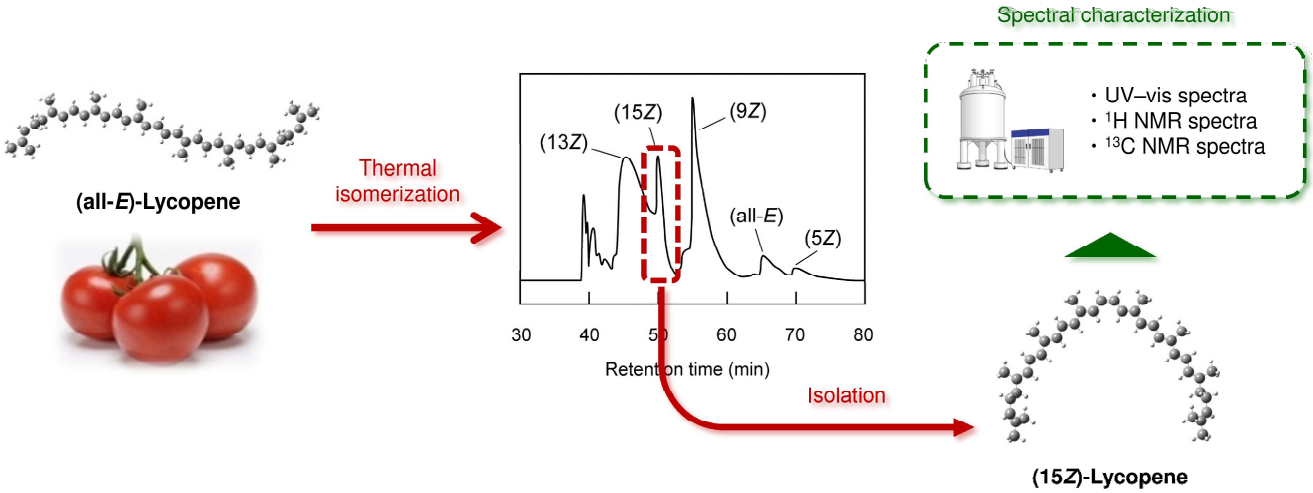

3.2. Introduction

Lycopene has a large number of geometric isomers caused by *E*/*Z* isomerization at arbitrary sites within the eleven conjugated double bonds, and 71 kinds of *Z*-isomers are theoretically possible [1]. However, it is a small part of them have been characterized by spectral methods such as UV–vis, ^{1}H, and ^{13}C NMR spectroscopy. The structural assignments and UV–vis spectral features of (5*Z*)-, (9*Z*)- and (13*Z*)-lycopene, the predominant *Z*-isomers generated during heat [1,2] or photoirradiation treatment [3,4], were demonstrated through the successful acquisition of highly purified preparations of the isomers by using a series of chromatographies [2]. The other theoretically-possible mono-*Z*-isomer by heating, (15*Z*)-lycopene (Figure 1), was rationally synthesized via a Wittig reaction [5,6], but could not be identified during the heat or photoirradiation process, possibly because of thermodynamic instability and the presence of a small

amount of the lycopene isomer generated by isomerization [7]. On the other hand, the structure [8,9], thermal isomerization [10,11], and bioavailability and function [12,13] of a similar symmetrical carotenoid of (15*Z*)-*β*-carotene have been extensively examined.

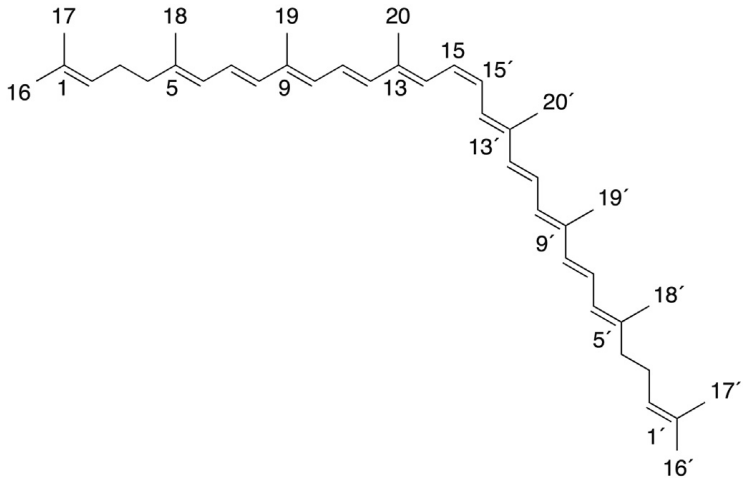

Figure 1. Chemical structure of (15*Z*)-lycopene. (15*Z*)-Lycopene in this study was purified from a mixture of lycopene isomers, which was prepared by heating (all-*E*)-lycopene of a tomato origin.

In the present study, (15*Z*)-lycopene with high purity was prepared from a mixture of lycopene isomers thermally converted from the all-*E* form of a tomato origin, and structural characterization was performed by spectral methods including UV–vis, ^{1}H, and ^{13}C NMR spectroscopy. This results of this study will provide an insight into (15*Z*)-lycopene and validate previous descriptions of spectral properties of a theoretically-synthesized 15*Z*-isomer [14–19], including those of the synthetic

(15*Z*)-lycopene [5,6].

3.3. Materials and methods

3.3.1. General

Analytical grade acetone, CH_2Cl_2, DIEPA, ethanol and MTBE were obtained from Nakaraitesuku Co., Ltd. (Kyoto, Japan), $CDCl_3$ was obtained from Sceti Co., Ltd. (Tokyo, Japan), and HPLC-grade methanol was obtained Sigma-Aldrich Co. (St. Louis, MO, USA). Hexane obtained from a solvent-dispensing system supplied by Glass Contour (Nikko Hansen & Co., Ltd., Osaka, Japan) under a nitrogen atmosphere after a preliminary distillation. DFT calculations were performed with the Gaussian 09 software (Rev. D.01), and conformational search was done using CONFLEX 7 program (Rev. B, Conflex corp., Tokyo) [20].

3.3.2. Preparation of (all-*E*)-lycopene

(all-*E*)-Lycopene was isolated from tomato paste (Kagome Co., Ltd., Tokyo; lycopene content, 8–12 g/kg) using procedures similar to those previously described [1,2], i.e., extraction with CH_2Cl_2, recrystallization from benzene, and washing with acetone and ethanol under shading conditions: 750 mg of a fine red crystalline powder

from 140 g of a tomato sample; reversed-phase HPLC, ≥99.0% purity. Purified lycopene was stored at −80 °C until just before use.

3.3.3. Thermal isomerization of lycopene

Purified (all-*E*)-lycopene (110 mg), which was dissolved in 170 mL of benzene, was transferred into a 300-mL stainless steel pressure vessel (TP300KG, Unicontrols Co., Ltd., Chiba, Japan), purged with argon, and then heated at 79 °C for 19 h in an oil bath. These procedures were conducted on five batches of the lycopene solution. The yield of isomerization to *Z*-forms was estimated to be nearly 70% of all lycopene isomers by the reversed-phase HPLC method.

3.3.4. Isolation of (15*Z*)-lycopene

Purification of the 15*Z*-isomer from the mixture of thermally-isomerized lycopene was conducted using three-step column chromatography. All procedures were carried out at room temperature, and light exposure was kept to a minimum throughout purification. A batch of the lycopene mixture, which was isomerized in benzene, was evaporated to dryness under reduced pressure, and then dissolved in 5.0 mL of hexane. The insoluble residues (ca. 40 mg), which mostly consisted of (all-*E*)-lycopene, were

removed using a 0.2-μm polytetrafluoroethylene membrane filter (DISMIC-25HP, Advantec, Tokyo) prior to chromatographic separations. The supernatant was divided into six potions and repeatedly applied to HPLC on three normal-phase columns tandemly connected under the following conditions: column, Nucleosil 300-5 (3 × 250-mm in length, 10-mm inner diameter, 5-μm particle size, GL Sciences Inc., Tokyo); solvent, hexane/DIPEA (500:1, v/v); flow rate, 2.0 mL/min; column temperature, ambient; photodiode array detector (SPD-M10AVP, Shimadzu, Kyoto, Japan). These procedures were applied to the other four batches, and the fractions with retention times of 49.5–52.0 min were collected and evaporated to dryness, leaving 13.4 mg of a red-brown substance. The resulting partially-purified sample was dissolved in 5.0 mL of hexane, and separated again under the same chromatographic conditions, except for the solvent (hexane/DIPEA [2000:1, v/v]). The eluted fractions with retention times of 56.0–60.0 min were combined, evaporated, and dried under reduced pressure. The resulting red substances (2.6 mg) were dissolved in 1.5 mL of benzene, and added to reversed-phase HPLC under the following conditions: column, YMC Carotenoid (250 × 10-mm inner diameter, 5-μm particle size, YMC, Kyoto); solvent A, methanol/MTBE/H_2O (75:15:10, v/v/v); solvent B, methanol/MTBE/H_2O (7:90:3, v/v/v); gradient, started with 100% eluent A and ended with 100% eluent B over a

period of 35 min; flow rate 3.0 mL/min; column temperature, 22 °C. The fractions with retention times of approximately 24.7 min were collected and dried *in vacuo*, resulting in the 15*Z*-isomer being obtained: 0.6 mg of fine red crystalline powder; reversed-phase HPLC, 97.2% purity; normal-phase HPLC, ≥99.9%. The purity of (15*Z*)-lycopene by reversed- and normal-phase HPLC was estimated by peak area integration at 470 nm, as previously reported [1,3].

3.3.5. NMR spectroscopy

The NMR spectra of (15*Z*)-lycopene were recorded on a JMN-LA400 FT NMR spectrometer (JEOL, Tokyo) at 400 MHz for ^{1}H and 100 MHz for ^{13}C. Chemical shifts were recorded as a δ value (ppm) using tetramethylsilane as an internal standard. Spectra were observed in C_6D_6 as well as $CDCl_3$.

3.3.6. Computational analysis

The geometric optimization of (all-*E*)- and (15*Z*)-lycopene was performed with DFT as implemented in Gaussian 09 using the B3LYP functional and 6'31G(d) basis set including a zero point vibrational energy correction. Prior to the calculation for (all-*E*)-lycopene, the structures of the conjugated all-*E*-polyenes, C_nH_{n+2} (n = 4–22,

even number) were optimized at the ground singlet states, and followed by the methylated undecaenes TMTU (Figure 2A) and HMHU (Figure 2B). The structure of HMHU was estimated using initial conformers at 30º intervals of the dihedral angles of the free rotation in a stepwise manner for two ethyl groups, and (all-*E*)-lycopene was then estimated in the same way. The initial conformations of (all-*E*)-lycopene were also ascertained using the CONFLEX method and MMFF94s force field. (15*Z*)-lycopene and the other mono-*Z*-isomers were similarly optimized by referring to the results of the all-*E*-isomer. Twisted TS geometries were obtained using a TS search. Vibrational frequency calculations were carried out in all cases to confirm the stationary point. Energy differences between the ground state and TS electronic energies corresponded to the activation energy of the isomerization reaction.

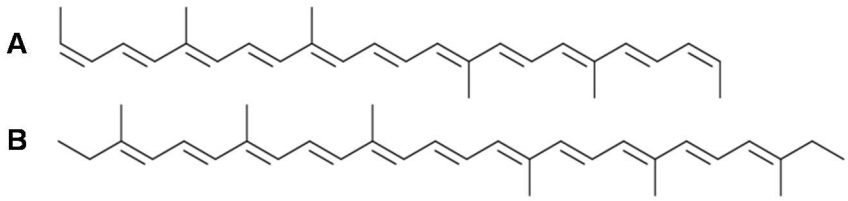

Figure 2. Chemical structures of (A) TMTU and (B) HMHU.

3.4. Results and discussion

3.4.1. Isolation of (15*Z*)-lycopene thermally generated from a tomato sample

The occurrence of (15*Z*)-lycopene from (all-*E*)-lycopene during a heating has been

suggested by several studies, and this has mainly been based on analyses of UV–vis spectra, in which the *Z*-peak ratio of the isomer, D_B/D_{II}, was estimated to be 75–79% in a HPLC mobile phase [2,16,19]. However, the existence of the *Z*-isomer from a natural source has not yet been demonstrated. In the present study, a purification procedure for (15*Z*)-lycopene was exploited using an elaborate HPLC technique. Prior to isolating the *Z*-isomer, the geometric isomerization of (all-*E*)-lycopene, which was purified from tomato paste, was conducted by heating at 79 °C for 19 h under optimal conditions that excluded oxygen and light irradiation. Among the possible geometrical types for lycopene in the isomerized mixture, any isomers containing the *Z*-configuration in the molecule were considered to be more soluble in the hexane solvent than (all-*E*)-lycopene [21]. The remaining (all-*E*)-lycopene (40 mg in each batch; ca. 30% of all isomers of lycopene) was effectively removed by filtration only, and the other crude *Z*-isomers were then prepared using this simple fractionation technique.

In the first chromatographic purification step, three normal-phase HPLC columns connected in tandem were applied to separate (15*Z*)-lycopene (retention time, 49.5–52.0 min; D_B/D_{II}, 79% [2]) from the crude fraction (Figure 3A). The ratio of (15*Z*)-lycopene to all isomers was estimated to be no more than 10% by comparisons with the peak areas; taking into account the previous removal of insoluble (all-*E*)-lycopene, the

amount of the 15*Z*-isomer produced during the thermal process was very small, typically a few percent or less. These results could reflect the relatively low generation rate and/or relatively higher free energy of the 15*Z*-isomer [7,22]. On the other hand, large amounts of (9*Z*)- and (13*Z*)-lycopene were observed with peak retention times of approximately 55 and 45 min, respectively, which is consistent with previous findings [2,17,19]. A second normal-phase HPLC was then applied to the partially-purified fraction under the same conditions as those for the columns and mobile phase, except for the amine concentration. HPLC separation equipped with a reversed-phase column was conducted on fractions abundant in (15*Z*)-lycopene, which resulted in 0.6 mg of the highly purified 15*Z*-isomer (Figure 3B) being successfully obtained from 556 mg of (all-*E*)-lycopene as a starting material. The purity of (15*Z*)-lycopene was estimated to be 97.2% by reversed-phase HPLC analysis, in which the small amount of impurities would have been (all-*E*)-lycopene generated from the reversion of (15*Z*)-lycopene to (all-*E*)-lycopene during the chromatographic procedure, because the peak retention time of approximately 33 min showed the all-*E*-isomer (Figure 3B), which was easily removed in the purification process. Similar findings were previously observed in the purification of other mono-*Z*-isomers [2]. The actual purity of (15*Z*)-lycopene was then considered to be sufficiently high to be subjected to structural characterization using

NMR spectroscopy, as the value estimated in normal-phase HPLC analysis was high (≥99.9%). Therefore, pure (15*Z*)-lycopene was now obtained from the thermally isomerized lycopene sample of a natural origin. The fine control of the concentration of amine in the normal-phase HPLC eluent led to the discovery of the isomer.

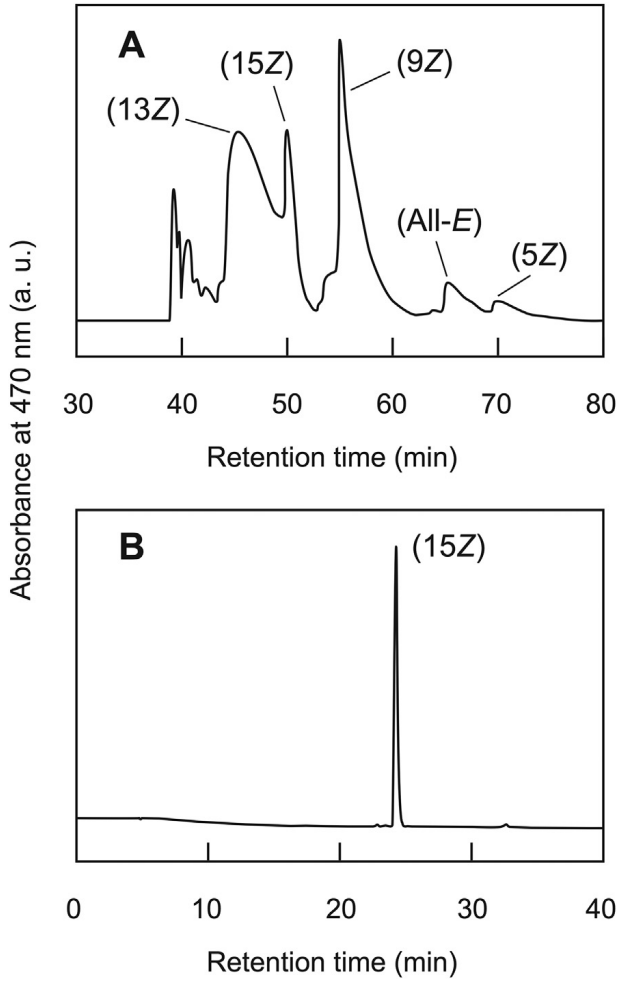

Figure 3. Separation of (A) geometrical isomers of lycopene, generated during a heating process, by normal-phase chromatography as the first purification step (solvent: hexane/DIPEA [500:1], v/v) and (B) purified (15*Z*)-lycopene was then analyzed by reversed-phase HPLC.

3.4.2. Characterization of (15*Z*)-lycopene by NMR spectroscopy

As noted in many previous studies [2,14–19], (15*Z*)-lycopene derived from natural sources has been identified tentatively by the D_B/D_{II} ratio on the basis of UV–vis spectroscopy i.e. the relative intensity of the *Z*-peak at approximately 360 nm to the absorption maximum of the isomer. In the present study, in order to confirm the occurrence of (15*Z*)-lycopene from natural sources, an attempt to characterize the isomer was conducted using NMR spectroscopy including two-dimensional analyses as well as ^{1}H and ^{13}C NMR, in combination with comparisons to the spectral data obtained from the synthesized (15*Z*)-lycopene [5,6]. The spectral analyses of lycopene demonstrated that the solubility of the *Z*-isomer in both $CDCl_3$ and C_6D_6 was higher than that of (all-*E*)-lycopene [21]; therefore, these spectra could be measured at a relatively higher concentration (1.0 mg/mL) in each solvent. This property facilitated measurements, especially in the case of ^{13}C and two-dimensional NMR analyses.

Proton (Figure 4) and ^{13}C spectra of the purified (15*Z*)-lycopene were listed in Table 1 and Table 2, respectively. By considering differences in the geometric structures of (15*Z*)- and (all-*E*)-lycopene, it is reasonable to assume that the 15*Z*-isomer exhibited more distinctive chemical shift values around the center of the molecule as compared to those of the all-*E*-isomer, but had equivalent values at the terminals. For example, the

large and lower magnetic field shifts of H–C(14) and H–C(14′) in (15*Z*)-lycopene were predictable because each proton was placed in diamagnetic anisotropy due to the π-systems between C(13) and C(13′), and vice versa for the H–C(15) and H–C(15′) protons of the 15*Z*-isomer [21]. The values of the chemical shift in (15*Z*)-lycopene around the center of the molecule were different from those of the *all-E* form, and were also consistent with the results obtained from synthetic data [5] for both nuclear species in $CDCl_3$ (Tables 1 and 2): for example, $\Delta\delta$ = 0.43 ppm for H–C(14) and H–C(14′); −0.23 ppm for H–C(15) and H–C(15′). Similar results were obtained with the other solvent C_6D_6, and the chemical shift values of C(14), C(14′), C(15), and C(15′) on (15*Z*)-lycopene were clearly different from those of the all-*E*-isomer. Furthermore, the coupling constants for (15*Z*)-lycopene in ^{1}H NMR, which were not reported even for synthetic ones [5], were determined in both solvents. The coupling system between H−C(14), H−C(14′) and H−C(15), H−C(15′) were observed separately in C_6D_6, whereas their corresponding signals in $CDCl_3$ overlapped with those of H−C(11), H−C(11′) and H−C(12), H−C(12′), respectively, and could only be assigned to multiplets (Table 1). The observed spin signal in C_6D_6 was attributed to the AA′BB′ type system and similar coupling was recognized in some carotenoids, such as prolycopene [5,8] and (all-*E*)-lycopene [1], which had the centrosymmetric structure in their molecules. As

described previously [1], NMR measurements of carotenoids in C_6D_6 in addition to $CDCl_3$ solvents effectively detected and discriminated spectral differences based on the physical properties of the solvent, such as polarity, resonance, and viscosity. This study successfully confirmed the existence of (15*Z*)-lycopene derived from a natural source and the validity of the characterization of the synthetic lycopene [5,6] and others [14–19]. The unambiguous determination attained in this study will also assist in identifying the unidentified *Z*-isomers occurring in natural sources and those generated from the isomerization of lycopene during the heating and irradiation process, especially for the di-*Z*-isomer with a centrosymmetric structure such as (5*Z*,5′*Z*)- and (9*Z*,9′*Z*)-lycopene, as well as with a 15*Z*-configuration.

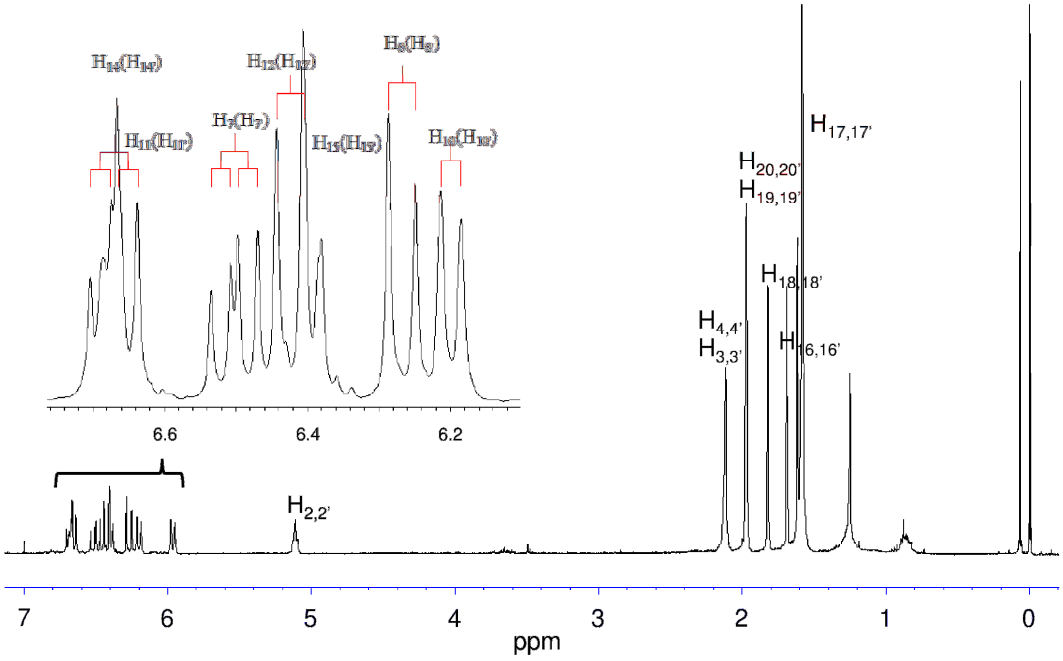

Figure 4. ^{1}H NMR spectrum of the purified (15*Z*)-lycopene. (400 MHz, $CDCl_3$).

Table 1. ^{1}H NMR assignment of (15*Z*)-lycopene thermally isomerized from (all-*E*)-lycopene of a tomato origin[a]

	in $CDCl_3$ [synthetic lycopene][b]			in C_6D_6		
proton	(15*Z*)	(all-*E*)[c]	$\Delta\delta$[d]	(15*Z*)	(all-*E*)[c]	$\Delta\delta$[d]
H–C(2), H–C(2′)	5.11 (*m*) [5.11]	5.11 (*m*) [5.11]		5.23 (*m*)	5.23 (*m*)	
2H–C(3), 2H–C(3′)	2.12 (*m*) [*ca.* 2.12]	2.11 (*m*) [*ca.* 2.11]		2.18 (*m*)	2.18 (*m*)	
2H–C(4), 2H–C(4′)	2.12 (*m*) [*ca.* 2.12]	2.11 (*m*) [*ca.* 2.11]		2.18 (*m*)	2.18 (*m*)	
H–C(6), H–C(6′)	5.96 (*d*, *J* = 10.8) [5.97]	5.95 (*d*, *J* = 11.0) [5.95]		6.16 (*d*, *J* = 11.1)	6.16 (*d*, *J* = 11.0)	
H–C(7), H–C(7′)	6.50 (*dd*, *J* = 15.0, 10.8) [6.50]	6.49 (*dd*, *J* = 15.0, 11.0) [6.49]		6.67 (*dd*, *J* = 15.1, 11.1)	6.67 (*dd*, *J* = 15.1, 11.0)	
H–C(8), H–C(8′)	6.27 (*d*, *J* = 15.0) [6.27]	6.25 (*d*, *J* = 15.0) [6.25]		6.43 (*d*, *J* = 15.1)	6.44 (*d*, *J* = 15.1)	
H–C(10), H–C(10′)	6.20 (*d*, *J* = 11.6) [6.20]	6.18 (*d*, *J* = 11.4) [6.18]		6.38 (*d*, *J* = 11.5)	6.36 (*d*, *J* = 11.6)	
H–C(11), H–C(11′)	6.67 (*dd*, *J* = 14.6, 11.6) [6.67]	6.64 (*dd*, *J* = 14.9, 11.4) [6.64]	0.03 [0.03]	6.80 (*dd*, *J* = 15.0, 11.5)	6.77 (*dd*, *J* = 15.0, 11.6)	0.03
H–C(12), H–C(12′)	6.43 (*d*, *J* = 14.6) [6.43]	6.35 (*d*, *J* = 14.9) [6.35]	0.08 [0.08]	6.52 (*d*, *J* = 15.0)	6.49 (*d*, *J* = 15.0)	0.03
H–C(14), H–C(14′)	6.67 (AA′BB′) [6.68]	6.24 (*m*) [6.25]	0.43 [0.43]	6.91 (AA′BB′)	6.34 (AA′BB′)	0.57
H–C(15), H–C(15′)	6.39 (AA′BB′) [6.40]	6.62 (*m*) [6.62]	–0.23 [–0.22]	6.47 (AA′BB′)	6.70 (AA′BB′)	–0.23
3H–C(16), 3H–C(16′)	1.692 (*s*) [1.692]	1.687 (*s*) [1.688]		1.670 (*s*)	1.674 (*s*)	
3H–C(17), 3H–C(17′)	1.620 (*s*) [1.619]	1.614 (*s*) [1.612]		1.563 (*s*)	1.568 (*s*)	
3H–C(18), 3H–C(18′)	1.824 (*s*) [1.825]	1.818 (*s*) [1.818]		1.740 (*s*)	1.749 (*s*)	
3H–C(19), 3H–C(19′)	1.975 (*s*) [1.978]	1.968 (*s*) [1.968]		1.911 (*s*)	1.925 (*s*)	
3H–C(20), 3H–C(20′)	1.970 (*s*) [1.969]	1.968 (*s*) [1.968]		1.878 (*s*)	1.876 (*s*)	

[a]Recorded at 400 MHz; δ in ppm (multiplicity, coupling constant in Hz); *s* = singlet, *d* = doublet, *dd* = doublet of doublets, *m* = multiplet. [b, c]Obtained from previous studies [1,5].
[d]Shift differences $\Delta\delta = \delta((Z)) - \delta((E))$ for $|\Delta\delta| > 0.02$ ppm.

Table 2. ^{13}C NMR assignment of (15*Z*)-lycopene thermally isomerized from (all-*E*)-lycopene of a tomato origin[a]

	in $CDCl_3$ [synthetic lycopene][b]			in C_6D_6		
carbon	(15*Z*)	(all-*E*)[c]	$\Delta\delta$[d]	(15*Z*)	(all-*E*)[c]	$\Delta\delta$[d]
C(1), C(1′)	131.75 [131.81]	131.72 [131.64]		131.63	131.61	
C(2), C(2′)	123.95 [123.85]	123.96 [124.12]		124.53	124.54	
C(3), C(3′)	26.68 [26.62]	26.70 [26.83]		27.15	27.13	
C(4), C(4′)	40.23 [40.22]	40.23 [40.30]		40.66	40.65	
C(5), C(5′)	139.55 [139.63]	139.47 [139.30]		139.02	138.99	
C(6), C(6′)	125.71 [125.59]	125.74 [125.94]		126.78	126.81	
C(7), C(7′)	124.89 [124.82]	124.79 [124.87]		125.39	125.32	
C(8), C(8′)	135.38 [135.33]	135.40 [135.54]		136.20	136.20	
C(9), C(9′)	136.34 [136.31]	136.15 [136.15]		136.59	136.41	
C(10), C(10′)	131.48 [131.49]	131.55 [131.64]		132.30	132.40	
C(11), C(11′)	125.50 [125.45]	125.15 [125.21]	0.35	126.01	125.68	0.33
C(12), C(12′)	137.56 [137.53]	137.35 [137.46]		138.19	138.02	
C(13), C(13′)	137.27 [137.24]	136.56 [136.54]	0.71 [0.70]	137.50	136.82	0.68
C(14), C(14′)	127.00 [126.98]	132.64 [132.71]	−5.6 [−5.7]	*ca.* 128.1[e]	133.41	*ca.* −5.3[e]
C(15), C(15′)	125.62 [125.56]	130.07 [130.17]	−4.5 [−4.6]	126.16	130.72	−4.6
C(16), C(16′)	25.69 [25.76]	25.68 [25.66]		25.94	25.85	
C(17), C(17′)	17.70 [17.73]	17.70 [17.70]		17.74	17.77	
C(18), C(18′)	16.96 [16.97]	16.99 [16.97]		16.93	16.93	
C(19), C(19′)	12.91 [12.94]	12.90 [12.90]		13.09	13.00	
C(20), C(20′)	12.50 [12.52]	12.79 [12.81]		12.58	12.90	−0.32

[a]Recorded at 100 MHz. [b, c]Obtained and revised from previous studies [1,5]. [d]Shift differences $\Delta\delta = \delta((Z)) - \delta((E))$ for $|\Delta\delta| > 0.30$ ppm. [e]Overlapped with the solvent peak.

3.4.3. Computational simulation of isomerization of (all-*E*)-lycopene to (15*Z*)-lycopene and other mono-*Z*-isomers.

A computational approach to examine the geometrical isomerization of (all-*E*)-lycopene to 15*Z*- and other mono-*Z*-isomers was performed using the Gaussian program by considering conformational changes in the terminal moieties of the molecule, each of which contained two methylene groups at C(3)/C(4) and C(3′)/C(4′) with lower rotational barriers. Calculations of the free energy for a series of polyenes were antecedent to those of (all-*E*)-lycopene and the *Z*-isomers: the energies of the all-*E*-polyene C_nH_{n+2} were estimated in the order of the molecular formula, starting from buta-1,3-diene (*n* = 4) to (3*E*,5*E*,7*E*,9*E*,11*E*,13*E*,15*E*,17*E*,19*E*)-docosa-1,3,5,7,9,11,13,15,17,19,21-undecaene (*n* = 22). The alkylated undecaenes of TMTU and HMHU were then calculated as described in the Materials and Methods section. An estimation for the full-length (all-*E*)-lycopene molecule was then carried out and followed by the mono-*Z*-isomers. In addition to the individual conformational changes at the two methylene groups of the terminal regions of the molecule, two conformation types were considered as the initial conformer in the calculation of the free energy of (all-*E*)-lycopene: namely, the *syn*-like conformer of lycopene which has terminal groups on the same side of the central planar

conjugated polyene (Figure 5A,B), and the *anti*-like conformer which has the terminal units on the opposite sides of each other (Figure 5C,D). The energy of the *syn*-like structure of (all-*E*)-lycopene was calculated as a more stable conformer than that of the *anti*-like conformer, although this difference was too small to be significant (Table 3, Figure 5A–D).

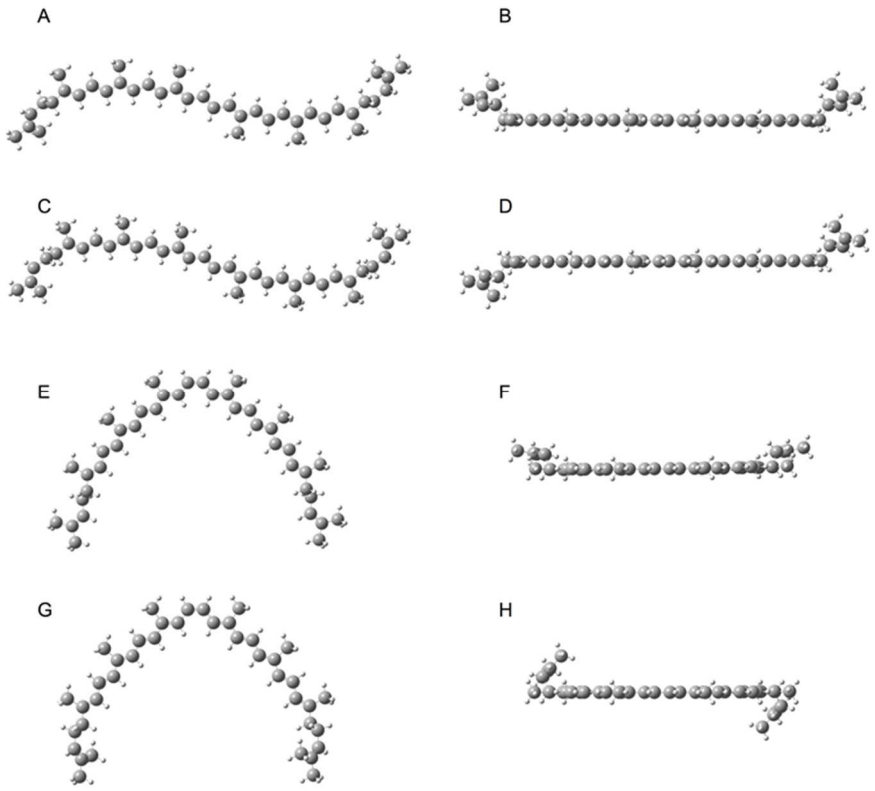

Figure 5. Calculated minimum-energy conformation of (A–D) (all-*E*)-lycopene and (E–H) (15*Z*)-lycopene. The left figures (top views) show outlooks from a different angle of lycopene, corresponding to the conformation on the right side (side views). C(3)/C(4) and C(3′)/C(4′) groups at the terminal regions of the molecule in A, B, E, and F are on the same side (*syn*-like conformation) to the 11 conjugated double bonds in the planar configuration of lycopene, while those in C, D, G, and H are on the opposite side (*anti*-like conformation).

Calculations with initial conformers estimated by the CONFLEX method also supported these results (data not shown). The energies of the (15*Z*)-lycopene conformers in the *syn*-like and *anti*-like types were then evaluated by referring to that of (all-*E*)-lycopene, and those of (5*Z*)-, (9*Z*)-, and (13*Z*)-lycopene were estimated by the same method. The results obtained showed that the energy of (15*Z*)-lycopene was the highest among the isomers and the order of stability was as follows: (all-*E*)- ≈ (5*Z*)- > (9*Z*)- > (13*Z*)- > (15*Z*)-lycopene (Table 3). The order of the relative stability of the isomers was consistent with that of a previous study [7]. Free energies were also calculated for the constitutional isomers of lycopene, (all-*E*)-*β*-carotene and (15*Z*)-*β*-carotene, using the same procedure. These energies were estimated to be −62.3 and −51.5 kJ/mol, respectively, with reference to the value of (all-*E*)-lycopene in the *syn*-like form as zero, which also suggested the relatively labile nature of lycopene, as shown in the experimental results [23,24].

Moreover, the activation energies of the isomerization from (all-*E*)-lycopene in the *syn*-like form to each *Z*-isomer were evaluated in the singlet state from energy differences between the ground state and TS electronic energies. The energy to (13*Z*)-lycopene was experimentally determined to be 99.6 kJ/mol in a benzene solvent (Figure 6), and was calculated as 87.9 kJ/mol in the present study (Table 3), implying

that this theoretical approach is appropriate for evaluating energies. The values to (15*Z*)-lycopene were then calculated as 90.4 kJ/mol and 91.2 kJ/mol at the twisted angles of +94.7° and −95.0°, respectively (Table 3, Figure 7). The other thermally-preferable isomers were estimated using the same method, and activation energies were determined in the order of (13*Z*)- < (15*Z*)- < (9*Z*)- < (5*Z*)-lycopene, for which the geometry of the methylene units did not influence the values obtained (Table 3). This order was supported by previous findings [7] as well as experimental data [1]. Consequently, (15*Z*)-lycopene was the more preferred isomer on the basis of kinetic parameters, but was unfavorable according to thermodynamic considerations: the back reaction to the all-*E* form could readily occur and give isomers other than the 15*Z* form. As discussed above, we only obtained 0.6 mg of (15*Z*)-lycopene with higher purity from 556 mg of (all-*E*)-lycopene. However, this result was reasonable because the ratio of (15*Z*)-lycopene to the all-*E* form was estimated to be 1:39, calculated according to the equation of $K = \exp(-\Delta G/RT)$ (*K*, equilibria constant; *R*, gas constant; *T*, absolute temperature), and the difference between the calculated value and the experimental value would be caused by a lack of the calculation accuracy (disregard of the solvent effects or lack of the base function accuracy) or non-reaching of the isomerization reaction to a equilibrium state.

(15*Z*)-Lycopene was thermally generated and purified from a natural source, and mainly identified by an NMR technique for the first time as a natural origin. Moreover, the occurrence and availability of the 15*Z*-isomer were also discussed on the basis of the calculation method, which provided a rational explanation for the experimental results obtained. Thus, a focus on the basic strategy, which tends to be avoided in these days of fast technology and chemistry, will contribute to basic and applied studies on carotenoids through the benefit of highly developed instrumental measurements.

Table 3. Calculated gibbs free energy (ΔG) of lycopene isomers and activation energy (ΔE_a) of rotational barriers for the isomerization process of (all-*E*)-lycopene to (mono-*Z*)-lycopene at the S_0 state

lycopene	ΔG^a (kJ/mol)		$\Delta E_a{}^b$ (Φ^c) (kJ/mol)
	syn-like	*anti*-like	
(all-*E*)	0.00	0.318	
(5*Z*)	0.042	0.339	148.1 (+99.5°), 148.1 (−100.5°)
(9*Z*)	4.02	4.52	100.8 (+95.7°)
(13*Z*)	4.35	4.52	87.9 (+95.8°), 87.9 (−96.2°)
(15*Z*)	11.6	10.8	90.4 (+94.7°), 91.2 (−95.0°)

[a]The energies (in kJ/mol) are presented with reference to (all-*E*)-lycopene in the S_0 state. Calculations were performed in the *syn*- and *anti*-like conformation of the C(3)/C(4) and C(3′)/C(4′) groups at the terminal regions of the lycopene molecule to the 11 conjugated double bonds in the planar configuration (see also Figure 5). [b]Calculated from the *syn*-like conformation of (all-*E*)-lycopene (see Figure 5A,B). [c]Dihedral angle (Φ) of C(*n*−1)–C(*n*)–C(*n*+1)–C(*n*+2) for (*nZ*)-lycopene (*n* = 5, 9, and 13) and C(14)–C(15)–C(14′)–C(15′) for (15*Z*)-lycopene. Clockwise and counter-clockwise rotations were examined.

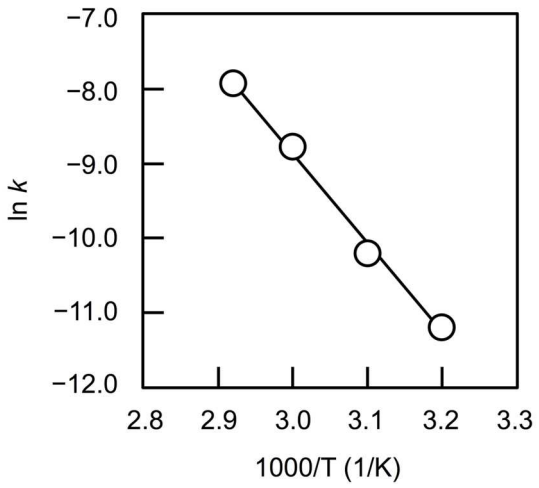

Figure 6. Arrhenius plots of thermal isomerization of (all-*E*)-lycopene to (13*Z*)-lycopene in benzene. Experimental conditions were described in detail previously [1].

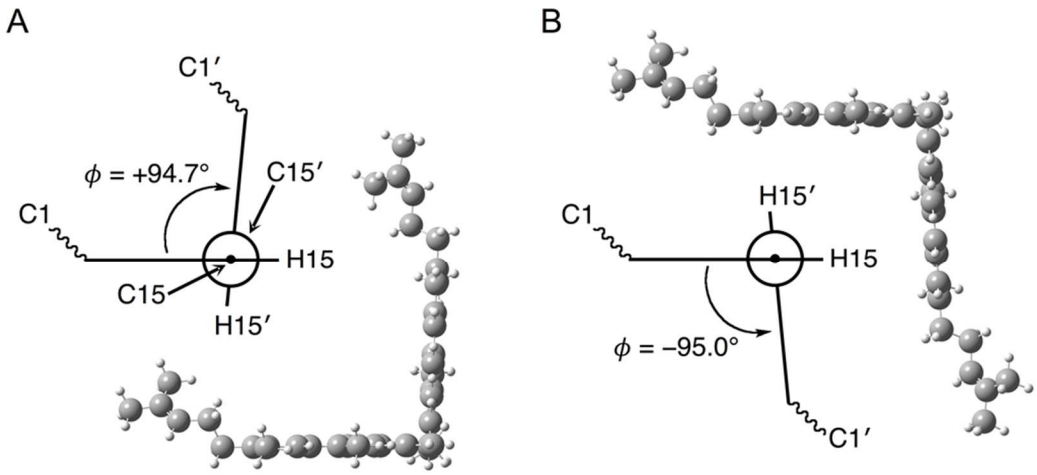

Figure 7. Calculated geometries of lycopene in twisted TSs with dihedral angles of (A) +94.7° and (B) −95.0° at the C(14)–C(15)–C(15′)–C(14′) position.

3.5. Reference

[1] Takehara, M., Nishimura, M., Kuwa, T., Inoue, Y., Kitamura, C., Kumagai, T., Honda, M. Characterization and thermal isomerization of (*all-E*)-lycopene. *J. Agric. Food Chem.* **2014**, *62*, 264–269.

[2] Honda, M., Takahashi, N., Kuwa, T., Takehara, M., Inoue, Y., Kumagai, T. Spectral characterization of *Z*-isomers of lycopene formed during heat treatment and solvent effects on the *E*/*Z* isomerization process. *Food Chem.* **2015**, *171*, 323–329.

[3] Honda, M., Igami, H., Kawana, T., Hayashi, K., Takehara, M., Inoue, Y., Kitamura, C. Photosensitized *E/Z* isomerization of (*all-E*)-lycopene aiming at practical applications. *J. Agric. Food Chem.* **2014**, *62*, 11353–11356.

[4] Heymann, T., Raeke, J., Glomb, M. A. Photoinduced isomerization of lycopene and application to tomato cultivation. *J. Agric. Food Chem.* **2013**, *61*, 11133–11139.

[5] Hengartner, U., Bernhard, K., Meyer, K., Englert, G., Glinz, E. Synthesis, isolation, and NMR-spectroscopic characterization of fourteen (*Z*)-isomers of lycopene and of some acetylenic didehydro- and tetradehydrolycopenes. *Helv. Chim. Acta* **1992**, *75*, 1848–1865.

[6] Isler, O., Gutmann, H., Lindlar, H., Montavon, M., Rüegg, R., Ryser, G., Zeller, P. Synthesen in der Carotinoid-Reihe. 6. Mitteilung. Synthese von Crocetindialdehyd und

Lycopin. *Helv. Chim. Acta* **1956**, *39*, 463–473.

[7] Guo, W.-H., Tu, C.-Y., Hu, C.-H. Cis-trans Isomerizations of *β*-carotene and lycopene: a theoretical study. *J. Phys. Chem. B* **2008**, *112*, 12158–12167.

[8] Englert, G. NMR spectroscopy. In *Carotenoids*; Britton, G., Liaaen-Jensen, S., Pfander, H., Eds.; Birkhäuser Verlag: Basel, Switzerland, **1995**, Vol. *1B*: Spectroscopy, pp 147–260.

[9] Koyama, Y., Hosomi, M., Hashimoto, H., Shimamura, T. ^{1}H NMR spectra of the all-*trans*, 7-*cis*, 9-*cis*, 13-*cis* and 15-*cis* isomers of *β*-carotene: elongation of the double bond and shortening of the single bond toward the center of the conjugated chain as revealed by vicinal coupling constants. *J. Mol. Struct.* **1989**, *193*, 185–201.

[10] Kuki, M., Koyama, Y., Nagae, H. Triplet-sensitized and thermal isomerization of all-trans, 7-cis, 9-cis, 13-cis and 15-cis isomers of *β*-carotene: configurational dependence of the quantum yield of isomerization via the T_1 state. *J. Phys. Chem.* **1991**, *95*, 7171–7180.

[11] Doering, W. von E., Sotiriou-Leventis, C., Roth, W. R. Thermal interconversions among 15-*cis*-, 13-*cis*-, and *all-trans-β*-carotene: kinetics, Arrhenius parameters, thermochemistry, and potential relevance to anticarcinogenicity of *all-trans-β*-carotene. *J. Am. Chem. Soc.* **1995**, *117*, 2747–2757.

[12] Grune, T., Lietz, G., Palou, A., Ross, A. C., Stahl, W., Tang, G., Thurham, D., Yin, S.-A., Biesalski, H. K. *β*-Carotene is an important vitamin A source for human. *J. Nutr.* **2010**, *140*, 2268S–2285S.

[13] Yeum, K.-J., Russell, R. M. Carotenoid bioavailability and bioconversion. *Annu. Rev. Nutr.* **2002**, *22*, 483–504.

[14] Emenhiser, C., Sander, L. C., Schwartz, S. J. Capability of a polymeric C_{30} stationary phase to resolve *cis–trans* carotenoid isomers in reversed-phase liquid chromatography. *J. Chromatogr. A* **1995**, *707*, 205–216.

[15] Fröhlich, K., Conrad, J., Schmid, A., Breithaupt, D. E., Böhm, V. Isolation and structural elucidation of different geometrical isomers of lycopene. *Int. J. Vitam. Nutr. Res.* **2007**, *77*, 369–375.

[16] Lee, M. T., Chen, B. H. Separation of lycopene and its *cis* isomers by liquid chromatography. *Chromatographia* **2001**, *54*, 613–617.

[17] Schierle, J., Bretzel, W., Bühler, I., Faccin, N., Hess, D., Steiner, K., Schüep, W. Content and isomeric ratio of lycopene in food and human blood plasma. *Food Chem.* **1997**, *59*, 459–465.

[18] Stahl, W., Sundquist, A. R., Hanusch, M., Schwarz, W., Sies, H. Separation of *β*-carotene and lycopene geometrical isomers in biological samples. *Clin. Chem.* **1993**,

39, 810–814.

[19] Yeum, K.-J., Booth, S. L., Sadowski, J.A., Liu, C., Tang, G.: Krinsky, N. I., Russell, R. M. Human plasma carotenoid response to the ingestion of controlled diets high in fruits and vegetables. *Am. J. Clin. Nutr.* **1996**, *64*, 594–602.

[20] Goto, H., Obata, S., Nakayama, N., Ohata, K. CONFLEX 7; Conflex: Tokyo, Japan, **2012**.

[21] Moss, G. P., Weedon, B. C. L. Chemistry of the carotenoids. In *Chemistry and Biochemistry of Plant Pigments*; Goodwin, T. W., Ed.; Academic Press: London, U.K., **1976**; Vol. *1*, pp 149–224.

[22] Chasse, G. A., Mak, M. L., Deretey, E., Farkas, I., Torday, L. L., Papp, J. G., Sarma, D. S. R., Agarwal, A., Chakravarthi, S., Agarwal, S., Rao, A. V. An *ab initio* computational study on selected lycopene isomers. *J. Mol. Struct. Thermochem.* **2001**, *571*, 27–37.

[23] Lee, M. T., Chen, B. H. Stability of lycopene during heating and illumination in a model system. *Food Chem.* **2002**, *78*, 425–432.

[24] Chen, B. H., Huang, J. H. Degradation and isomerization of chlorophyll a and *β*-carotene as affected by various heating and illumination treatments. *Food Chem.* **1998**, *62*, 299–307.

Chapter 4

Effects of solvent and temperature on E/Z isomerization of (all-E)-Lycopene

4.1. Table of contents

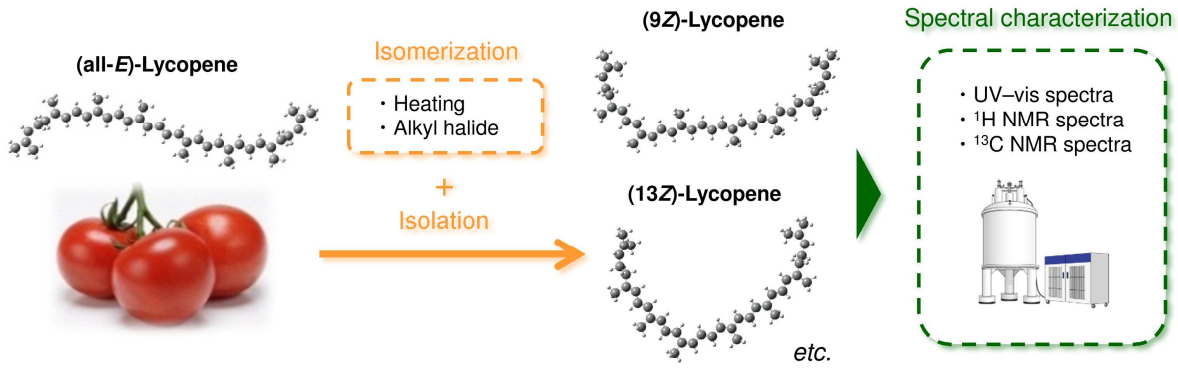

4.2. Introduction

The *E*/*Z* isomerization of carotenoids upon heating has been demonstrated for some representative compounds, including *β*-carotene, lutein, and zeaxanthin [1−4]. It has been also reported that astaxanthin was isomerized by heating in organic solvents, and a higher rate of isomerization was achieved in alkyl halides such as CH_2Cl_2 and $CHCl_3$ [5,6]. However, there are few reports discussing the effect of solvents on the *E*/*Z* isomerization of lycopene; consequently, the present investigation was conducted to characterize the isomerization of lycopene in various organic solvents. Based on the study of astaxanthin [5], we focused on the solvent effects of alkyl halides including CH_2Cl_2, $CHCl_3$, carbon CCl_4, and CH_2Br_2, as well as acetone, hexane, and benzene, other commonly used solvents in the study of carotenoids. Furthermore, the influence of temperature on *Z*-isomerization was investigated for each solvent.

Prior to the investigation of solvent effects on lycopene isomerization, (9*Z*)- and

(13*Z*)-lycopene, predominantly formed during the heating process, were exhaustively purified from heat-treated tomato paste and characterized by UV–vis and NMR spectroscopy, and their molar extinction coefficients were successfully determined for the first time. These fundamental spectroscopic data are essential for the investigation of the solvent effects on the *E*/*Z* isomerization of lycopene.

4.3. Materials and methods

4.3.1. Chemicals

HPLC-grade acetone, hexane, benzene, CH_2Cl_2, $CHCl_3$, CCl_4, and CH_2Br_2 were obtained from Kanto Chemical Co., Inc. (Tokyo, Japan). DIPEA was purchased from Tokyo Chemical Industry Co., Ltd. (Tokyo). (all-*E*)-Lycopene was obtained by a method described previously [7] or was provided by Wako Pure Chemical Industries, Ltd. (Osaka, Japan).

4.3.2. Isomerization of (all-*E*)-lycopene

(all-*E*)-Lycopene was dissolved in the respective solvents at a concentration of 0.1 mg/mL, and the solutions were filtered through a 0.2-μm PTFE membrane filter (Advantec Co., Ltd., Tokyo). A 5-mL sample was transferred from each of the solutions

to a 10-mL screw-capped tube. The headspace was filled with nitrogen gas, and the tube was tightly capped to prevent oxygen entry through the closure. The isomerization of (all-*E*)-lycopene was conducted at 4 °C and 50 °C in the dark. After the reaction, the solvent was removed from the reaction tube by a nitrogen gas stream, and the residue was re-dissolved in hexane. Normal-phase HPLC was used to analyze the lycopene isomers.

4.3.3. HPLC analysis

Normal-phase HPLC analysis was conducted according to the method described by Schierle et al. (1997) [8] with some modifications. The sample was cooled to 5 °C using an autosampler with a cooler (L-2200, Hitachi Ltd., Tokyo) immediately before the analysis. The detection wavelength of the compound was set at 460 nm (L-2455, Hitachi Ltd.) where the differences in molar extinction coefficients among lycopene isomers are relatively smaller. The mobile phase consisted of hexane containing 0.1% DIPEA and the stationary phase consisted of three Nucleosil 300-5 columns connected in tandem (3 × 250 mm in length, 4.6 mm inner diameter, 5 μm particles, GL Sciences Inc., Tokyo). The flow rate and column temperature were set at 1 mL/min and 30 °C, respectively. Reversed-phase HPLC analysis was performed according to the method of

Takehara et al. (2014) [7].

4.3.4. Isolation and identification of (9*Z*)- and (13*Z*)-lycopene

In older to characterization of the major lycopene *Z*-isomers, (9*Z*)- and (13*Z*)-lycopene, generated by thermal isomerization, they were isolated by preparative HPLC. (all-*E*)-Lycopene was dissolved in benzene at a concentration of 0.7 mg/mL, and the solution was heated at 75 °C for 14.5 h in the dark. After heating, the solvent was evaporated on a rotary evaporator, and the residue was dissolved in hexane at a concentration of 14.8 mg/mL. After filtering through a 0.2-μm PTFE membrane filter, the solution was injected into the normal-phase HPLC instrument at room temperature as described above, except for the mobile phase (hexane/DIPEA (400:1 v/v)) and flow rate (2.0 mL/min). Under these conditions, fractions of crude (9*Z*)-lycopene at a retention time of 48.8–54.2 min and crude (13*Z*)-lycopene at 39.5–43.2 min were isolated and applied to a second normal-phase chromatographic separation using a hexane/DIPEA mobile phase at 700:1 (v/v) for the 9*Z*-isomer or 2000:1 (v/v) for the 13*Z*-isomer. Finally, the third normal-phase chromatographic separation was conducted with hexane/DIPEA (500:1 v/v) to further purify (13*Z*)-lycopene.

4.3.5. UV–vis and NMR spectroscopic analyses of (all-*E*)-, (9*Z*)-, and (13*Z*)-lycopene

UV–vis spectra of the purified lycopene isomers were measured in hexane over a scanning range of 200–600 nm, and the λ maxima and minima of the compounds were determined. Spectra were recorded with a Hitachi U-3010 spectrophotometer (Tokyo). The absorption at 460 nm was also measured to give an accurate estimation of the concentration of lycopene isomers by comparing the molar extinction coefficient of (all-*E*)-lycopene to those of (9*Z*)- and (13*Z*)-lycopene at that wavelength.

(9*Z*)-Lycopene and (13*Z*)-lycopene were identified by ^{1}H and ^{13}C NMR spectroscopic analysis. NMR spectra of the lycopene isomers were recorded using a JEOL JMN-LA400 FT 400 NMR spectrometer (Tokyo) at 400 MHz (for ^{1}H) and 100 MHz (for ^{13}C). Chemical shifts were recorded as the δ value in ppm using tetramethylsilane as an internal standard. Spectra were obtained in C_6D_6 as well as in $CDCl_3$.

4.3.6. Evaluation of isomerization rate

In order to evaluate the effect of solvent species on isomerization of (all-*E*)-lycopene, the reaction rate constants were calculated. Namely, assuming a first-order reaction, the increment in the concentration of total *Z*-isomers with

isomerization time was fitted to the equation (1) shown below:

$$\ln C = -kt + \ln C_0 \quad (1)$$

where C and C_0 are the concentration and initial concentration of (all-*E*)-lycopene, respectively, k is the reaction rate constant, and t is the reaction time. Only the linear portion of the plot between the natural log of concentration and time was considered. Numerical values are presented as mean ± SD.

4.4. Results and discussion

4.4.1. General profile of the thermal isomerization of (all-*E*)-lycopene

The overall isomerization progress of (all-*E*)-lycopene was estimated as the total amount of *Z*-isomers in various organic solvents over 24 h, and was described as a percentage represented by the ratio of the amount of *Z*-isomers to the total amount of lycopene isomers including the (all-*E*)-form (Figure 1). The isomerization ratios at 4 °C increased gradually in CH_2Cl_2 and $CHCl_3$, reaching 19.7% and 11.4%, respectively, over 24 h (Figure 1A). In CH_2Br_2, the isomerization ratio of the *Z*-isomers exceeded 60% within the first hour, whereas ratio increments were hardly observed in acetone, hexane, benzene, and CCl_4 at this temperature for the period of time tested. Alternatively, at the relatively higher temperature of 50 °C, the isomerization ratios of

the *Z*-isomers increased in all of the organic solvents tested (Figure 1B): CH_2Cl_2, 77.8%; CH_2Br_2, 75.0%; $CHCl_3$, 48.4%; acetone, hexane, benzene, and CCl_4, 34.7–38.1. Thus, promoted *Z*-isomerization of (all-*E*)-lycopene has been first demonstrated in CH_2Br_2 as well as CH_2Cl_2 and $CHCl_3$, whilst some experiments were carried out on astaxanthin [5,6].

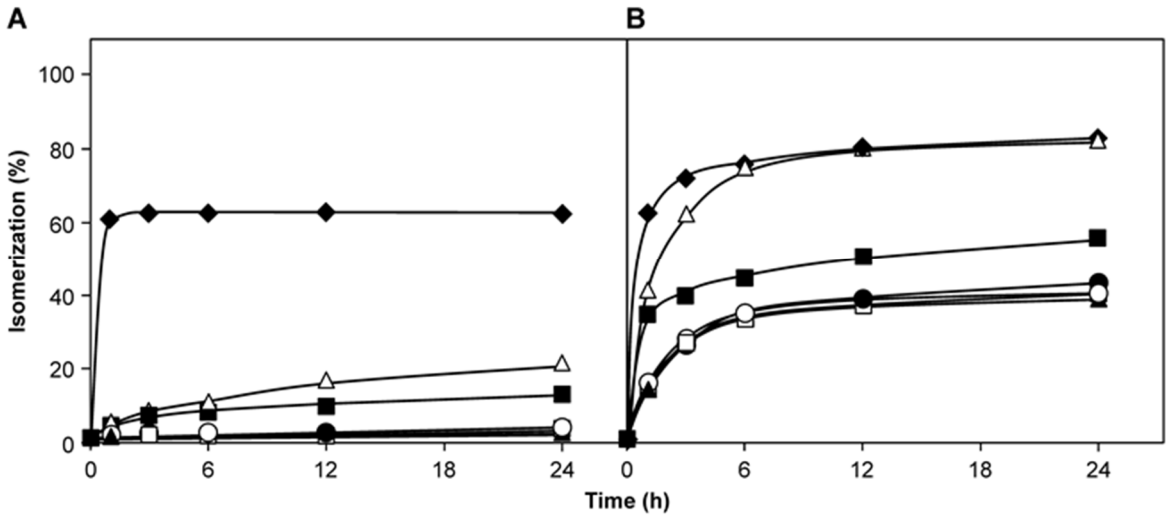

Figure 1. Changes in the content of (*Z*)-lycopene isomers thermally isomerized at (A) 4 °C and (B) 50 °C in various organic solvents: (●) acetone; (○) hexane; (▲) benzene; (△) CH_2Cl_2; (■) $CHCl_3$; (□) CCl_4; (◆) CH_2Br_2. Isomerization was expressed as a percentage of the amount of *Z*-isomers to the total amount of lycopene isomers including (all-*E*)-lycopene.

The thermally isomerized lycopene solutions obtained at 50 °C over 24 h (Figure 1B) were separated on a normal-phase HPLC column. The typical chromatograms of these samples are shown in Figure 2 as well as that of purified (all-*E*)-lycopene (unheated).

The predominant *Z*-isomer emerged in benzene as (13*Z*)-lycopene (Figure 2B), while many kinds of other geometrical isomers, including (5*Z*)-, (9*Z*)-, and (13*Z*)-lycopene were observed in a CH_2Cl_2 solvent system (Figure 2C).

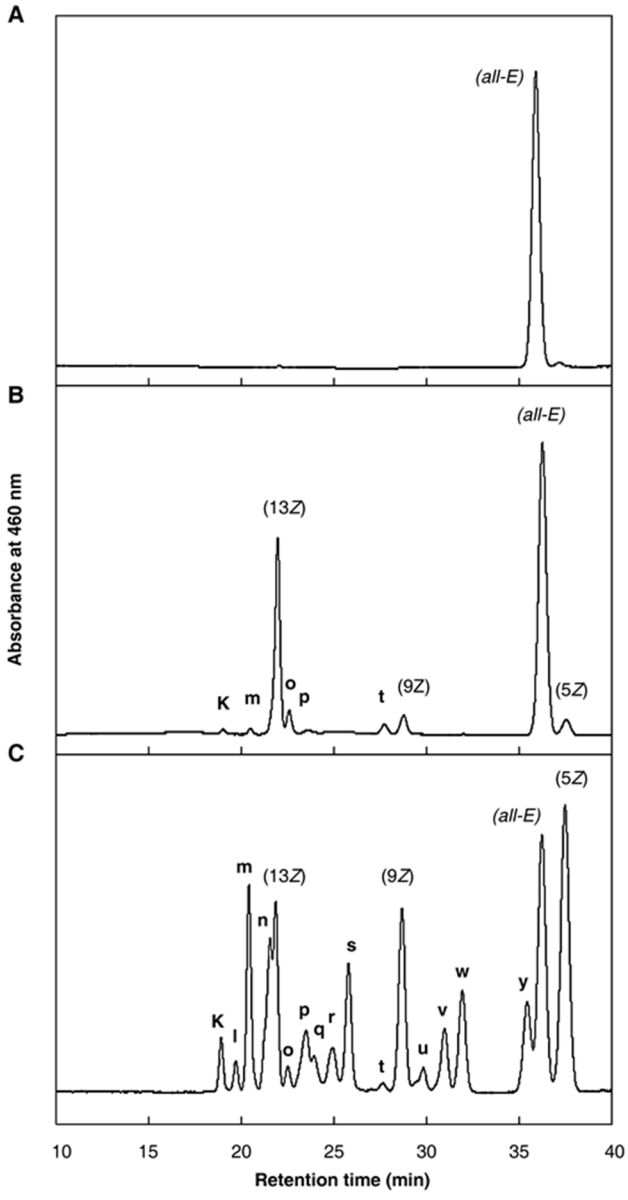

Figure 2. Normal-phase HPLC chromatograms of (A) (all-*E*)-lycopene and thermally generated *Z*-isomers at 50 °C for 24 h in (B) benzene and (C) CH_2Cl_2. Three (mono-*Z*)-lycopene designated in the charts were tentatively identified according to the literature [9–11], and ascertained by ^{1}H and ^{13}C NMR spectroscopic analyses.

This characteristic difference in the isomerization profiles can lead to the selective enrichment of a desirable isomer by taking advantage of the properties of the solvent, as discussed below. The absorption maxima for each peak **k**–**y** in the chromatogram were also measured using a photodiode-array detector (Table 1). Several peaks were subsequently identified as certain geometrical isomers according to the visible spectral data and retention times in HPLC described in the literatures [9−11], as well as the characterizations by NMR spectroscopy carried out in this study. The absorption maxima of the di-*Z*-isomers, (9*Z*,13′*Z*)- and (9*Z*,13*Z*)-lycopene (peaks **k** and **q**, respectively) showed a remarkable hypsochromic shift as compared to that of (all-*E*)-lycopene. On the other hand, those of the di-*Z*-isomers including a peripheral *Z*-configuration gave a relatively lower displacement, such as (5*Z*,9′*Z*)- (peak **s**), (5*Z*,9*Z*)- (peak **w**), and (5*Z*,5′*Z*)-lycopene (peak **y**). The relative intensities of the *Z*-peak are also shown in Table 1 as % D_B/D_{II}, in which larger values were observed for (13*Z*)- and (15*Z*)-lycopene isomers having a *Z*-configuration around the center of the molecule [9−11].

Table 1 Absorption maxima (λ_{max}) and relative intensities of the *Z*-peak (% D_B/D_{II}) for geometrical lycopene isomers separated by a normal-phase chromatographic column

Peak	Lycopene isomer	λ_{max} (nm)	D_B/D_{II} (%)	Peak	Lycopene isomer	λ_{max} (nm)	D_B/D_{II} (%)
k	(9*Z*,13′*Z*)[a]	360, 433, 457, 487	30.4	**s**	(5*Z*,9′*Z*)[a]	361, 438, 464, 495	13.4
l	UZ[b]	361, 432, 457, 487	31.7	**t**	UZ	361, 432, 457, 485	28.3
m	UZ	360, 437, 462, 493	45.4		(9*Z*)[c]	361, 438, 464, 495	13.0
n	UZ	360, 438, 462, 492	51.7	**u**	UZ	356, 433, 456, 487	12.2
	(13*Z*)[c]	361, 437, 463, 494	52.4	**v**	(5*Z*,9*Z*,5′*Z*)[a]	361, 438, 463, 495	12.6
o	(15*Z*)[a]	360, 442, 466, 497	79.0	**w**	(5*Z*,9*Z*)[a]	361, 438, 464, 495	11.8
p	UZ	359, 431, 454, 484	22.5	**y**	(5*Z*,5′*Z*)[a]	443, 470, 501	ND[d]
q	(9*Z*,13*Z*)[a]	361, 433, 456, 488	23.5		(all-*E*)[c]	444, 470, 501	ND
r	UZ	361, 433, 457, 487	16.5		(5*Z*)[c]	444, 470, 501	ND

Values as well as peak designation were obtained from the chromatogram in Fig. 3C with a mobile phase of hexane containing 0.1% DIPEA for lycopene isomers generated during heating in CH_2Cl_2 at 50 °C for 24 h. [a]Tentatively identified according to previous works [9–11] [b]Unidentified *Z*-isomer of lycopene. [c]Identified by NMR measurements: among them, assignments of highly purified (9*Z*)- and (13*Z*)-lycopene isomers are shown in the Tables 2 and 3. [d]Not detected.

4.4.2. Purification and characterization of (9*Z*)- and (13*Z*)-lycopene

In order to obtain accurate estimations of the concentrations of (9*Z*)- and (13*Z*)-lycopene, these isomers were purified from the *Z*-isomer mixture obtained by heating in benzene at 75 °C. From a starting material weight of 2,000 mg of (all-*E*)-lycopene, 90 mg of the 9*Z*-isomer (reversed-phase HPLC, 98.8% purity; normal-phase HPLC, ≥ 99.9%) and 18.4 mg of the 13*Z*-isomer (reversed-phase HPLC, 97.0%; normal-phase HPLC, ≥ 99.9%) were obtained. The relatively lower purities of the compounds yielded by reversed-phase HPLC was caused by the presence of (all-*E*)-lycopene which would be attributed to the isomerization to the all-*E*-form during the chromatographic procedure; the all-*E*-isomer could be easily separated from these *Z*-isomers by the aforementioned purification steps.

The structures of purified (9*Z*)- and (13*Z*)-lycopene were ascertained by ^{1}H and ^{13}C NMR spectroscopic analyses (Figure 3), and these assignments are listed along with those of the all-*E*-form (Table 2, 3). NMR measurements were performed in two solvents, $CDCl_3$ and C_6D_6, in order to acquire characteristic NMR signals as observed in the previous analysis of (all-*E*)-lycopene [8]. The shift differences ($\Delta\delta$) against the values of (all-*E*)-lycopene were larger around the *Z*-double-bond structures of the lycopene isomers in the measurements of both nuclei and both solvents. Principal

assignments for the (9*Z*)- and (13*Z*)-lycopene were in good agreement with those of the values previously reported in $CDCl_3$, including synthetic ones [9], and more sophisticated identifications were achieved for the coupling constants in this work. The spin signals attributed to AA′BB′-type systems were more distinctively observed in C_6D_6 for H–C(14), H–C(14′), H–C(15), and H–C(15′) of (9*Z*)-lycopene, while simple doublet of doublet (dd) patterns were obtained for the protons of (13*Z*)-lycopene as a result of the apparent loss of molecular symmetry.

The absorption maxima and molar extinction coefficients of (9*Z*)- and (13*Z*)-lycopene were determined in hexane to be 1.64×10^5 $M^{-1} \cdot cm^{-1}$ at 465 nm and 137×10^3 $M^{-1} \cdot cm^{-1}$ at 464 nm, respectively (Figure 4 and Table 4). The hypsochromic shift accompanying the hypochromic effects of the *Z*-isomers has made it difficult for researchers to estimate the concentrations of isomerized lycopene in solution from chromatographic measurements. The molar extinction coefficients of (9*Z*)-, (13*Z*)-, and (all-*E*)-lycopene, predominant isomers formed during the heating process, were also measured at 460 nm in the same solvent. These values, determined as 1.28×10^5, 1.47×10^5 and 1.18×10^5 $M^{-1} \cdot cm^{-1}$, respectively, could facilitate the compensation of isomer concentrations in the chromatographic analyses, and aid in the accurate estimation of the isomerization profile of lycopene during the thermal process. In addition, the *Z*-peak

ratios of D_B/D_{II} were calculated from the values in Table 4 as 14.0% for the 9*Z*-form and 56.2% for the 13*Z*-form, which are compatible with the values presented in Table 1 and other literature values [10,12].

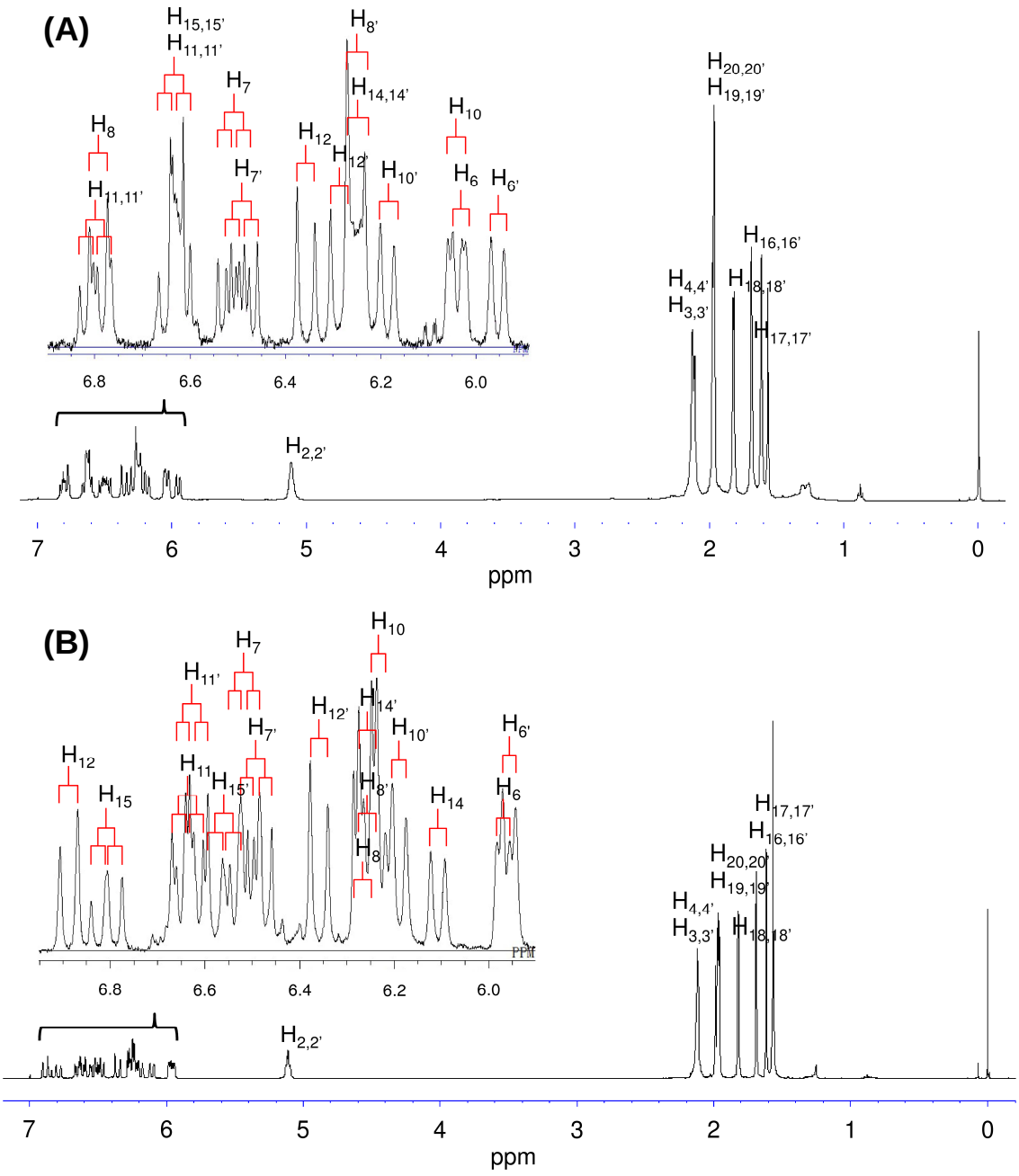

Figure 3. ^{1}H NMR spectra of the purified (A) (9*Z*)- and (B) (13*Z*)-lycopene. (400 MHz, $CDCl_3$).

Table 2 ^{1}H NMR assignment of (9*Z*)- and (13*Z*)-lycopene isomers from tomato

	δ in ppm in $CDCl_3$ [$\Delta\delta$][a]			δ in ppm in C_6D_6 [$\Delta\delta$][a]		
	(all-*E*)[b]	(9*Z*)	(13*Z*)	(all-*E*)[b]	(9*Z*)	(13*Z*)
H–C(2) H–C(2′)	5.11 (m)	5.11 (m)	5.11 (m)	5.23 (m)	5.23 (m)	5.23 (m)
2H–C(3) 2H–C(3′)	2.11 (m)	2.13 (m)	2.12 (m)	2.18 (m)	2.17 (m)	2.17 (m)
2H–C(4) 2H–C(4′)	2.11 (m)	2.13 (m)	2.12 (m)	2.18 (m)	2.17 (m)	2.17 (m)
H–C(6)	5.95	6.04 (d, *J* = 10.6) [0.09]	5.97 (d, *J* = 10.8)	6.16 (d, *J* = 11.0)	6.16 (d, *J* = 10.6)	6.16 (d, *J* = 11.0)
H–C(6′)	(d, *J* = 11.0)	5.95 (d, *J* = 10.8)	5.95 (d, *J* = 10.8)		6.16 (d, *J* = 10.9)	6.16 (d, *J* = 10.7)
H–C(7)	6.49	6.52 (dd, *J* = 10.6, 15.1) [0.03]	6.52 (dd, *J* = 10.8, 15.3) [0.03]	6.67	6.69 (dd, *J* = 10.6, 15.2)	6.68 (dd, *J* = 11.0, 14.9)
H–C(7′)	(dd, *J* = 11.0, 15.0)	6.48 (dd, *J* = 10.8, 15.0)	6.49 (dd, *J* = 10.8, 15.1)	(dd, *J* = 11.0, 15.1)	6.67 (dd, *J* = 10.9, 15.1)	6.67 (dd, *J* = 10.7, 15.2)
H–C(8)	6.25 (d, *J* = 15.0)	6.80 (d, *J* = 15.1) [0.55]	6.26 (d, *J* = 15.3)	6.44 (d, *J* = 15.1)	7.09 (d, *J* = 15.2) [0.65]	6.46 (d, *J* = 14.9)
H–C(8′)		6.25 (d, *J* = 15.0)	6.25 (d, *J* = 15.1)		6.44 (d, *J* = 15.1)	6.44 (d, *J* = 15.2)
H–C(10)	6.18 (d, *J* = 11.4)	6.04 (d, *J* = 11.0) [–0.14]	6.23 (d, *J* = 11.5) [0.05]	6.36 (d, *J* = 11.6)	6.18 (d, *J* = 11.5) [–0.18]	6.38 (d, *J* = 11.6)
H–C(10′)		6.19 (d, *J* = 11.5)	6.19 (d, *J* = 11.3)		6.35 (d, *J* = 11.2)	6.35 (d, *J* = 11.5)
H–C(11)	6.64	6.80 (dd, *J* = 11.0, 14.7) [0.16]	6.64 (dd, *J* = 11.5, 14.8)	6.77	7.03 (dd, *J* = 11.5, 15.0) [0.26]	6.77 (dd, *J* = 11.6, 14.9)
H–C(11′)	(dd, *J* = 11.4, 14.9)	6.63 (dd, *J* = 11.5, 14.8)	6.63 (dd, *J* = 11.3, 14.6)	(dd, *J* = 11.6, 15.0)	6.77 (dd, *J* = 11.2, 14.9)	6.77 (dd, *J* = 11.5, 14.8)
H–C(12)	6.35 (d, *J* = 14.9)	6.28 (d, *J* = 14.7) [–0.07]	6.88 (d, *J* = 14.8) [0.53]	6.49 (d, *J* = 15.0)	6.44 (d, *J* = 15.0) [–0.05]	7.06 (d, *J* = 14.9) [0.57]
H–C(12′)		6.36 (d, *J* = 14.8)	6.36 (d, *J* = 14.6)		6.48 (d, *J* = 14.9)	6.50 (d, *J* = 14.8)
H–C(14)	6.24 (m)	6.25 (m)	6.11 (d, *J* = 11.7) [–0.13]	6.34 (AA′of AA′BB′ system)	6.34 (AA′of AA′BB′ system)	6.14 (d, *J* = 12.0) [–0.20]
H–C(14′)			6.25 (d, *J* = 11.6)			6.35 (d, *J* = 12.1)
H–C(15)	6.62 (m)	6.63 (m)	6.81 (dd, *J* = 11.7, 13.8) [0.19]	6.70 (BB′of AA′BB′ system)	6.69 (BB′of AA′BB′ system)	6.93 (dd, *J* = 12.0, 13.9) [0.23]
H–C(15′)			6.56 (dd, *J* = 11.6, 13.8) [–0.06]			6.62 (dd, *J* = 12.1, 13.9) [–0.08]
3H–C(16) 3H–C(16′)	1.687 (s)	1.690 (s)	1.691 (s)	1.674 (s)	1.665 (s) 1.670 (s)	1.669 (s)
3H–C(17) 3H–C(17′)	1.614 (s)	1.621 (s) 1.616 (s)	1.618 (s)	1.568 (s)	1.558 (s) 1.565 (s)	1.563 (s)
3H–C(18) 3H–C(18′)	1.818 (s)	1.828 (s) 1.818 (s)	1.822 (s)	1.749 (s)	1.724 (s) [–0.03] 1.746 (s)	1.745 (s)
3H–C(19) 3H–C(19′)	1.968 (s)	1.981 (s) 1.969 (s)	1.960 (s) 1.967 (s)	1.925 (s)	1.971 (s) [0.05] 1.923 (s)	1.919 (s) 1.924 (s)
3H–C(20) 3H–C(20′)	1.968 (s)	1.969 (s)	1.974 (s) 1.989 (s)	1.876 (s)	1.848 (s) [–0.03] 1.871 (s)	1.937 (s) [0.06] 1.876 (s)

Recorded at 400 MHz; s = singlet, d = doublet, dd = doublet of doublets, m = multiplet. Coupling constants are given in Hz. [a]Shift differences: $\Delta\delta = \delta\,(Z) - \delta\,(E)$ for $|\Delta\delta| > 0.02$ ppm. [b]Obtained from the reference [7].

Table 3 ^{13}C NMR assignment of (9*Z*)- and (13*Z*)-lycopene isomers from tomato

	δ in ppm in $CDCl_3$ [$\Delta\delta$][a]			δ in ppm in C_6D_6 [$\Delta\delta$][a]		
	(all-*E*)[b]	(9*Z*)	(13*Z*)	(all-*E*)[b]	(9*Z*)	(13*Z*)
C(1)	131.72	131.81	131.77	131.58	131.68	131.63
C(1′)		131.76	131.75		131.60	131.60
C(2)	123.96	123.88	123.93	124.50	124.50	124.53
C(2′)		123.94	123.94			124.50
C(3)	26.70	26.68	26.68	27.10	27.13	27.14
C(3′)					27.10	
C(4)	40.23	40.23	40.23	40.62	40.63	40.65
C(4′)		40.27				
C(5)	139.47	140.44 [0.97]	139.75	138.95	139.98 [1.03]	139.25
C(5′)		139.50	139.45		139.96 [1.01]	138.92
C(6)	125.74	125.78	125.67	126.77	126.80	126.80
C(6′)		125.71	125.71		126.78	126.74
C(7)	124.79	126.31 [1.52]	125.00	125.31	126.76 [1.45]	125.54
C(7′)		124.78	124.73		125.29	125.26
C(8)	135.40	127.23 [−8.17]	135.30	136.17	*ov*	136.04
C(8′)		135.41	135.41		136.20	136.21
C(9)	136.15	134.62 [−1.53]	136.36	136.37	134.76 [−1.61]	135.06 [−1.31]
C(9′)		136.13	136.06		136.35	136.29
C(10)	131.55	129.95 [−1.60]	131.48	132.39	130.90 [−1.49]	132.26
C(10′)		131.55	131.54		132.41	132.40
C(11)	125.15	123.91 [−1.24]	126.42 [1.27]	125.66	124.43 [−1.23]	126.89 [1.23]
C(11′)		125.10	125.09		125.62	125.62
C(12)	137.35	136.65 [−0.70]	129.14 [−8.21]	138.00	137.40 [−0.60]	129.89 [−8.11]
C(12′)		137.37	137.38		138.04	138.06
C(13)	136.56	136.46	134.90 [−1.66]	136.83	136.72	136.66
C(13′)		136.49	136.87		136.80	137.11
C(14)	132.64	132.44	130.93 [−1.71]	133.39	133.22	131.79 [−1.60]
C(14′)		132.64	132.48		133.40	133.21
C(15)	130.07	129.96	128.77 [−1.30]	130.70	130.59	126.52 [−4.18]
C(15′)		130.07	129.23 [−0.84]		130.74	129.88 [−0.82]
C(16)	25.68	25.72	25.70	25.84	25.85	25.86
C(16′)		25.71				
C(17)	17.70	17.71	17.71	17.73	17.75	17.77
C(17′)					17.76	
C(18)	16.99	16.96	16.97	16.90	16.92	16.92
C(18′)		17.00	16.95			
C(19)	12.90	20.83 [7.93]	12.94	12.98	21.00 [8.02]	13.02
C(19′)		12.91	12.89		13.00	12.99
C(20)	12.79	12.89	20.71 [7.92]	12.86	12.92	20.83 [7.97]
C(20′)		12.79	12.77		12.97	12.86

Recorded at 100 MHz; *ov* = overlapped. [a]Shift differences: $\Delta\delta = \delta(Z) - \delta(E)$ for $|\Delta\delta| > 0.5$ ppm. [b]Obtained from the reference [7].

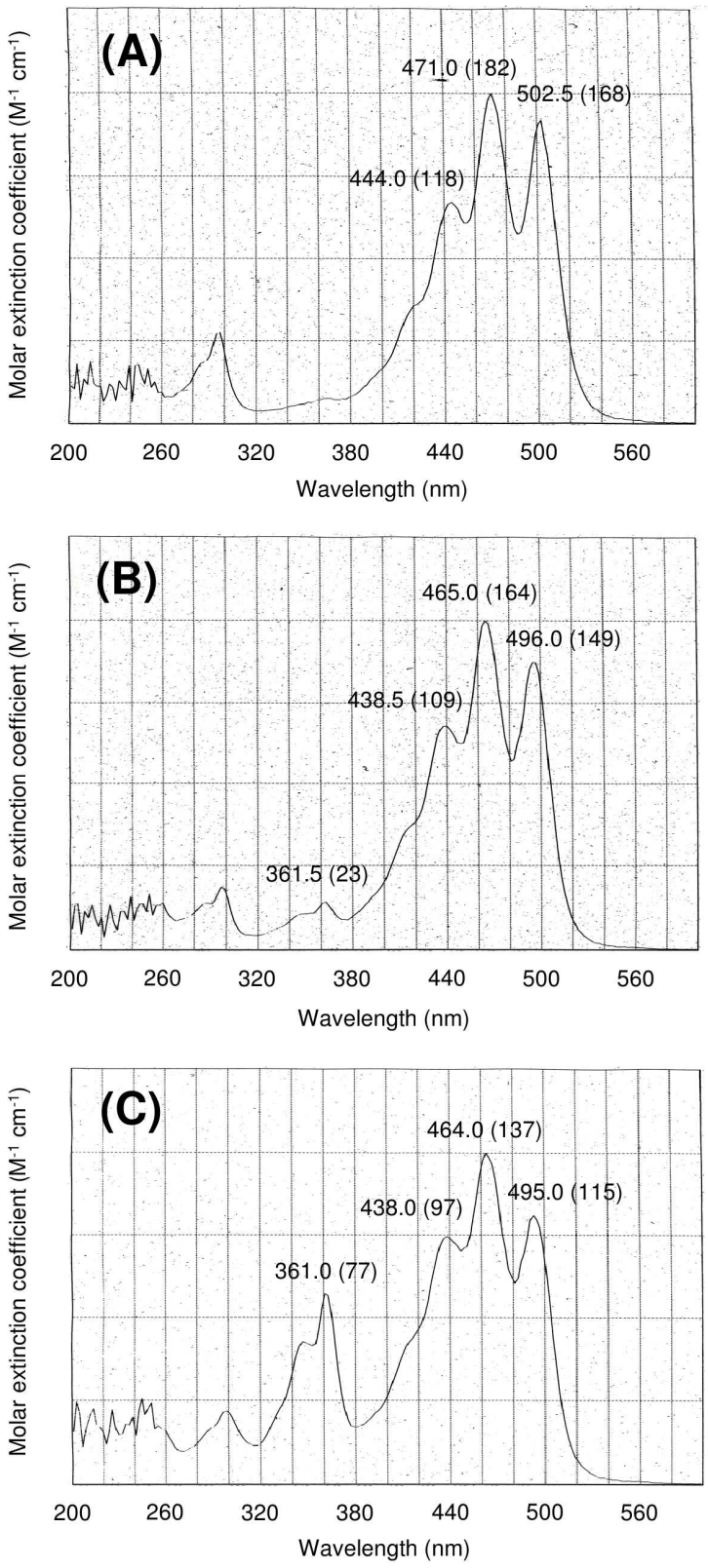

Figure 4. Ultraviolet (UV) spectra of the purified (A) (all-*E*)-, (B) (9*Z*)- and (C) (13*Z*)-lycopene in hexane.

Table 4 Absorption maxima and minima and molar extinction coefficients of lycopene isomers purified from thermally processed tomato paste

Isomer	λ_B[a]	λ_1	λ_{min}	λ_2	λ_{min}	λ_3
(all-*E*)[b]	ND[c]	444.0	454.5	471.0	488.0	502.5
		(118)	(102)	(182)	(95)	(168)
(9*Z*)	361.5	438.5	449.0	465.0	482.0	496.0
	(23)	(109)	(95)	(164)	(87)	(149)
(13*Z*)	361.0	438.0	448.5	464.0	481.0	495.0
	(77)	(97)	(84)	(137)	(73)	(115)

Solvent, hexane; λ in nm; values in parentheses, $\varepsilon \times 10^{-3}$. [a]Absorption maximum for *Z*-peak. [b]Modified from the literature [7]. [c]Not detected.

4.4.3. Thermal isomerization of lycopene and relevant solvent effects

Isomerization of (all-*E*)-lycopene to the individual *Z*-isomers was investigated in several organic solvents at 4 °C and 50 °C (Figure 5), in which (9*Z*)- and (13*Z*)-lycopene were estimated in a manner compensating for the different molar extinction coefficients described above. In benzene at 4 °C, (all-*E*)-lycopene was hardly isomerized to the *Z*-forms (Figure 5A), and similar observations were made in acetone, hexane, and CCl_4 (data not shown). In CH_2Cl_2 and $CHCl_3$ at 4 °C, the content of (all-*E*)-lycopene gradually decreased with the concomitant emergence of the *Z*-isomers (Figure 5B,C). After 24 h incubation, the ratios of (5*Z*)- and (13*Z*)-lycopene reached 10.3% in CH_2Cl_2 and 8.8% in $CHCl_3$, respectively, as the predominant isomer. A rapid decrease in the all-*E*-content was observed in CH_2Br_2, followed by an increment of (5*Z*)-lycopene to 27.7% during the first several hours (Figure 5D). The degree of the solvent effect on isomerization was thus demonstrated (Figure 5B–D), and the rate constants for isomerization to *Z*-isomers were calculated as the first-order reaction of (all-*E*)-lycopene elimination as follows: $(1.52 \pm 0.61) \times 10^{-5}$ s^{-1} in CH_2Cl_2; $(8.0 \pm 0.5) \times 10^{-6}$ s^{-1} in $CHCl_3$; $> 1.0 \times 10{-}^{3}$ s^{-1} in CH_2Br_2. These results indicated that (5*Z*)-lycopene was likely to be a predominant product in the solvents having a relatively strong solvent effect (Figure 5B,D), while the (13*Z*)-isomer was prominent in solvents

with a weak effect (Figure 5C).

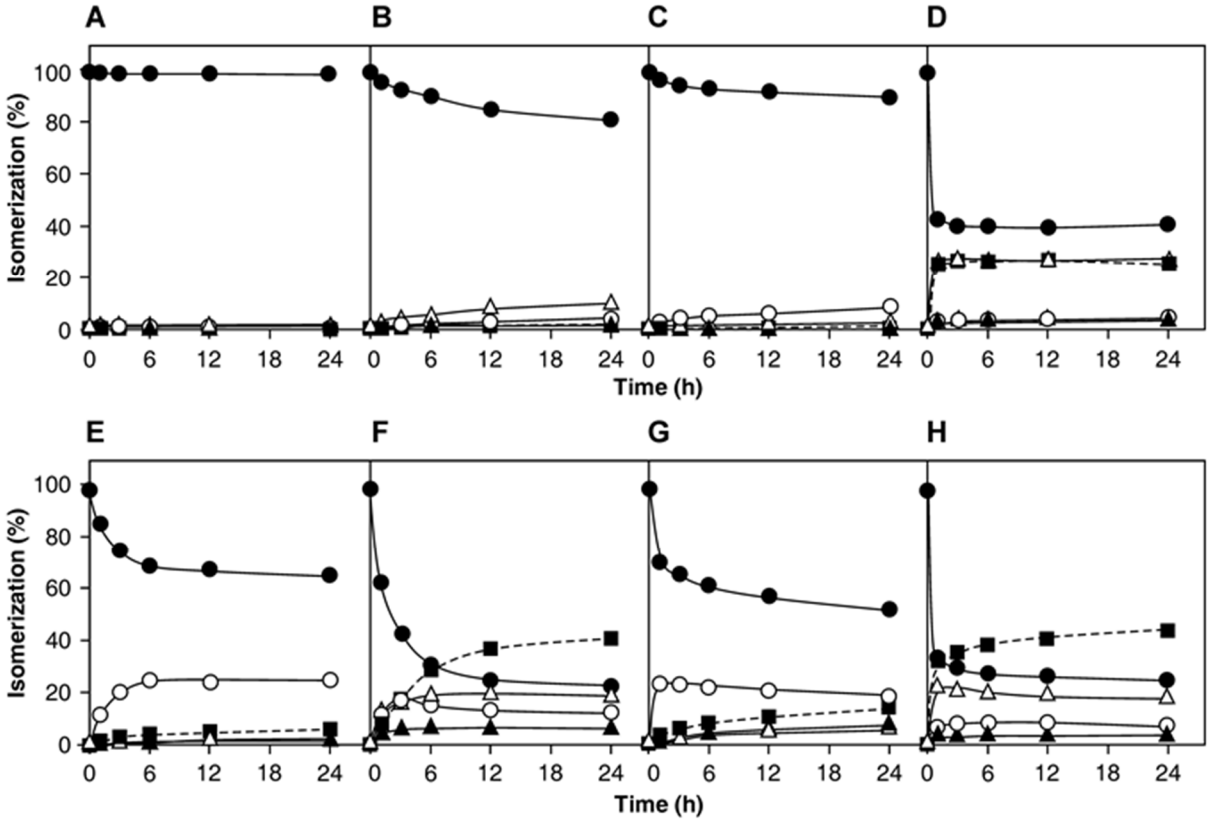

Figure 5. Thermal isomerization of (all-*E*)-lycopene to individual *Z*-isomers (A to D) at 4 °C and (E to H) at 50 °C in (A, E) benzene, (B, F) CH_2Cl_2, (C, G) $CHCl_3$ and (D, H) CH_2Br_2. Changes in the isomer content are presented with regard to the total amount of lycopene isomers resulting at each point of sampling: (●) (all-*E*)-lycopene; (○) (13*Z*)-lycopene; (▲) (9*Z*)-lycopene; (△) (5*Z*)-lycopene; (■) total amount of the other *Z*-isomers.

At the relatively higher temperature of 50 °C (Figure 5E–H), the isomerization ratios of the *Z*-isomers were accelerated in the all the organic solvents above in comparison with those at 4 °C. The rate constants for isomerization to the *Z*-isomers at

50 °C were calculated to be $(3.4 \pm 0.4) \times 10^{-5}$ s^{-1} in benzene, $(1.41 \pm 0.28) \times 10^{-4}$ s^{-1} in CH_2Cl_2, $(8.7 \pm 0.3) \times 10^{-5}$ s^{-1} in $CHCl_3$, and $> 1.0 \times 10^{-3}$ s^{-1} in CH_2Br_2. The rate constants in the other solvents examined were approximately equal to that of benzene: $(3.3 \pm 0.8) \times 10^{-5}$ s^{-1} in acetone; $(3.7 \pm 0.3) \times 10^{-5}$ s^{-1} in hexane; $(3.3 \pm 0.1) \times 10^{-5}$ s^{-1} in CCl_4 (data not shown). Similar tendencies were also obtained at this temperature, namely, the rate constants for isomerization were larger in solvents with a strong solvent effect, generating (5*Z*)-lycopene as a predominant isomer; in contrast, (13*Z*)-lycopene was predominant in solvents with a weaker effect. The isomerization profiles to the individual isomers in acetone, hexane, and CCl_4 were also in good accordance with that of benzene. In CH_2Cl_2 and $CHCl_3$, (13*Z*)-lycopene emerged as the predominant isomer and gradually decreased after reaching its maximum of ca. 20% after the initial 2–3 h, at which time the other *Z*-isomers started to increase. These observations were described in previous studies [8,13]. According to [14], the potential energies of all-*E*- and mono-*Z*-isomers are in the order of (all-*E*)- > (5*Z*)- > (9*Z*)- > (13*Z*)-lycopene, and the magnitude of the activation energies of the isomerization from (all-*E*)-lycopene to (mono-Z)-lycopene are (5*Z*)- > (9*Z*)- > (13*Z*)-lycopene. These computational results are well accounted for in our experimental findings. Namely, (13*Z*)-lycopene was kinetically favored, while the 5*Z*-isomer was thermodynamically preferred. In CH_2Cl_2

and CH_2Br_2, a strong solvent effect should lower the isomerization activation energies to the 5*Z*-isomer. Once the thermodynamically stable *Z*-isomer of lycopene was produced, (di-*Z*)- and (tri-*Z*)-lycopene isomers having *Z*-configuration at C(13 or 13′) and C(9 or 9′) could easily be generated because of the lower activation energies of subsequent isomerization reactions.

The mechanism of the conversion of (all-*E*)-lycopene to *Z*-isomers, as depicted below, could be explained in a similar manner to that of *Z*-isomerization of (all-*E*)-*β*-carotene by Fe-MCM-41 or titanium tetrachloride [15–18]:

$$(\text{Lycopene})_E - e^- \rightleftharpoons (\text{Lycopene}^{\bullet+})_E \quad (2)$$

$$(\text{Lycopene}^{\bullet+})_E \rightleftharpoons (\text{Lycopene}^{\bullet+})_Z \quad (3)$$

$$(\text{Lycopene}^{\bullet+})_Z + e^- \rightleftharpoons (\text{Lycopene})_Z \quad (4)$$

The carbon atom of an alkyl halide is partially positive because of the difference in electronegativity between the carbon and halogen atoms, leaving the carbon atom susceptible to attack by a chemical species with high electron density. According to the Lewis definition, CH_2Br_2, $CHCl_3$, and CH_2Cl_2 are defined as acids because they are electron acceptors, while lycopene is a base owing to its electron-rich conjugated double-bond structure. Therefore, it is quite likely that the carbon atoms of the alkyl halides are associated with the double-bond moieties of (all-*E*)-lycopene.

When (all-*E*)-lycopene was dissolved in these alkyl halides, isomerization progressed in the following order: CH_2Br_2 > CH_2Cl_2 > $CHCl_3$. The differences in the strengths of the solvent effect among these solvents can be explained by the hard and soft acids and bases (HSAB) theory [19–21]. According to the HSAB theory, a soft Lewis acid/soft Lewis base pair or a hard Lewis acid/hard Lewis base pair will react easily because of the formation of strong bonds. The strength of the charge on the carbon atoms can be arranged in ascending order of $CHCl_3$, CH_2Cl_2 and CH_2Br_2 on the basis of electronegativity, and the softness of the acid is indicated by the reversed order. Lycopene can be classified as a soft base because it has a large polarizability owing to the eleven conjugated double bonds in its structure; isomerization occurred in these solvents in that order preferentially. On the other hand, the apparently contradictory result at 4 °C in CCl_4 (Figure 1A) makes the effect worthy of further study.

So far, $CHCl_3$ and CH_2Cl_2 have been commonly used in various applications with lycopene, such as an extraction solvent [22,23], mobile phase in HPLC analysis [24,25], and as an entrainer in supercritical extraction [26]. It would be more appropriate to pay attention to lycopene processing with these solvents, instead of estimating the apparent quantity of the *Z*-isomers.

4.5. Reference

[1] Aman, R., Schieber, A., Carle, R. Effects of heating and illumination on *trans–cis* isomerization and degradation of *β*-carotene and lutein in isolated spinach chloroplasts. *J. Agric. Food Chem.* **2005**, *53*, 9512–9518.

[2] Knockaert, G., Pulissery, S. K., Lemmens, L., Van Buggenhout, S., Hendrickx, M., Van Loey, A. Carrot *β*-carotene degradation and isomerization kinetics during thermal processing in the presence of oil. *J. Agric. Food Chem.* **2012**, *60*, 10312–10319.

[3] Subagio, A., Morita, N., Sawada, S. Thermal isomerization of (all-*trans*)-lutein in a benzene solution. *Biosci. Biotechnol. Biochem.* **1998**, *62*, 2453–2456.

[4] Updike, A. A., Schwartz, S. J. Thermal processing of vegetables increases cis isomers of lutein and zeaxanthin. *J. Agric. Food Chem.* **2003**, *51*, 6184–6190.

[5] Yuan, J.-P., Chen, F. Isomerization of *trans*-astaxanthin to *cis*-isomers in organic solvents. *J. Agric. Food Chem.* **1999**, *47*, 3656–3660.

[6] Yuan, J.-P., Chen, F. Kinetics for the reversible isomerization reaction of *trans*-astaxanthin. *Food Chem.* **2001**, *73*, 131–137.

[7] Takehara, M., Nishimura, M., Kuwa, T., Inoue, Y., Kitamura, C., Kumagai, T., Honda, M. Characterization and thermal isomerization of (*all-E*)-lycopene. *J. Agric. Food Chem.* **2014**, *62*, 264–269.

[8] Schierle, J., Bretzel, W., Bühler, I., Faccin, N., Hess, D., Steiner, K., Schüep, W. Content and isomeric ratio of lycopene in food and human blood plasma. *Food Chem.* **1997**, *59*, 459–465.

[9] Hengartner, U., Bernhard, K., Meyer, K., Englert, G., Glinz, E. Synthesis, isolation, and NMR-spectroscopic characterization of fourteen (*Z*)-isomers of lycopene and of some acetylenic didehydro- and tetradehydrolycopenes. *Helv. Chim. Acta* **1992**, *75*, 1848–1865.

[10] Fröhlich, K., Conrad, J., Schmid, A., Breithaupt, D. E., Böhm, V. Isolation and structural elucidation of different geometrical isomers of lycopene. *Int. J. vitam. Nutr. Res.* **2007**, *77*, 369–375.

[11] Glaser, T., & Albert, K. Hyphenation of modern extraction techniques to LC–NMR for the analysis of geometrical carotenoid isomers in functional food and biological tissues. In K. Albert (Ed.), *On-line LC–NMR and related techniques*, New York: John Wiley & Sons, Ltd. **2002**; pp 129–140.

[12] Lee, M. T., Chen, B. H. Separation of lycopene and its *cis* isomers by liquid chromatography. *Chromatographia* **2001**, *54*, 613–617.

[13] Lambelet, P., Richelle, M., Bortlik, K., Franceschi, F., Giori, A. M. Improving the stability of lycopene *Z*-isomers in isomerised tomato extracts. *Food chem.* **2009**, *112*,

156–161.

[14] Guo, W.-H., Tu, C.-Y., Hu, C.-H. *Cis–trans* isomerizations of *β*-carotene and lycopene: a theoretical study. *J. Phys. Chem. B* **2008**, *112*, 12158–12167.

[15] Gao, Y., Kispert, L. D. Reaction of carotenoids and ferric chloride: equilibria, isomerization, and products. *J. Phys. Chem. B* **2004**, *107*, 5333–5338.

[16] Gao, Y., Kispert, L. D., Konovalova, T. A., Lawrence, J. N. Isomerization of carotenoids in the presence of MCM-41 molecular sieves: EPR and HPLC studies. *J. Phys. Chem. B* **2004**, *108*, 9456–9462.

[17] He, Z., Gao, G., Hand, E. S., Kispert, L. D., Strand, A., Liaaen-Jensen, S. Iodine-catalyzed *R*/*S* isomerization of allenic carotenoids. *J. Phys. Chem. A* **2002**, *106*, 2520–2525.

[18] Rajendran, V., Chen, B. H. Isomerization of *β*-carotene by titanium tetrachloride catalyst. *J. Chem. Sci.* **2007**, *119*, 253–258.

[19] Pearson, R. G. Hard and soft acids and bases. *J Am. Chem. Soc.* **1963**, *85*, 3533–3539.

[20] Pearson, R. G. Hard and soft acids and bases, HSAB, part I: fundamental principles. *J. Chem. Edu.* **1968**, *45*, 581–587.

[21] Pearson, R. G. Hard and soft acids and bases, HSAB, part II: underlying theories.

J. Chem. Edu. **1968**, *45*, 643–648.

[22] Tiziani, S., Schwartz, S. J., Vodovotz, Y. Profiling of carotenoids in tomato juice by one- and two-dimensional NMR. *J. Agric. Food Chem.* **2006**, *54*, 6094–6100.

[23] Topal, U., Sasaki, M., Goto, M., Hayakawa, K. Extraction of lycopene from tomato skin with supercritical carbon dioxide: effect of operating conditions and solubility analysis. *J. Agric. Food Chem.* **2006**, *54*, 5604–5610.

[24] Broich, C. R., Gerber, L. E., Erdman, J. W., Jr. Determination of lycopene, α- and β-carotene and retinyl esters in human serum by reversed-phase high performance liquid chromatography. *Lipids* **1983**, *18*, 253–258.

[25] Thurnham, D. I., Smith, E., Flora, P. S. Concurrent liquid-chromatographic assay of retinol, α-tocopherol, β-carotene, α-carotene, lycopene, and β-cryptoxanthin in plasma, with tocopherol acetate as internal standard. *Clin. Chem.***1988**, *34*, 377–381.

[26] Cadoni, E., De Giorgi, M. R., Medda, E., Poma, G. Supercritical CO_2 extraction of lycopene and β-carotene from ripe tomatoes. *Dyes Pig.* **1999**, *44*, 27–32.

Chapter 5

Photosensitized E/Z isomerization of (all-E)-lycopene aiming at practical applications

5.1. Table of contents

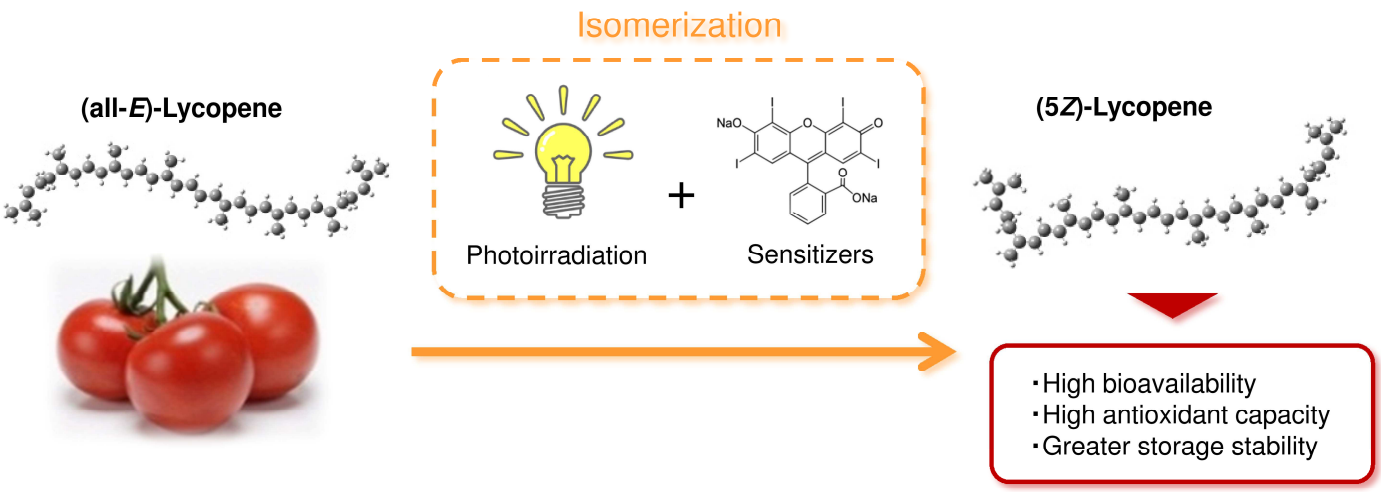

5.2. Introduction

To isomerize (all-*E*)-carotenoids to *Z*-isomers, heat treatment has been the typical method used so far [1−4]. There are some reports on the photosensitized *E*/*Z* isomerization of carotenoids, an alternative method to thermal processing, which has been confined to (all-*E*)-*β*-carotene [5,6]. However, it is not clear that the reaction also occurs about lycopene. Here, we report on the first instance of photoisomerization of (all-*E*)-lycopene using various photosensitizers, including edible ones, aiming at practical applications.

5.3. Materials and methods

5.3.1. Chemicals

Analytical grade acetone, ethyl acetate and MTBE were obtained from Nakaraitesuku Co., Ltd. (Kyoto, Japan), and HPLC-grade methanol was obtained Sigma-Aldrich Co. (St. Louis, MO, USA). Hexane was obtained from a solvent dispensing system supplied by Glass Contour (Nikko Hansen & Co., Ltd., Osaka, Japan) under a nitrogen atmosphere. MB (Figure 1A) was purchased from Nacalai Tesque, Inc. (Kyoto, Japan), and chlorophyll *a*, erythrosine, and RB (Figure 1B–D) were purchased from Wako Pure Chemical Industries, Ltd. (Osaka).

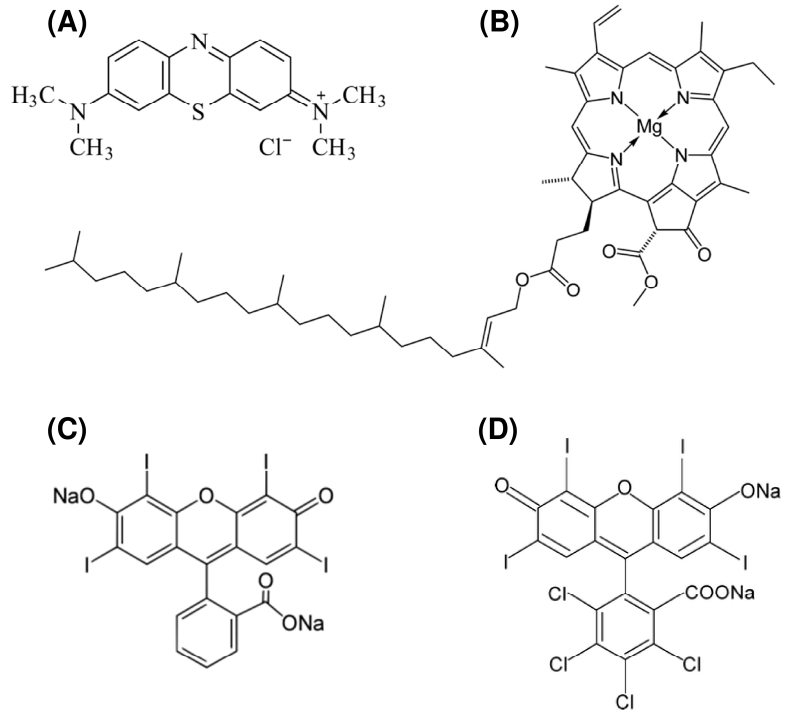

Figure 1. Chemical structures of the photosensitizers used in this study: (A) methylene blue; (B) chlorophyll *a*; (C) erythrosine; (D) rose bengal.

5.3.2. Preparation of (all-*E*)-lycopene

(all-*E*)-Lycopene was obtained from tomato paste (Kagome Co., Ltd., Tokyo, Japan; lycopene content, 8–12 g/kg) as described in previous reports [3,4]: 360 mg of fine red crystalline powder from 70.4 g of tomato material; reversed-phase HPLC, ≥ 99.1% purity.

5.3.3. Photosensitized isomerization of (all-*E*)-lycopene

To the (all-*E*)-lycopene solution in acetone (2×10^{-5} mol/L), MB, chlorophyll *a*, erythrosine or RB were added at the same molar ratio as lycopene. After nitrogen gas was bubbled through the solutions, samples were irradiated by xenon lamp (XB-50101AA, Ushio Inc., Tokyo) equipped with optical filters corresponding to the absorption wavelength of the individual sensitizers: MB and chlorophyll *a*, irradiation range ≥ 600 nm (LV0610 optical filter, Asahi Spectra Co., Ltd., Tokyo); erythrosine and RB, 480 to 600 nm (GIF filter, Nikon Corporation, Tokyo). The photosensitization reaction was conducted at 32 °C for 60 min in a 10 × 10 mm glass container with a lid. The reaction mixtures were sampled and the contents of lycopene isomers were analyzed by reversed-phase HPLC based on the peak areas.

The time-dependent photoisomerization behavior in acetone, ethyl acetate, and

hexane was also investigated under the same conditions as described above using erythrosine and RB, both of which are legitimate, stable and sufficiently inexpensive to be applicable for practical use.

5.3.4. HPLC analysis

Z-Isomers of lycopene were separated with a C_{30} carotenoid column (250 × 4.6 mm inner diameter, 5 μm particles, YMC, Kyoto) using two mobile phases consisting of (A) methanol/ MTBE/H_2O (75:15:10, v/v/v) and (B) methanol/MTBE/H_2O (7:90:3, v/v/v). The gradient profile was as follows: 0–3 min, 0–27% B linear; 3–15 min, 27–55% B; 15–25 min, 55–65% B; 25–35 min, 65–85% B; 35–40 min, 85–95% B; 40–48min, 95–100% B. Flow rate was 1.0 mL/min and column temperature was maintained at 25 °C. The quantification of *Z*-isomers of lycopene was performed by peak area integration at 470 nm using a UV–vis detector (JASCO Co., Tokyo).[4] (13*Z*)-, (9*Z*)-, (all-*E*)-, and (5*Z*)-lycopene were identified by peaks with the retention times of 33.8, 37.9, 42.4, and 42.9 min, respectively, with this system.

5.4. Results and discussion

5.4.1. Photoisomerization with various sensitizers

The photoisomerization of (all-*E*)-lycopene to the corresponding *Z*-forms was performed in acetone in the presence of four kinds of sensitizers using filtered light. After irradiation with 480–600-nm light for 60 min, the concentrations of undecomposed lycopene remaining in solution were determined to be 1.5×10^{-5} mol/L (with MB), 1.7×10^{-5} mol/L (chlorophyll *a*), and 1.7×10^{-5} mol/L (without sensitizer) under ≥ 600-nm light irradiation; 0.7×10^{-5} mol/L (erythrosine), 1.0×10^{-5} mol/L (RB), and 1.9×10^{-5} mol/L (without sensitizer) by the HPLC analysis, typical chromatograms shown in Figure 2. The total amounts of *Z*-isomers relative to the remaining lycopene after the reaction were 57.4%, 51.3%, 47.7%, and 46.4% with MB, chlorophyll *a*, erythrosine, and RB, respectively (Table 1). On the other hand, the blank tests irradiated at the light regions more than 600 nm and between 480 and 600 nm without sensitizer resulted in a *Z*-isomer content of only 7.4% and 7.7%, respectively. To the best of our knowledge, photoisomerization of (all-*E*)-lycopene was previously conducted by Stahl and co-workers [7], and Lee and Chen [8]. However, Stahl and co-workers [7] performed the iodine-catalyzed isomerization; the iodine is inedible, and the reaction mechanism would contain a radical process principally [9]. Then, Lee and Chen [8] carried out the isomerization of (all-*E*)-lycopene by direct light irradiation for 60 min, obtained a few percent of *Z*-isomers. Our results obviously indicated that the usage of

sensitizer and filtered light resulted in an accelerated isomerization of (all-*E*)-lycopene to *Z*-isomers. MB was the most efficient sensitizer for the isomerization among the reagents tested; however, it is not approved for use in food processing. In contrast, chlorophyll *a*, erythrosine, and RB are usable in such industrial fields, and therefore erythrosine appears to be the most suitable sensitizer for (all-*E*)-lycopene isomerization.

As for the individual *Z*-isomers generated, several *Z*-isomers of lycopene were observed in the HPLC chart in addition to (5*Z*)-, (9*Z*)-, and (13*Z*)-lycopene (Figure 2B) predominantly contained in processed food [1,10]. In all cases with the above sensitizers after 60-min irradiation, (5*Z*)-lycopene showed the greatest increase to 39.9%, 31.7%, 37.7%, and 29.9% relative to the remaining lycopene with MB, chlorophyll *a*, erythrosine, and RB, respectively (Table 1). On the other hand, (9*Z*)-, (13*Z*)-, and other *Z*-isomers increased to less than 10% with each sensitizer under the same irradiation duration. (5*Z*)-Lycopene exhibits higher bioavailability [10] and antioxidant activity [11] compared to (all-*E*)-lycopene and possibly to (9*Z*)- and (13*Z*)-lycopene. In addition, (5*Z*)-lycopene is estimated to be thermodynamically more stable than (9*Z*)- and (13*Z*)-lycopene according to the results of quantum chemistry calculations [12]. Therefore, we believe that photosensitized isomerization is an effective method to produce lycopene isomers with sophisticated functionalities and

greater storage stability among the *Z*-isomers.

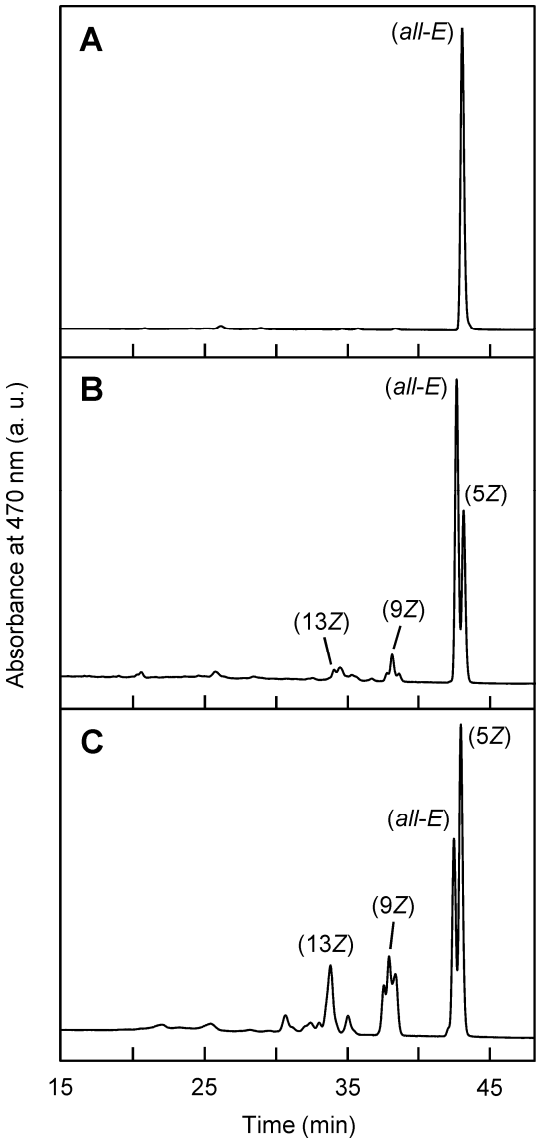

Figure 2. Reversed-phase HPLC charts of (A) (all-*E*)-lycopene and photoirradiated lycopene with rose bengal (RB) as a sensitizer (B) in acetone and (C) in hexane at 32 °C for 60 min. Unidentified peaks contain multi-(*Z*)-isomers as well as other mono-(*Z*)-isomer(s).

Table 1. Photoisomerization of (all-*E*)-lycopene to individual *Z*-isomers with methylene blue (MB), chlorophyll *a*, erythrosine, and rose cengal (RB) as sensitizers

		content (%)[a]				
sensitizer	irradiation (nm)	total *Z*-isomers[b]	5*Z*	9*Z*	13*Z*	other-*Z*[c]
MB	≥ 600	57.4 ± 3.8	39.9 ± 3.3	7.1 ± 0.6	3.6 ± 0.2	6.8 ± 1.3
chlorophyll *a*	≥ 600	51.3 ± 5.9	31.7 ± 2.8	7.1 ± 1.3	3.4 ± 0.6	9.1 ± 3.8
no sensitizer	≥ 600	7.4 ± 0.6	ND[d]	3.2 ± 1.2	3.2 ± 0.7	0.9 ± 0.5
erythrosine	480–600	47.7 ± 1.7	37.7 ± 1.2	7.6 ± 0.3	1.2 ± 1.2	1.2 ± 1.2
RB	480–600	46.4 ± 0.7	29.9 ± 1.0	6.8 ± 0.02	3.3 ± 0.5	6.4 ± 1.0
no sensitizer	480–600	7.7 ± 2.0	ND[d]	1.2 ± 1.0	4.4 ± 0.9	2.1 ± 0.5

[a]Percentage content of *Z*-isomers of lycopene isomerized from (all-*E*)-form by photoirradiation for 60 min in acetone. Values were represented as mean ± standard errors (n = 3). [b]Total amount of *Z*-isomers of lycopene. [c]Sum of *Z*-isomers of lycopene other than (5*Z*)-, (9*Z*)- and (13*Z*)-forms. [d]Not detected.

5.4.2. Time course of the photosensitized isomerization of lycopene and solvent effects on the content of *Z*-isomers

In order to determine the optimum condition for photosensitized isomerization of (all-*E*)-lycopene, the sensitizers erythrosine and RB approved for use in food processing and have good isomerization efficiency, as mentioned above, were used. The time course examinations of photosensitized isomerization of lycopene were carried out with the sensitizers in acetone (Figures 3A,B). The total amount of *Z*-isomers of lycopene with erythrosine was slightly greater than with RB, and (5*Z*)-lycopene constituted the majority of *Z*-isomers with both sensitizers. Using erythrosine, (9*Z*)-lycopene, a kinetically-preferable isomer, initially emerged and likely reversed to the (all-*E*)-form with time.

Next, solvent effects on isomerization with the two sensitizers was investigated using ethyl acetate (Figures 3C,D) and hexane (Figures 3E,F), both of which are approved for use in the food, drink and dietary supplement manufacturing industries. After irradiation in ethyl acetate for 60 min, the concentrations of lycopene remaining in solutions were 0.6×10^{-5} mol/L with both erythrosine and RB; on the other hand, relatively higher levels of lycopene were obtained in hexane: 1.7×10^{-5} mol/L with erythrosine and 1.4×10^{-5} mol/L with RB. The total amounts of *Z*-isomers relative to the remaining lycopene

after 60-min irradiation were 80.4%, 67.6%, and 47.7% in hexane, ethyl acetate, and acetone, respectively (Figures 3E,C,A), and a similar tendency was also observed with RB (Figures 3F,D,B). As for the individual *Z*-isomers, (5*Z*)-lycopene was again predominantly produced in each condition and both (9*Z*)-lycopene and (13*Z*)-lycopene exceeded 10% by content after 60-min irradiation with erythrosine (Figure 3E) or RB (Figures 2C, 3F) in hexane. In addition, the total amount of other *Z*-isomers except for (5*Z*)-, (9*Z*)- and (13*Z*)-lycopene was also markedly increased in hexane, 19.7% and 19.4% with erythrosine and RB, respectively. These results demonstrate that the usage of a less polar solvent not only accelerated *Z*-isomerization but also was effective in suppressing the decomposition of lycopene. To explain the higher rate of the photosensitized isomerization of (all-*E*)-lycopene to the *Z*-isomers, it could be reasonable to investigate the energy gap between the photosensitizer in an excited triplet state and the (all-*E*)-lycopene in a triplet state [5,6,13].

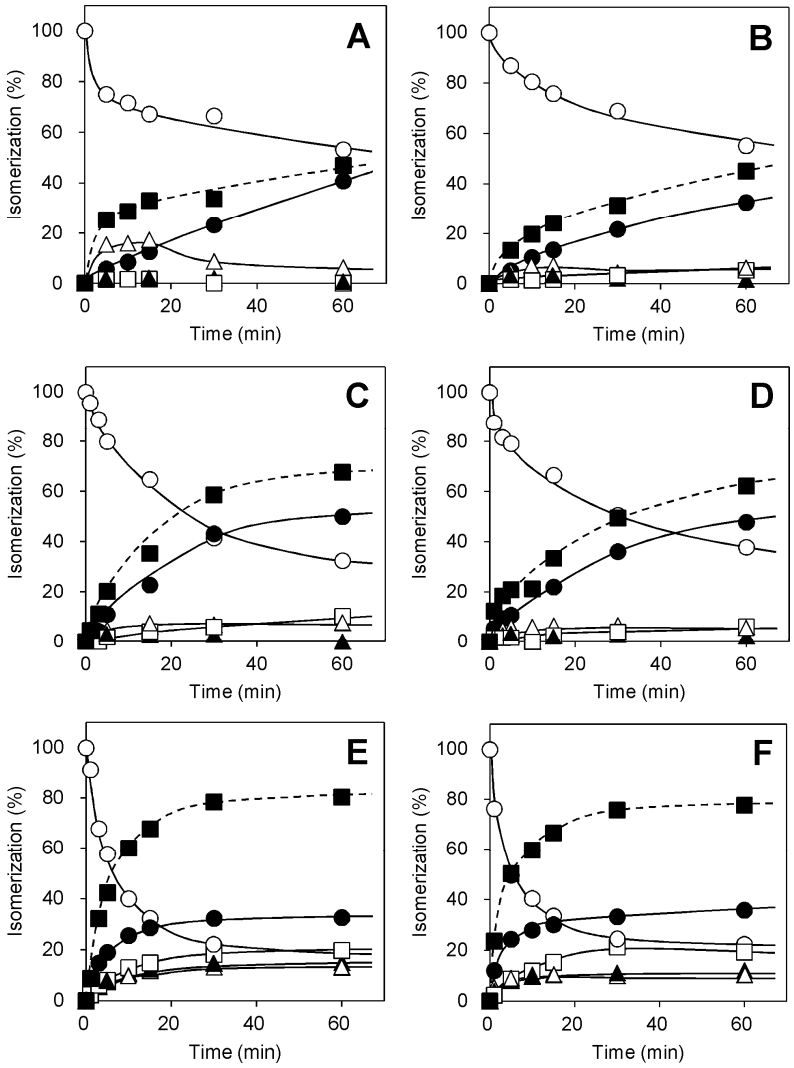

Figure 3. Photoisomerization of (all-*E*)-lycopene to individual *Z*-isomers in (A, B) acetone, (C, D) ethyl acetate, and (E, F) hexane with (A, C, E) erythrosine and (B, D, F) RB as a sensitizer under 480–600 nm light irradiation. Changes in the isomer content are presented relative to the total amount of lycopene isomers at each sampling point: (○) (all-*E*)-lycopene; (●) (5*Z*)-lycopene; (△) (9*Z*)-lycopene; (▲) (13*Z*)-lycopene; (□) other *Z*-isomers including those unidentified; (■) total amount of *Z*-isomers.

In conclusion, the photoisomerization of (all-*E*)-lycopene to *Z*-isomers with sensitizer and filtered light has proven to be more effective than thermal isomerization.

In particular, the reaction condition with erythrosine in hexane under 60-min irradiation at wavelengths between 480 nm and 600 nm was the best method to enrich the content of *Z*-isomers and suppress the decomposition of lycopene. These findings will contribute to the development of facile isomerization of (all-*E*)-lycopene to *Z*-isomers in the fields of food, drink and dietary supplement manufacturing.

5.5. Reference

[1] Schieber, A., Carle, R. Occurrence of carotenoid *cis*-isomers in food: technological, analytical, and nutritional implications. *Trends Food Sci. Technol.* **2005**, *16*, 416–422.

[2] Richelle, M., Lambelet, P., Rytz, A., Tavazzi, I., Mermoud, A.-F., Juhel, C., Borel, P., Bortlik, K. The proportion of lycopene isomers in human plasma is modulated by lycopene isomer profile in the meal but not by lycopene preparation. *Br. J. Nutr.* **2012**, *107*, 1482–1488.

[3] Honda, M., Takahashi, N., Kuwa, T., Takehara, M., Inoue, Y., Kumagai, T. Spectral characterization of *Z*-isomers of lycopene formed during heat treatment and solvent effects on the *E*/*Z* isomerization process. *Food Chem.* **2015**, *171*, 323–329.

[4] Takehara, M., Nishimura, M., Kuwa, T., Inoue, Y., Kitamura, C., Kumagai, T., Honda, M. Characterization and thermal isomerization of (*all-E*)-lycopene. *J. Agric. Food Chem.* **2014**, *62*, 264–269.

[5] Jensen, N. H., Nielsen, A. B., Wilbrandt, R. Chlorophyll *a* sensitized trans–cis photoisomerization of *all-trans-β*-carotene. *J. Am. Chem. Soc.* **1982**, *104*, 6117–6119.

[6] Kuki, M., Koyama, Y., Nagae, H. Triplet-sensitized and thermal isomerization of all-trans, 7-cis, 9-cis, 13-cis and 15-cis isomers of *β*-carotene: configurational

dependence of the quantum yield of isomerization via the T_1 state. *J. Phys. Chem.* **1991**, *95*, 7171–7180.

[7] Stahl, W., Sundquist, A. R., Hanusch, M., Schwarz, W., Sies, H. Separation of *β*-carotene and lycopene geometrical isomers in biological samples. *Clin. Chem*. **1993**, *39*, 810–814.

[8] Lee, M. T., Chen, B. H. Stability of lycopene during heating and illumination in a model system. *Food Chem.* **2002**, *78*, 425–431.

[9] Ideses, R, Shani, A. Study of the radical mechanism of iodine-catalyzed isomerization of conjugated diene systems. *J. Am. Oil Chem. Soc*. **1989**, *66*, 948–952.

[10] Richelle, M., Lambelet, P., Rytz, A., Tavazzi, I., Mermoud, A.-F., Juhel, C., Borel, P., Bortlik, K. The proportion of lycopene isomers in human plasma is modulated by lycopene isomer profile in the meal but not by lycopene preparation. *Br. J. Nutr.* **2012**, *107*, 1482–1488.

[11] Müller, L., Goupy, P., Fröhlich, K., Dangles, O., Caris-Veyrat, C., Böhm, V. Comparative study on antioxidant activity of lycopene (*Z*)-isomers in different assays. *J. Agric. Food Chem.* **2011**, *59*, 4504–4511.

[12] Guo, W.-H., Tu, C.-Y., Hu, C.-H. cis–trans Isomerizations of *β*-carotene and lycopene: a theoretical study. *J. Phys. Chem. B.* **2008**, *112*, 12158–12167.

[13] DeRosa, M. C., Crutchley, R. J. Photosensitized singlet oxygen and its applications. *Coord. Chem. Rev.* **2002**, *233–234*, 351–371.

Chapter 6

Enhanced E/Z isomerization of (all-E)-lycopene by employing iron(III) chloride as a catalyst

6.1. Table of contents

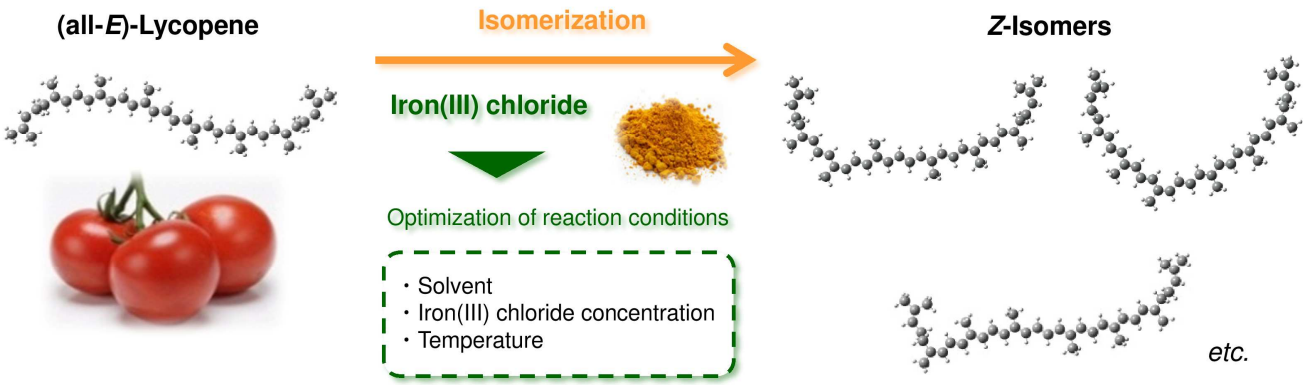

6.2. Introduction

There have been some reports on the *E*/*Z* isomerization of carotenoids, except for lycopene, using a catalyst such as iron(III) chloride [1,2], Fe-MCM-41 [3,4], and titanium tetrachloride [5], but no observations from the perspective of both isomerization efficiency and recovery of the carotenoids have been published. In connection with our studies of *E*/*Z* isomerization, we report here on the first instance of catalytic *E*/*Z* isomerization of (all-*E*)-lycopene using iron(III) chloride applicable to industrial manufacturing in the fields of food, drink and dietary supplements. In this study, to understand the *E*/*Z* isomerization characteristics of lycopene using the catalyst, the effects of reaction solvent, concentration of iron(III) chloride, and reaction temperature were investigated, and the reaction condition was optimized. This new procedure will be an effective tool for *E*/*Z* isomerization of lycopene and will contribute

to the understanding of the catalytic isomerization process regarding lycopene.

6.3. Materials and methods

6.3.1. Chemicals

(all-*E*)-Lycopene was purified as previously described [6,7] or obtained from Wako Pure Chemical Industries, Ltd. (Osaka, Japan). Iron(III) chloride was purchased from Wako Pure Chemical Industries, Ltd. HPLC-grade hexane, acetone, ethyl acetate, benzene and CH_2Cl_2 were obtained from Kanto Chemical Co., Inc. (Tokyo, Japan). DIPEA was purchased from Tokyo Chemical Industry Co., Ltd. (Tokyo).

6.3.2. *E*/*Z* Isomerization of (all-*E*)-lycopene using iron(III) chloride

(all-*E*)-Lycopene was dissolved in acetone, ethyl acetate, benzene, or CH_2Cl_2 at a concentration of 0.1 mg/mL, and a suitable amount of iron(III) chloride was added to the solution. From each of the solutions, 5 mL of sample was immediately transferred to a 10-mL screw-capped tube, the headspace was purged with nitrogen gas, and the tube was tightly capped to prevent oxygen from coming into contact with the solution. The isomerization reaction was conducted at a specified temperature for up to 24 h under darkness. The reaction mixtures at a given time during the isomerization were filtered

through a 0.2-μm polytetrafluoroethylene membrane filter (Advantec Co., Ltd., Tokyo) before the HPLC separation.

6.3.3. HPLC analysis

Normal-phase HPLC analysis with a photodiode array detector (L-2455; Hitachi Ltd., Tokyo) was conducted according to the method described previously [7]. Briefly, the analysis was performed on three Nucleosil 300-5 columns connected in tandem (3 × 250 mm in length, 4.6 mm inner diameter, 5 μm particle size; GL Sciences Inc., Tokyo) with hexane containing 0.1% DIPEA, at a flow rate of 1.0 mL/min, and a column temperature at 30 °C. The quantification of lycopene isomers was performed by peak area integration at 460 nm.

6.3.4. Evaluation of the decomposition rate

The decomposition of lycopene associated with isomerization reaction was evaluated. Assuming that the decomposition of lycopene is approximated by first order kinetics, the decomposition rate constant (k) can be calculated according to the equation: $\ln(C/C_0) = -kt$, where C and C_0 are the concentration and initial concentration of lycopene isomers, respectively, and t is the reaction time. Only the linear portion of the plot

between the natural log of concentration and time was considered. Numerical values are presented as mean ± SD.

6.4. Results and discussion

6.4.1. Profile of isomerization of (all-*E*)-lycopene to *Z*-isomers in the presence of Iron(III) chloride

The normal-phase HPLC charts of (all-*E*)-lycopene (purity, ≥99.0%) and generated *Z*-isomers of lycopene by the reaction with iron(III) chloride are shown in Figure 1. (13*Z*)-Lycopene predominantly emerged as a *Z*-isomer at 20 °C for one hour with iron(III) chloride at a concentration of 5.0×10^{-4} mg/mL in acetone (Figure 1B), while a number of *Z*-isomers including (5*Z*)-, (9*Z*)-, and (13*Z*)-lycopene were observed with a relatively high level of the catalyst (1.6×10^{-2} mg/mL) (Figure 1C). Each peak (**a**–**l**) designated in the chromatogram was also characterized using a photodiode-array detector. Several *Z*-isomers of lycopene were identified according to the retention times in HPLC, visible spectral data, and the relative intensities of the *Z*-peak as % D_B/D_{II} described in previous researches (Table 1) [7–13].The absorption spectra of the isomers having a 13*Z*-configuration around the center of the molecule, such as (9*Z*,13′*Z*)- and (9*Z*,13*Z*)-lycopene (peaks **a** and **h**, respectively) as well as (13*Z*)-lycopene, showed

significant blueshifts, and the values of % D_B/D_{II} increased considerably compared with that of (all-*E*)-lycopene. However, those of the isomers containing a peripheral *Z*-configuration, such as (5*Z*,9′*Z*)- and (5*Z*,5′*Z*)-lycopene (peaks **i** and **l**) as well as (5*Z*)-lycopene, were relatively lower.

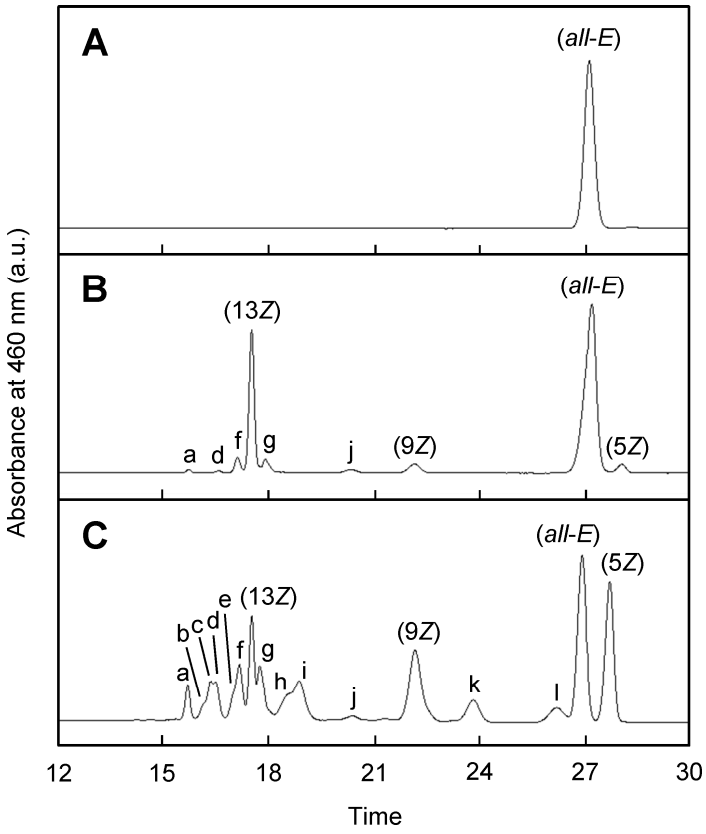

Figure 1. Normal-phase high-performance liquid chromatographic analysis of (A) (all-*E*)-lycopene and catalytically generated *Z*-isomers using iron(III) chloride at a concentration of (B) 5.0×10^{-4} mg/mL or (C) 1.6×10^{-2} mg/mL at 20 °C for one hour in acetone. The lycopene was prepared at an initial concentration of 0.1 mg/mL. (5*Z*)-, (9*Z*)-, and (13*Z*)-lycopene designated in the charts were identified according to the previous studies [7–13]. Some of the peaks (**a**–**l**) were tentatively identified as shown in Table 1.

Table 1 Absorption maxima (λ_{max}) and relative intensities of the *Z*-peak (% D_B/D_{II}) for geometrical lycopene isomers separated and observed using normal-phase high-performance liquid chromatography[a]

peak	lycopene isomer[b]	retention time (min)	λ_{max} (nm)		D_B/D_{II} (%)	
			in-line	Reported [7–13]	in-line	Reported [7–13]
a	(9Z,13′Z)	15.7	361, 436, 459, 489	360, 433, 457, 487	25.4	30.4
b	UZ[c]	16.2	361, 435, 459, 489	UZ	19.2	UZ
c	UZ	16.4	361, 436, 460, 491	UZ	21.6	UZ
d	UZ	16.5	360, 439, 465, 495	UZ	39.3	UZ
e	UZ	17.0	361, 436, 460, 493	UZ	27.9	UZ
f	UZ	17.2	361, 440, 465, 496	UZ	40.1	UZ
	(13*Z*)	17.5	361, 439, 464, 494	361, 437, 463, 494	43.3	52.4
g	UZ	17.8	360, 435, 459, 488	UZ	25.0	UZ
h	(9Z,13*Z*)	18.6	360, 432, 455, 488	361, 433, 456, 488	26.2	23.5
i	(5Z,9′Z)	18.9	361, 440, 464, 495	361, 438, 464, 495	17.1	13.4
j	UZ	21.3	360, 436, 462, 485	UZ	24.7	UZ
	(9Z)	22.2	361, 439, 465, 496	361, 438, 464, 495	12.7	13.0
k	(5Z,9Z)	23.8	361, 439, 464, 496	361, 438, 464, 495	12.2	11.8
l	(5Z,5′Z)	26.2	443, 470, 502	443, 470, 501	ND[d]	ND
	(all-*E*)	26.9	444, 470, 502	443, 470, 501	ND	ND
	(5*Z*)	27.7	444, 470, 502	443, 470, 501	ND	ND

[a]Values and peak designations were obtained from the chromatograms in Figure 1B,C with a mobile phase of hexane containing 0.1% *N,N*-diisopropylethylamine for lycopene isomers generated during catalytic reaction with iron(III) chloride at 20 °C for one hour in acetone.
[b]Assigned by the literature [7–13]. [c]Unidentified *Z*-isomer of lycopene. [d]Not detected.

6.4.2. Effect of solvent on isomerization of (all-*E*)-lycopene with iron(III) chloride

Isomerization of (all-*E*)-lycopene (0.1 mg/mL) to *Z*-isomers was investigated in the presence of iron(III) chloride (1.0×10^{-3} mg/mL) at 20 °C in several solvents, including ones permitted for use in food and beverage production. The total contents of *Z*-isomers converted were estimated to range between 50–80% when the remaining lycopene without decomposition was taken as 100% (Table 2), and showed an increase in efficiency in the following order: CH_2Cl_2 > benzene > acetone > ethyl acetate. Relatively higher isomerization contents in CH_2Cl_2 and benzene might be caused by differences in the solvation states, because the absorption maxima of lycopene were characteristically red-shifted in these solvents compared with acetone and ethyl acetate [6]. Some studies have also reproducibly reported that *Z*-isomerization of carotenoids including lycopene were promoted in halogenated solvents, such as CH_2Cl_2, $CHCl_3$ and dibromomethane [7,14,15].

Table 2 Isomerization of (all-*E*)-lycopene to *Z*-isomers with iron(III) chloride in four organic solvents: acetone, ethyl acetate, benzene, and dichloromethane (CH_2Cl_2)[a]

solvent	remaining lycopene (%)[b]	content (%)[c]					
		(all-*E*)	total *Z*[d]	(5*Z*)	(9*Z*)	(13*Z*)	other *Z*[e]
acetone	96.5 ± 1.6	48.5 ± 2.1	51.5 ± 2.1	10.4 ± 1.0	9.5 ± 0.7	18.1 ± 0.5	13.4 ± 0.8
	[95.3 ± 1.6]	[59.8 ± 3.2]	[60.2 ± 3.2]	[15.2 ± 1.3]	[10.7 ± 1.0]	[16.2 ± 0.8]	[18.1 ± 1.4]
ethyl acetate	98.9 ± 0.4	49.2 ± 0.3	50.8 ± 0.3	5.2 ± 1.2	11.5 ± 1.0	22.2 ± 0.1	11.9 ± 1.3
	[88.7 ± 5.3]	[46.6 ± 4.7]	[53.4 ± 4.7]	[7.5 ± 1.4]	[12.3 ± 0.4]	[22.2 ± 1.2]	[11.4 ± 3.3]
benzene	99.7 ± 0.3	38.6 ± 0.2	61.4 ± 0.2	4.2 ± 0.1	21.8 ± 0.1	14.7 ± 0.1	20.6 ± 0.7
	[94.7 ± 7.9]	[37.9 ± 0.3]	[62.1 ± 0.3]	[4.6 ± 0.2]	[21.8 ± 0.8]	[14.5 ± 0.4]	[21.1 ± 0.2]
CH_2Cl_2	79.4 ± 3.6	21.6 ± 0.5	78.4 ± 0.5	19.7 ± 0.1	12.0 ± 0.1	7.7 ± 0.2	38.9 ± 0.7
	[47.5 ± 1.9]	[17.3 ± 0.4]	[82.7 ± 0.4]	[20.1 ± 0.5]	[10.2 ± 0.4]	[6.3 ± 0.4]	[46.1 ± 0.4]

[a](all-*E*)-Lycopene and iron(III) chloride were prepared at concentrations of 0.1 mg/mL and 1.0×10^{-3} mg/mL, respectively, and were incubated at 20 °C for 3 h [or 12 h]. Values are presented as mean ± standard error. [b]Remaining ratio of total amount of lycopene isomers without decomposition by the reaction with iron(III) chloride. [c]Percentage content of *Z*-isomers of lycopene relative to the total amount of lycopene isomers at each sampling time. [d]Total content of *Z*-isomers of lycopene. [e]Sum of *Z*-isomers of lycopene other than (5*Z*)-, (9*Z*)-, and (13*Z*)-forms.

In terms of each *Z*-isomer generated, it was demonstrated that the content of (5*Z*)-lycopene increased temporally in each solvent tested, whereas (13*Z*)-lycopene maintained constant values or decreased (Table 2). According to computational methods, the magnitudes of the activation energy of isomerization from (all-*E*)-lycopene to each (mono-*Z*)-isomer were estimated in the following order: (5*Z*)- > (9*Z*)- > (13*Z*)-lycopene, and the relative potential energy of (mono-*Z*)-lycopene on the basis of (all-*E*)-lycopene was in the order: (13*Z*)- > (9*Z*)- > (5*Z*)- ≈ (all-*E*)-lycopene [16,17]. Taking into account the increase in other *Z*-isomers of lycopene, kinetically-favored (13*Z*)-lycopene was produced immediately after the reaction and was followed by the reversed reaction to (all-*E*)-lycopene and subsequent isomerization to thermodynamically-stable (5*Z*)-lycopene or (multi-*Z*)-lycopene containing the 5*Z*-configuration [16,17]. Such tendencies for the isomerization were also observed in the thermal isomerization of (all-*E*)-lycopene [6,7]. In benzene, (9*Z*)-lycopene markedly increased compared with the other solvents tested, while, in CH_2Cl_2, (5*Z*)-lycopene and the other *Z*-isomers of lycopene markedly increased. This characteristic difference in the isomerization preference would lead to the selective enrichment of an isomer with desirable *Z*-configuration by taking advantage of the solvent properties.

The remaining ratios of total amount of lycopene isomers without decomposition

after the 12-h reaction were higher in the order of acetone > benzene > ethyl acetate > CH_2Cl_2 (Table 2). Lycopene was hardly decomposed in acetone and benzene: the remaining ratios of lycopene after the 12-h reaction were both more than 90%. On the other hand, in CH_2Cl_2, the remaining lycopene after 3 h and 12 h was only 79.4% and 47.5%, respectively. It has been reported that astaxanthin, a kind of carotenoid, was also decomposed in CH_2Cl_2 [14]. Together with the availability of acetone and ethyl acetate in food processing in many countries, the two solvents are considered to be suitable for use in the isomerization of (all-*E*)-lycopene for the food, beverage, and dietary supplement manufacturing industries. In comparison with ethyl acetate, acetone is able to isomerize (all-*E*)-lycopene to *Z*-isomers more efficiently and largely without lycopene decomposition. To optimize the isomerization reaction for compatibility with food processing, experiments were performed using acetone as a solvent in the following sections.

6.4.3. Dependence of iron(III) chloride concentration on isomerization of (all-*E*)-lycopene

The isomerization of (all-*E*)-lycopene (0.1 mg/mL) was investigated using iron(III) chloride at concentrations ranging from 5.0×10^{-4} to 1.6×10^{-2} mg/mL (Figure 2). The

more catalyst was added to the reaction solution, the greater the production of *Z*-isomers of lycopene. The total contents of *Z*-isomers reached about 40% within one hour with an iron(III) chloride concentration of 5.0×10^{-4} mg/mL, and were maintained at a constant level for 24 h (Figure 2A). On the other hand, with a catalyst concentration of 1.0×10^{-3} mg/mL, the total content of *Z*-isomers was progressively increased after an initial burst of conversion and reached about 60% for 24 h (Figure 2B). Moreover, at higher concentrations of no less than 2.0×10^{-3} mg/mL, more than 80% isomerization was attained for a 24-h period at longest (Figure 2C–F). As for individual isomers, (13*Z*)-lycopene mainly increased with iron(III) chloride at concentrations of 5.0×10^{-4} and 1.0×10^{-3} mg/mL. In the case of catalyst at a concentration of no less than 2.0×10^{-3}, (5*Z*)- and the other *Z*-isomers emerged as the predominant isomers. However, while (13*Z*)-lycopene initially increased during 1–2 h of reaction with iron(III) chloride at all concentrations tested, it gradually decreased concomitant with the increase in the other *Z*-isomers. The computational approach discussed above accounts for this isomerization profile. Namely, (13*Z*)-lycopene which has a low activation energy was remarkably increased at a relatively lower concentration of iron(III) chloride, and (5*Z*)-lycopene which has a higher activation energy but lower potential energy increased remarkably at a relatively higher catalyst concentration. In addition, once the

thermodynamically stable (5*Z*)-isomer of lycopene has been formed, (di-*Z*)- and (tri-*Z*)-lycopene isomers can be easily generated because of the lower activation energies of the subsequent isomerization reactions.

Since all of the lycopene was degraded in the presence of iron(III) chloride at concentrations of 8.0×10^{-3} and 1.6×10^{-2} mg/mL, their time courses were limited to 12 h (Figure 2E) and 3 h (Figure 2F), respectively. As is often seen in the general catalytic reaction, the higher the concentration of iron(III) chloride, the faster the decomposition of lycopene. The decomposition rate constants were $(1.9 \pm 0.2) \times 10^{-6}$ s^{-1}, $(1.8 \pm 0.6) \times 10^{-6}$ s^{-1}, $(1.8 \pm 0.5) \times 10^{-6}$ s^{-1}, $(9.2 \pm 2.6) \times 10^{-6}$ s^{-1}, $(3.1 \pm 0.6) \times 10^{-5}$ s^{-1}, and $(1.2 \pm 0.5) \times 10^{-4}$ s^{-1} with iron(III) chloride concentrations of 5.0×10^{-4}, 1.0×10^{-3}, 2.0×10^{-3}, 4.0×10^{-3}, 8.0×10^{-3}, and 1.6×10^{-2} mg/mL, respectively. Up to an iron(III) chloride concentration of 2.0×10^{-3} mg/mL (the molar ratio of lycopene to iron(III) chloride is 1:0.066), lycopene was hardly decomposed during the reaction: the total amount of the remaining lycopene was 90.3% with 2.0×10^{-3} mg/mL catalyst for 0.1 mg/mL of (all-*E*)-lycopene in acetone for 24 h at 20 °C. Therefore, to exploit this isomerization procedure for practical applications, it is preferable that the molar ratio of lycopene to iron(III) chloride is 1:0.1 or less, which can suppress the decomposition of lycopene and increase the content of *Z*-isomers efficiently.

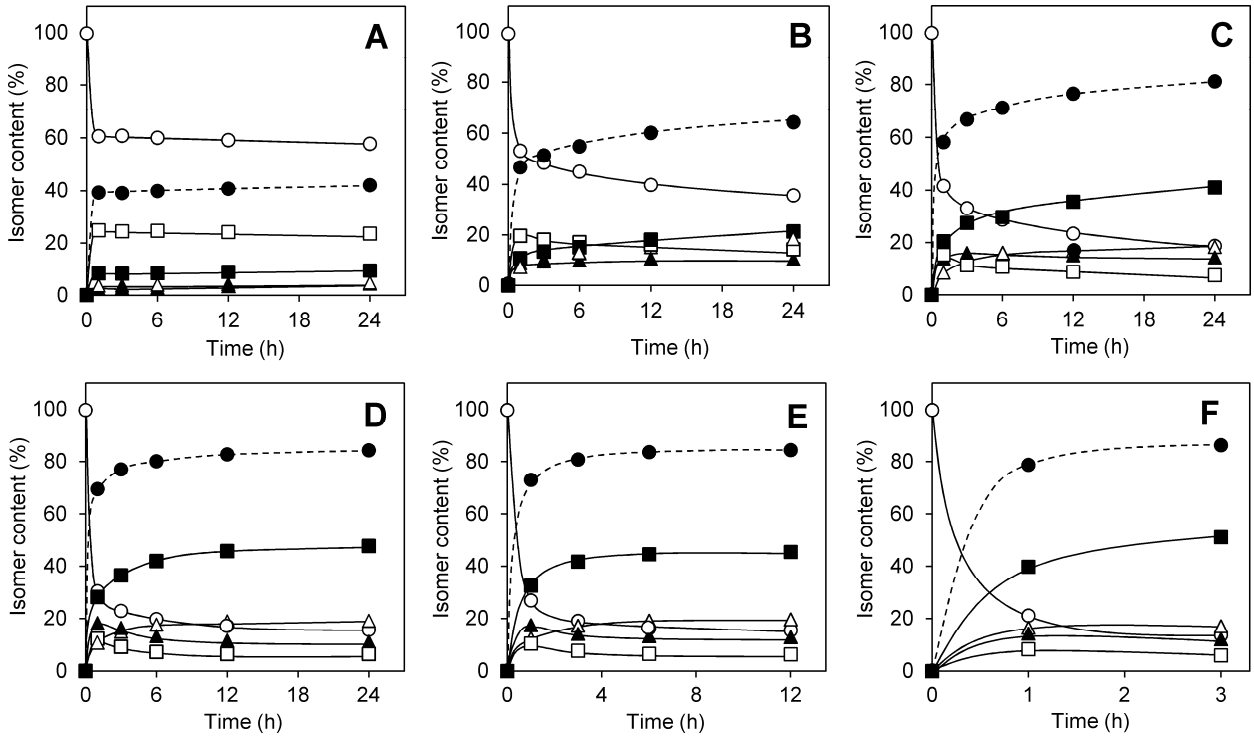

Figure 2. Isomerization of (all-*E*)-lycopene to *Z*-isomers using iron(III) chloride at concentrations of (A) 5.0×10^{-4} mg/mL, (B) 1.0×10^{-3} mg/mL, (C) 2.0×10^{-3} mg/mL, (D) 4.0×10^{-3} mg/mL, (E) 8.0×10^{-3} mg/mL, and (F) 1.6×10^{-2} mg/mL at 20 °C in acetone. The lycopene was prepared at an initial concentration of 0.1 mg/mL. Changes in the isomer content (%) are presented relative to the total amount of lycopene isomers at each sampling point: (○) (all-*E*)-lycopene; (●) total content of *Z*-isomers; (△) (5*Z*)-lycopene; (▲) (9*Z*)-lycopene; (□) (13*Z*)-lycopene; (■) sum of *Z*-isomers of lycopene other than (5*Z*)-, (9*Z*)-, and (13*Z*)-forms. Because of the higher decomposition levels of the lycopene (panels E and F), analyses were limited to shorter reaction durations (see also in the text).

6.4.4. Effect of reaction temperature on isomerization of (all-*E*)-lycopene with iron(III) chloride and a possible isomerization process

Using the above catalyst concentration of 1.0×10^{-3} mg/mL, the isomerization

temperature of (all-*E*)-lycopene in acetone was optimized in the range of 0–60 °C. As the reaction temperature was raised, the total content of *Z*-isomers of lycopene markedly increased (Table 3). Especially, the isomer content approached 80% within a few hours after heating at 60 °C. In addition, at a reaction temperature of 60 °C, the other *Z*-isomers of lycopene increased considerably because of the possible enhancement of (di-*Z*)- and (tri-*Z*)-lycopene containing (5*Z*)-configuration, as discussed above. Focusing on the reaction times of 3 h and 12 h, (5*Z*)-lycopene and other *Z*-isomers of lycopene increased in a time-dependent manner in each case, whereas (13*Z*)-lycopene decreased. (9*Z*)-Lycopene also increased temporally in the range of 0–40 °C while it decreased at the elevated temperature of 60 °C. Furthermore, the total amount of lycopene was hardly decreased during the reaction period: the remaining lycopene exceeded 90% of the initial dose in each measurement after 12 h (Table 3). Thus, a higher level of isomerization was successfully achieved at 60 °C while suppressing the decomposition of lycopene to a minimum, and is thus appropriate for practical applications.

Table 3 Influence of reaction temperature on isomerization of (all-*E*)-lycopene to *Z*-isomers with iron(III) chloride in acetone[a]

temperature (°C)	remaining lycopene (%)[b]	content (%)[c]					
		(all-*E*)	total *Z*[d]	(5*Z*)	(9*Z*)	(13*Z*)	other *Z*[e]
0	99.4 ± 2.6	50.6 ± 0.8	49.4 ± 0.8	10.6 ± 0.4	7.9 ± 0.4	18.7 ± 0.2	12.1 ± 0.1
	[97.4 ± 1.0]	[46.6 ± 2.9]	[53.4 ± 3.9]	[13.3 ± 2.5]	[8.1 ± 0.7]	[17.6 ± 1.0]	[14.4 ± 1.5]
20	96.5 ± 1.6	48.5 ± 2.1	51.5 ± 2.1	10.4 ± 1.0	9.5 ± 0.7	18.1 ± 0.5	13.4 ± 0.8
	[95.3 ± 1.6]	[59.8 ± 3.2]	[60.2 ± 3.2]	[15.2 ± 1.3]	[10.7 ± 1.0]	[16.2 ± 0.8]	[18.1 ± 1.4]
40	98.9 ± 0.2	44.2 ± 1.1	55.8 ± 1.1	8.3 ± 0.2	10.3 ± 0.6	20.6 ± 1.2	16.7 ± 0.9
	[92.5 ± 0.2]	[36.4 ± 2.0]	[63.6] ± 2.0	[11.0 ± 0.8]	[12.8 ± 0.2]	[18.2 ± 1.2]	[21.6 ± 2.1]
60	96.5 ± 5.1	20.1 ± 1.3	79.9 ± 1.3	13.6 ± 1.0	15.1 ± 0.5	13.7 ± 0.3	37.4 ± 0.9
	[94.3 ± 5.7]	[16.7 ± 0.6]	[83.3 ± 0.6]	[15.8 ± 0.4]	[13.5 ± 0.4]	[12.2 ± 0.5]	[41.8 ± 0.7]

[a](all-*E*)-Lycopene and iron(III) chloride were prepared at concentrations of 0.1 mg/mL and 1.0×10^{-3} mg/mL, respectively, and were incubated for 3 h [or 12 h] in acetone. Values are presented as mean ± standard error. [b]Remaining ratio of total amount of lycopene isomers without decomposition by the reaction with iron(III) chloride. [c]Percentage content of *Z*-isomers of lycopene relative to the total amount of lycopene isomers at each sampling time. [d]Total content of *Z*-isomers of lycopene. [e]Sum of *Z*-isomers of lycopene other than (5*Z*)-, (9*Z*)-, and (13*Z*)-forms.

We propose that the mechanism of *E*/*Z* isomerization of lycopene using iron(III) chloride could follow a similar process to that of (all-*E*)-*β*-carotene using iron(III) chloride [1,2], Fe-MCM-41 [3,4], or titanium tetrachloride [5] as described below:

$$(\text{Lycopene})_E + Fe^{3+} \rightleftharpoons (\text{Lycopene}^{\bullet+})_E + Fe^{2+} \quad (1)$$

$$(\text{Lycopene}^{\bullet+})_E + Fe^{3+} \rightleftharpoons (\text{Lycopene}^{2+})_E + Fe^{2+} \quad (2)$$

$$(\text{Lycopene}^{\bullet+})_E \rightleftharpoons (\text{Lycopene}^{\bullet+})_Z \quad (3)$$

$$(\text{Lycopene}^{2+})_E \rightleftharpoons (\text{Lycopene}^{2+})_Z \quad (4)$$

$$(\text{Lycopene}^{2+})_Z + Fe^{2+} \rightleftharpoons (\text{Lycopene}^{\bullet+})_Z + Fe^{3+} \quad (5)$$

$$(\text{Lycopene}^{\bullet+})_Z + Fe^{2+} \rightleftharpoons (\text{Lycopene})_Z + Fe^{3+} \quad (6)$$

First iron(III) ions in the catalyst accept an electron from (all-*E*)-lycopene, $(\text{Lycopene})_E$, and also from the resulting cations $(\text{Lycopene}^{\bullet+})_E$ shown in equilibriums (1) and (2). The cation species $(\text{Lycopene}^{\bullet+})_E$ and $(\text{Lycopene}^{2+})_E$, which are able to rotate at the electron-deficient site formerly double-bonded, isomerize to the corresponding *Z*-forms, $(\text{Lycopene}^{\bullet+})_Z$ and $(\text{Lycopene}^{2+})_Z$ in equilibriums (3) and (4), respectively. Finally, the *Z*-isomerized lycopene cation species accept the electron from iron(II) ions to form *Z*-isomers of lycopene in equilibriums (5) and (6).

In this study, we found that (all-*E*)-lycopene isomerizes to *Z*-isomers efficiently and largely without decomposition by employing an appropriate solvent and concentration

of iron(III) chloride as catalyst under optimized temperature: the isomerization ratio of (all-*E*)-lycopene (0.1 mg/mL) to *Z*-isomers and the total amounts of the remaining lycopene were attained at 79.9% and 96.5%, respectively, with 1.0×10^{-3} mg/mL iron(III) chloride in acetone for 3 h at 60 °C. This catalytic procedure is not only more effective in obtaining *Z*-isomers of lycopene exhibiting good functionalities, but is also applicable to industrial manufacturing in the fields of food, drink and dietary supplements requiring less facility investment.

6.5. Reference

[1] Wei, C. C., Gao, G., Kispert, L. D. Selected *cis*/*trans* isomers of carotenoids formed by bulk electrolysis and iron (III) chloride oxidation. *J. Chem. Soc., Perkin Trans. 2* **1997**, *4*, 783–786.

[2] Gao, Y., Kispert, L. D. Reaction of carotenoids and ferric chloride: equilibria, isomerization, and products. *J. Phys. Chem. B* **2003**, *107*, 5333–5338.

[3] Gao, Y., Kispert, L. D., Konovalova, T. A., Lawrence, J. N. Isomerization of carotenoids in the presence of MCM-41 molecular sieves: EPR and HPLC studies. *J. Phys. Chem. B* **2004**, *108*, 9456–9462.

[4] Kispert, L. D., Polyakov, N. E. Carotenoid radicals: cryptochemistry of natural colorants. *Chem. Lett.* **2010**, *39*, 148–155.

[5] Rajendran, V., Chen, B. H. Isomerization of β-carotene by titanium tetrachloride catalyst. *J. Chem. Sci*. **2007**, *119*, 253–258.

[6] Takehara, M., Nishimura, M., Kuwa, T., Inoue, Y., Kitamura, C., Kumagai, T., Honda, M. Characterization and thermal isomerization of (*all-E*)-lycopene. *J. Agric. Food Chem.* **2014**, *62*, 264–269.

[7] Honda, M., Takahashi, N., Kuwa, T., Takehara, M., Inoue, Y., Kumagai, T. Spectral characterization of *Z*-isomers of lycopene formed during heat treatment and solvent

effects on the *E*/*Z* isomerization process. *Food Chem.* **2015**, *171*, 323–329.

[8] Schierle, J., Bretzel, W., Bühler, I., Faccin, N., Hess, D., Steiner, K., Schüep, W. Content and isomeric ratio of lycopene in food and human blood plasma. *Food Chem.* **1997**, *59*, 459–465.

[9] Hengartner, U., Bernhard, K., Meyer, K., Englert, G., Glinz, E. Synthesis, isolation, and NMR-spectroscopic characterization of fourteen (*Z*)-isomers of lycopene and of some acetylenic didehydro- and tetradehydrolycopenes. *Helv. Chim. Acta* **1992**, *75*, 1848–1865.

[10] Fröhlich, K., Conrad, J., Schmid, A., Breithaupt, D. E., Böhm, V. Isolation and structural elucidation of different geometrical isomers of lycopene. *Int. J. Vitam. Nutr. Res.* **2007**, *77*, 369–375.

[11] Lee, M. T., Chen, B. H. Separation of lycopene and its *cis* isomers by liquid chromatography. *Chromatographia* **2001**, *54*, 613–617.

[12] Glaser, T., Albert, K. Hyphenation of modern extraction techniques to LC–NMR for the analysis of geometrical carotenoid isomers in functional food and biological tissues. In *On-line LC–NMR and related techniques*; Albert, K. Ed.; John Wiley & Sons Ltd.: New York, NY, **2002**; pp 129–140.

[13] Britton, G. UV/visible spectroscopy. In *Carotenoids*; Britton, G., Liaaen-Jensen,

S., Pfander, H., Eds.; Birkhäuser Verlag: Basel, Switzerland, **1995**; Vol. *1B*: Spectroscopy, pp 13–62.

[14] Yuan, J.-P., Chen, F. Isomerization of *trans*-astaxanthin to *cis*-isomers in organic solvents. *J. Agric. Food Chem.* **1999**, *47*, 3656–3660.

[15] Yuan, J.-P., Chen, F. Kinetics for the reversible isomerization reaction of *trans*-astaxanthin. *Food Chem.* **2001**, *73*, 131–137.

[16] Guo, W.-H., Tu, C.-Y., Hu, C.-H. Cis–trans isomerizations of *β*-carotene and lycopene: a theoretical study. *J. Phys. Chem. B* **2008**, *112*, 12158–12167.

[17] Chasse, G. A., Mak, M. L., Deretey, E., Farkas, I., Torday, L. L., Papp, J. G., Sarma, D. S. R., Agarwal, A., Chakravarthi, S., Agarwal, S., Rao, A. V. An *ab initio* computational study on selected lycopene isomers. *J. Mol. Struct. (Theochem)* **2001**, *571*, 27–37.

Chapter 7

Vegetable oil-mediated thermal isomerization of (all-E)-lycopene: facile and efficient production of Z-isomers

7.1. Table of contents

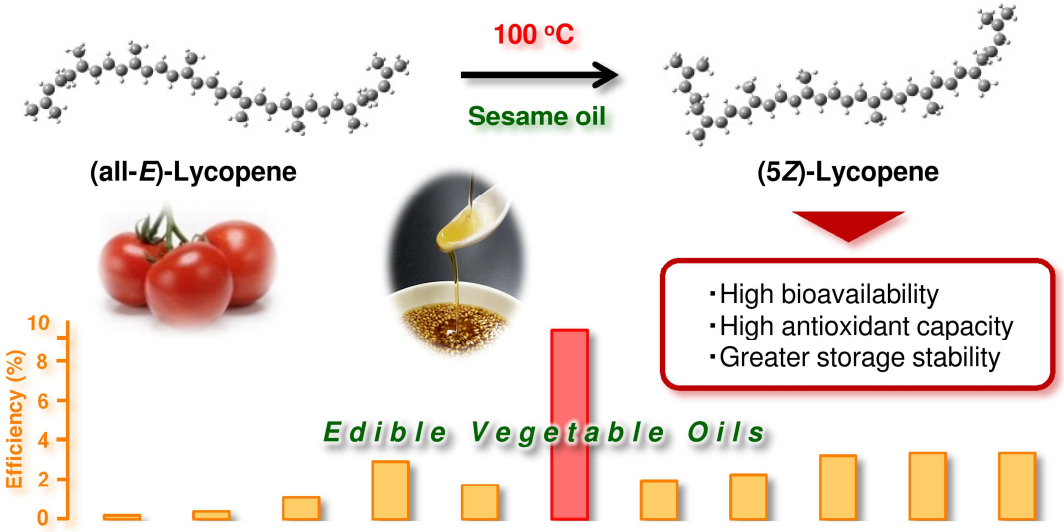

7.2. Introduction

As discussed in the previous chapter, we demonstrated basic studies on the thermal-[1] and photo-isomerization [2] of (all-*E*)-lycopene, and finally attained a greater isomerization to the corresponding *Z*-isomers (79.9% conversion) in the presence of a catalyst [3] almost without decomposition of lycopene (96.5% recovery). Although our developed methods showed high efficiency for geometrical isomerization of (all-*E*)-lycopene and are amenable to foods and beverages manufacturing, some organic solvents or food additives such as erythrosine and iron(III) chloride were employed in each procedure. Since the global trend is toward natural and additive-free foods and drinks, we embarked on a new study on lycopene preparations rich in *Z*-forms without

those chemical reagents. Several studies have also reported that some organic solvents, such as CH_2Cl_2 and $CHCl_3$, promoted thermal *Z*-isomerization of carotenoids including lycopene [4–6], and have stimulated interest in the possible effects induced by biogenic solvents like vegetable oils. Here, we investigated the potential of eleven different kinds of edible vegetable oils available in the market to isomerize (all-*E*)-lycopene to *Z*-isomers under heat treatment. This simple but effective method will be an alternative tool for the *Z*-isomerization of (all-*E*)-lycopene under conditions suitable for food processing.

7.3. Materials and methods

7.3.1. Chemicals

All solvents were of analytical-grade, except for the HPLC-grade methanol (Sigma-Aldrich Co., St. Louis, MO) and vegetable oils for cooking (perilla, linseed, grape seed, soybean, corn, sesame, rapeseed, rice bran, safflower seed, olive, and sunflower seed oils). The suppliers of the oils were summarized in Table 1 with some chemical properties [7–10].

Table 1. Iodine values (IVs), saponification values (SVs), and fatty acid (FA) compositions of the eleven vegetable oils tested[a]

			FA composition (wt%)						
vegetable oil	IV	SV	16:0	18:0	18:1	18:2	18:3	22:1	supplier
perilla	193–201	190–205	30–35	8	ND[b]	9	37	47	Benibana Foods Co., Ltd.
linseed	170–204	189–195	6–10	3–8	10–21	13–15	50–61	ND	Nippon Flour Mills Co., Ltd.
grape seed	124–150	188–194	6–11	3–7	12–28	58–78	≤1	≤0.3	Kikkoman Co., Ltd.
soybean	120–143	189–195	8–13	2–5	18–26	50–57	6–10	≤0.3	Ajinomoto Co., Inc.
corn	103–133	187–195	9–17	1–3	20–42	39–63	1–2	≤0.1	Ajinomoto Co., Inc.
sesame	104–120	186–195	8–12	5–7	34–46	37–48	≤1	ND	Takemoto Oil & Fat Co., Ltd.
rapeseed	94–120	168–181	2–6	1–3	8–60	11–23	5–13	5.0–60	Ajinomoto Co., Inc.
rice bran	90–115	180–199	14–23	1–4	38–48	21–42	≤3	ND	Tsuno Co., Ltd.
safflower seed[c]	80–100	186–194	4–6	1–2	70–84	9–20	≤1	≤0.3	The Nisshin OilliO Group, Ltd.
olive	80–88	184–196	8–20	1–5	55–83	4–21	≤2	ND	Ajinomoto Co., Inc.
sunflower seed[c]	78–90	182–194	4–6	2–5	43–72	19–45	≤1	ND	Showa Sangyo Co., Ltd.

[a]All values are obtained from literatures [7–10]. [b]Not detected. [c]Oil with high oleic acid content.

7.3.2. Purification of (all-*E*)-lycopene

(all-*E*)-Lycopene was obtained from tomato oleoresin (Lyc-O-Mato® 15%, LycoRed Ltd., Beer-Sheva, Israel) according to the previous description [1]: 493.4 mg of fine red crystalline powder from 3.12 g of tomato material; reversed-phase HPLC, ≥ 98.3% purity. Purified lycopene was stored at −80 °C until just before use.

7.3.3. Thermal isomerization of purified (all-*E*)-lycopene in vegetable oils

The edible vegetable oils used in this study were perilla, linseed, grape seed, soybean, corn, sesame, rapeseed, rice bran, safflower seed, olive, and sunflower seed oil. Purified (all-*E*)-lycopene was dispersed into each vegetable oil at the concentration of 10 mg/mL, and the residues were dissolved by sonication in an ice-cold bath (SUS-300, Shimadzu, Kyoto, Japan) at 300 W for 20 min. Almost no isomerization of (all-*E*)-lycopene was observed after the process. From each of the solutions, 25 μL of sample was withdrawn with a microsyringe, transferred to a small vial, and the headspace was purged with argon gas. Immediately, the vessels were tightly closed to minimize the oxygen exposure and placed in an oil-bath at 100 °C for 1 h or 3 h under dark conditions. After the thermal treatment, each reaction mixture was diluted in 5 mL of benzene and filtered through a 0.2-μm polytetrafluoroethylene membrane filter (Advantec Co., Ltd., Tokyo,

Japan) prior to the HPLC separation.

7.3.4. HPLC analysis

Reversed-phase HPLC analysis with a C_{30} carotenoid column (250 × 4.6 mm inner diameter, 5 μm particles, YMC, Kyoto) was conducted according to the method described previously [1]. The quantification of *Z*-isomers of lycopene was carried out by peak area integration at 470 nm by a UV–vis detector (JASCO Co., Tokyo), and the peaks were identified according to previous works [1–4].

7.4. Results and discussion

Purified (all-*E*)-lycopene samples dissolved in corn and sesame oils which are nearly equivalent in IVs and SVs and FA compositions (Table 1) [9,10] were thermally isomerized at 100 °C for 1 h. The resulting lycopene mixtures were separated on a reversed-phase HPLC column. The typical chromatogram of each sample is shown in Figure1, as well as that of intact (all-*E*)-lycopene. The predominant mono-*Z*-isomers produced were identified according to previous works [1–4] and defined spectral data for (5*Z*)-lycopene (Figure 2, 3 and Tables 2, 3). In corn oil (Figure 1B), (9*Z*)- and (13*Z*)-lycopene were prevailing except for the all-*E*-form, while (5*Z*)-lycopene and

putative (5*Z*,9′*Z*)- and (5*Z*,9*Z*)-isomers [11] were significantly increased in sesame oil (Figure 1C). These mono-*Z*-isomers are often found in the human body as well as in processed tomato products [12,13]. Some peaks assumed (multi-*Z*)-lycopene were also detected in both vegetable oils.

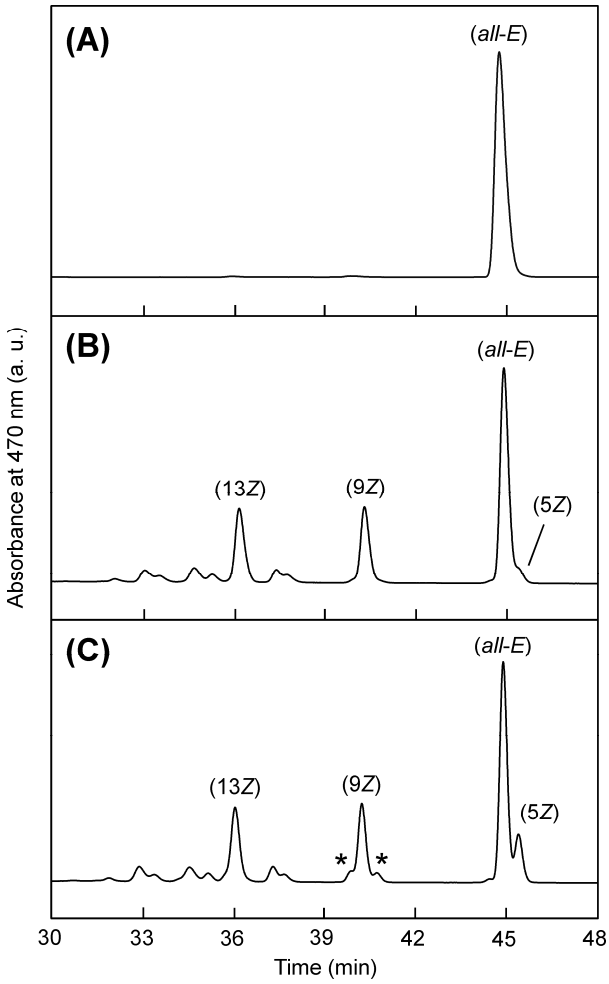

Figure 1. Reversed-phase HPLC chromatograms of (A) (all-*E*)-lycopene and thermally treated lycopene at 100 °C for 1 h in (B) corn oil and (C) sesame oil. Peaks with asterisks around the (9*Z*)-lycopene denote the di-*Z*-isomers having 5*Z*-configuration: (5*Z*,9′*Z*)-lycopene with the retention time of 40.6 min and (5*Z*,9*Z*)-lycopene of 41.4 min [11]. Unidentified peaks contain other mono-*Z*- and multi-*Z*-isomers.

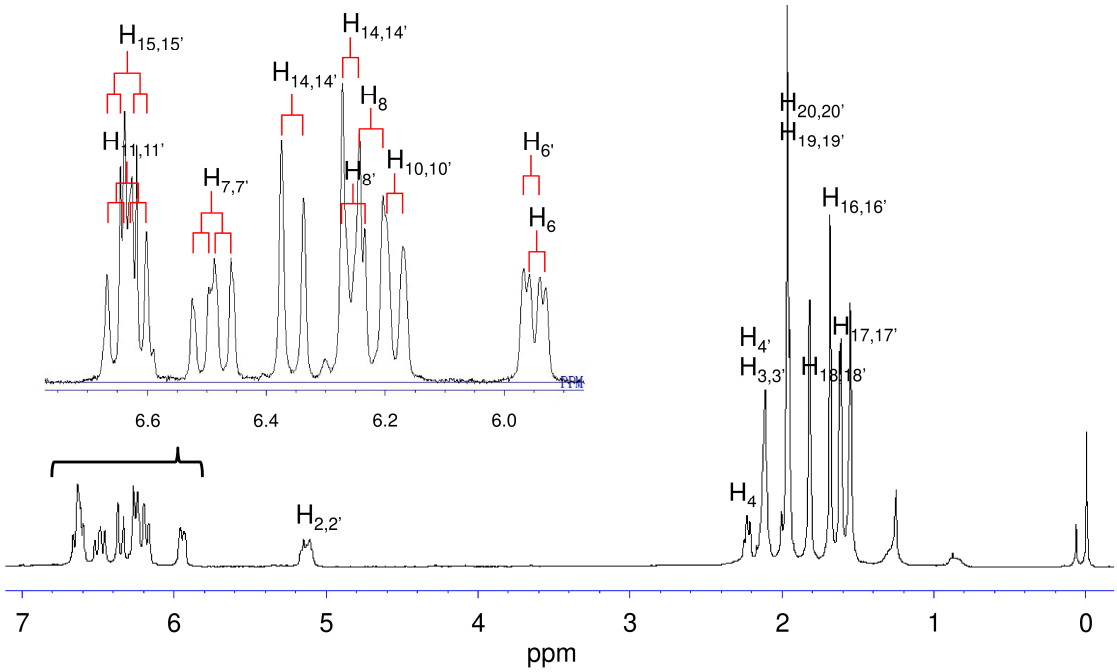

Figure 2. ^{1}H NMR spectrum of the purified (5*Z*)-lycopene. (400 MHz, $CDCl_3$).

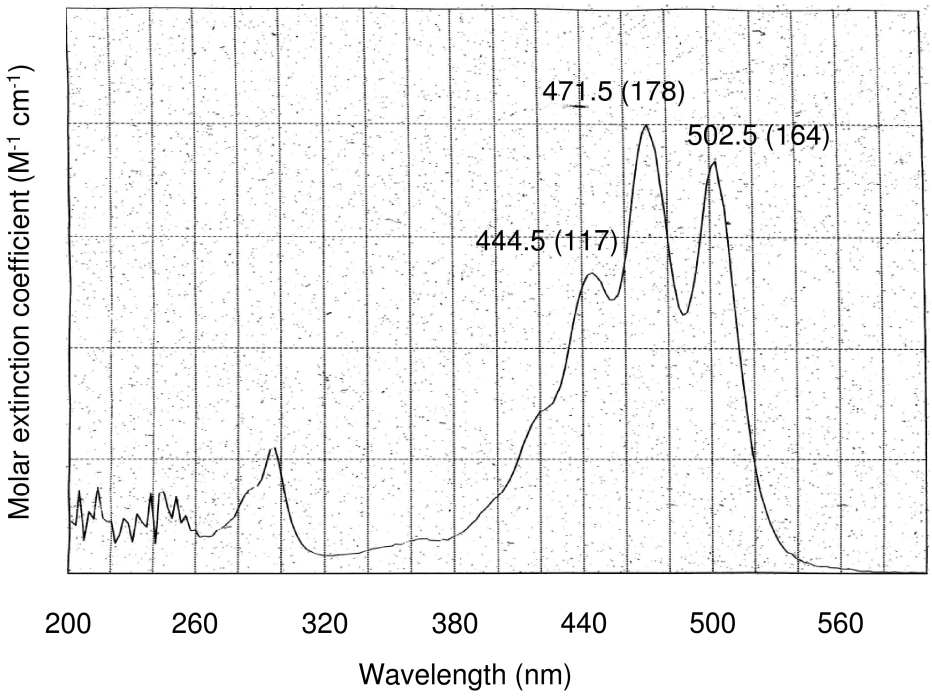

Figure 3. Ultraviolet (UV) spectra of the purified (5*Z*)-lycopene in hexane.

Table 2. Proton and ^{13}C NMR assignment of (5*Z*)-lycopene isomerized from (all-*E*)-lycopene of a tomato origin[a]

proton	δ in ppm (multiplicity, coupling constant in Hz) [$\Delta\delta$][b]		carbon	δ in ppm	
	(all-*E*)[c]	(5*Z*)		(all-*E*)[c]	(5*Z*)
			C(1)	131.72	132.00
			C(1′)		131.74
H–C(2)	5.11 (m)	5.15 [0.04]	C(2)	123.96	124.06
H–C(2′)		5.11	C(2′)		124.03
2H–C(3)	2.11 (m)	2.11 (m)	C(3)	26.70	26.87
2H–C(3′)			C(3′)		26.71
2H–C(4)	2.11 (m)	2.24 (t, *J* = 7.5) [0.03]	C(4)	40.23	32.82 [−7.41]
2H–C(4′)		2.11 (m)	C(4′)		40.25
			C(5)	139.47	139.49
			C(5′)		139.72
H–C(6)	5.95 (d, *J* = 11.0)	5.94 (d, *J* = 11.1)	C(6)	125.74	126.52 [0.78]
H–C(6′)		5.95 (d, *J* = 10.5)	C(6′)		125.74
H–C(7)	6.49 (dd, *J* = 15.0, 11.0)	6.49 (dd, *J* = 14.8, 11.1)	C(7)	124.79	124.69
H–C(7′)		6.49 (dd, *J* = 15.1, 10.5)	C(7′)		124.82
H–C(8)	6.25 (d, *J* = 15.0)	6.22 (d, *J* = 14.8) [−0.03]	C(8)	135.40	135.13
H–C(8′)		6.25 (d, *J* = 15.1)	C(8′)		135.40
			C(9)	136.15	136.17
			C(9′)		
H–C(10)	6.18 (d, *J* = 11.4)	6.19 (d, *J* = 11.9)	C(10)	131.55	131.57
H–C(10′)		6.19 (d, *J* = 11.7)	C(10′)		131.52
H–C(11)	6.64 (dd, *J* = 14.9, 11.4)	6.63 (m)	C(11)	125.15	125.15
H–C(11′)			C(11′)		
H–C(12)	6.35 (d, *J* = 14.9)	6.35 (d, *J* = 14.8)	C(12)	137.35	137.32
H–C(12′)		6.35 (d, *J* = 14.7)	C(12′)		137.37
			C(13)	136.56	136.54
			C(13′)		
H–C(14)	6.24 (m)	6.26 (m)	C(14)	132.64	132.63
H–C(14′)			C(14′)		
H–C(15)	6.62 (m)	6.63 (m)	C(15)	130.07	130.09
H–C(15′)			C(15′)		
3H–C(16)	1.687 (s)	1.687 (s)	C(16)	25.68	25.70
3H–C(16′)			C(16′)		
3H–C(17)	1.614 (s)	1.624 (s)	C(17)	17.70	17.62
3H–C(17′)		1.614 (s)	C(17′)		17.73
3H–C(18)	1.818 (s)	1.821 (s)	C(18)	16.99	24.16 [7.17]
3H–C(18′)			C(18′)		16.93
3H–C(19)	1.968 (s)	1.953 (s)	C(19)	12.90	12.90
3H–C(19′)		1.968 (s)	C(19′)		
3H–C(20)	1.968 (s)	1.968 (s)	C(20)	12.79	12.83
3H–C(20′)			C(20′)		

[a](5*Z*)-Lycopene was obtained in a photosensitized manner with methylene blue [2] from (all-*E*)-lycopene, and purified through a normal-phase HPLC column [4]. Spectra were recorded at 400 MHz for ^{1}H and 100 MHz for ^{13}C; *s* = singlet, *d* = doublet, *dd* = doublet of doublets, *m* = multiplet. [b]Shift differences $\Delta\delta = \delta((Z)) - \delta((E))$ for $|\Delta\delta| > 0.02$ ppm in ^{1}H, and for $|\Delta\delta| > 0.30$ ppm in ^{13}C. [c]Obtained from previous study [1].

Table 3. Absorption maxima and minima and molar extinction coefficients of lycopene isomers purified from processed tomato paste[a]

isomer	λ_B[b]	λ_1	λ_{min}	λ_2	λ_{min}	λ_3
(all-*E*)[c]	ND[d]	444.0 (118)	454.5 (102)	471.0 (182)	488.0 (95)	502.5 (168)
(5*Z*)[e]	ND	444.5 (117)	454.5 (101)	471.5 (178)	488.0 (93)	502.5 (164)
(9*Z*)[c]	361.5 (23)	438.5 (109)	449.0 (95)	465.0 (164)	482.0 (87)	496.0 (149)
(13*Z*)[c]	361.0 (77)	438.0 (97)	448.5 (84)	464.0 (137)	481.0 (73)	495.0 (115)

[a]Solvent, hexane; λ in nm; values in parentheses, $\varepsilon \times 10^{-3}$. [b]Absorption maximum for *Z*-peak. [c]Modified from the literature [4]. [d]Not detected. [e]Obtained in a photosensitized manner with methylene blue [2] from (all-*E*)-lycopene, and purified through a normal-phase HPLC column [4] (HPLC purity, 99.0%).

Thermal isomerization of (all-*E*)-lycopene to the *Z*-isomers was conducted in various kinds of vegetable oils having different IVs at 100 °C for 1 h. The percentage contents of the isomers obtained are listed in Table 4. The total content of *Z*-lycopene surpassed 58.8% after the heat treatment in sesame oil, and the values attained in the eleven vegetable oils were higher in the order corresponding to sesame > rice bran, grape seed, safflower seed, soybean, corn, linseed > olive, rapeseed, perilla > sunflower seed oil. As for the individual *Z*-isomers generated, profiles of components of the *Z*-isomers were almost the same amongst the tested vegetable oils except for sesame oil, in which (5*Z*)-lycopene increased approximately 3–5 times compared with the others. (5*Z*)-Lycopene was estimated to be kinetically unfavorable but thermodynamically more stable than (9*Z*)- and (13*Z*)-lycopene by the results of quantum chemistry calculations [14]. The preferential occurrence of (5Z)-lycopene from (all-*E*)-lycopene in sesame oil is considered to be independent of the IVs and SVs and FA composition, because these values were similar to those of corn oil [9,10]. Colle et al. (2013) also indicated that there was no correlation between these values and thermal isomerization tendencies of (all-*E*)-lycopene by the experiments of using olive and fish oils [15]. It can be supposed that the preference is due to the catalytic ingredients in sesame oil, such as iron, which increased a content of (5Z)-isomer [3] probably by lowering the activation energy

during isomerization to the corresponding isomer [14, 16]. In fact, the sesame oil used in this study contained rich minerals such as iron, copper, selenium and so on than other vegetable oils [17]. Interestingly, (5*Z*)-lycopene has been reported to show higher bioavailability [18] and antioxidant capacity [19] compared with (all-*E*)-lycopene and possibly to (9*Z*)- and (13*Z*)-lycopene.

The remaining ratios of total amount of lycopene isomers without decomposition were investigated under the above conditions, and found to be high in the following order: sunflower seed, sesame, soybean, rapeseed, corn, olive, safflower seed, rice bran (79.6–74.2%) > perilla, grape seed (55.8, and 54.1%, respectively) > linseed oil (38.8%). The decomposition of lycopene in oils showing higher remaining ratios, such as sunflower seed and sesame oils, would probably be suppressed by natural antioxidants contained in the oils, such as *α*-tocopherol and sesamol, respectively [10]. In fact, ^{1}H-NMR signals at 5.95 and 6.77–6.88 ppm, possibly derived from the spectra of lignan derivatives [20], were observed in a sesame oil used in this study (Figure 4). On the other hand, lycopene was largely degraded in perilla, linseed, and grape seed oil. The high IV of these oils brought about the accelerated decomposition of lycopene, because the double bonds in FAs can undergo the formation of peroxy radicals harmful to lycopene [10,15].

As a practically important criterion, efficiency of *Z*-isomerization with vegetable oils was assessed for the *Z*-isomers of lycopene in total amount and for 5*Z*-isomer, considering the remaining ratio of total amount of lycopene isomers without decomposition after the thermal treatment (Figure 5). In eight oils, more than 35% of the efficiency of total *Z*-isomerization could be attained for 1 h, whereas only two oils showed such high efficiency after 3 h (Figure 5A). When sesame oil was employed, the efficiency remained above 45% during the period tested, and in particular, (5*Z*)-lycopene production was threefold greater than the average of the other oils (Figure 5B). The thermal *Z*-isomerization efficiency of (all-*E*)-lycopene in sesame oil is estimated to be higher than in common organic solvents such as acetone, benzene and hexane: approximately 40% of total *Z*-isomers content and less than 3% of (5*Z*)-lycopene content by heating in those solvents, even without considering the decomposition of lycopene [4]. In perilla and linseed oils, however, the efficiencies were quite low at ca. 5% for total *Z*-isomers and less than 0.5% for (5*Z*)-lycopene for 3 h, because high decomposition ratios of lycopene depend on the high IVs discussed above.

Table 4. Isomerization of (all-*E*)-lycopene to *Z*-isomers in various vegetable oils by heating at 100 °C for 1 h[a]

	content (%)[b]					
vegetable oil	total *Z*[c]	(5*Z*)	(9*Z*)	(13*Z*)	other *Z*[d]	remaining lycopene (%)[e]
perilla	47.6 ± 3.8	1.4 ± 0.7	15.7 ± 1.3	15.1 ± 0.9	15.4 ± 1.5	55.8 ± 15.0
linseed	52.5 ± 5.9	2.8 ± 0.3	18.1 ± 2.6	14.3 ± 1.7	17.4 ± 2.0	38.8 ± 9.8
grape seed	54.3 ± 0.1	2.9 ± 0.1	17.6 ± 0.5	16.6 ± 0.8	17.2 ± 0.4	54.1 ± 0.1
soybean	53.6 ± 1.5	2.4 ± 1.2	17.3 ± 0.3	17.0 ± 0.3	17.0 ± 0.6	77.3 ± 2.3
corn	52.6 ± 7.0	2.0 ± 0.4	17.6 ± 3.1	16.0 ± 1.1	17.0 ± 3.6	76.2 ± 10.6
sesame	58.8 ± 2.7	8.6 ± 0.4	15.8 ± 0.7	15.1 ± 1.1	19.3 ± 1.2	78.3 ± 3.6
rapeseed	47.9 ± 4.1	3.0 ± 0.5	15.0 ± 1.6	14.4 ± 1.7	15.6 ± 1.6	76.5 ± 7.5
rice bran	54.5 ± 3.2	3.0 ± 1.1	18.1 ± 1.2	16.4 ± 0.2	17.0 ± 1.3	72.4 ± 6.6
safflower seed[f]	54.2 ± 2.5	2.8 ± 1.5	17.4 ± 1.3	17.1 ± 0.5	16.9 ± 0.9	74.2 ± 10.3
olive	49.7 ± 1.3	3.2 ± 1.2	16.0 ± 0.7	14.5 ± 1.1	16.1 ± 0.5	75.0 ± 3.5
sunflower seed[f]	44.8 ± 3.0	2.0 ± 0.5	14.6 ± 1.5	14.1 ± 0.7	14.1 ± 1.4	79.6 ± 7.3

[a]Values are presented as mean ± standard error (n = 3). [b]Percentage content of *Z*-isomers of lycopene relative to the total amount of lycopene isomers after the heating period. [c]Total content of *Z*-isomers of lycopene. [d]Sum of *Z*-isomers of lycopene other than 5*Z*-, 9*Z*-, and 13*Z*-forms. [e]Remaining ratio of total amount of lycopene isomers without decomposition during the thermal treatment. [f]Oil with high oleic acid content.

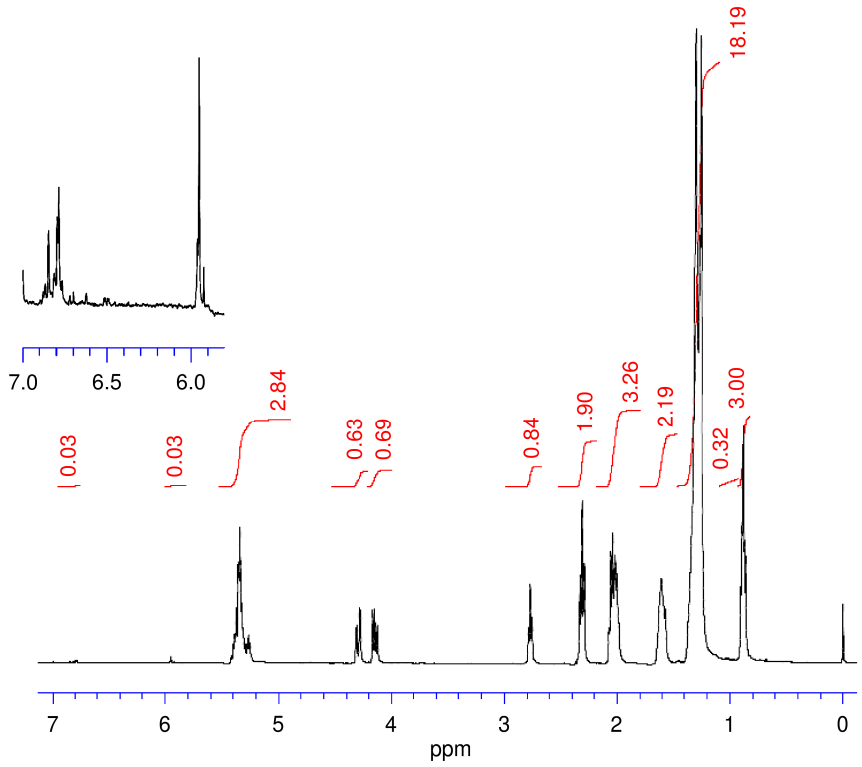

Figure 4. ^{1}H NMR spectrum of the sesame oil. The signals at 5.95 and 6.77–6.88 ppm, possibly derived from the spectra of lignan derivatives [18].

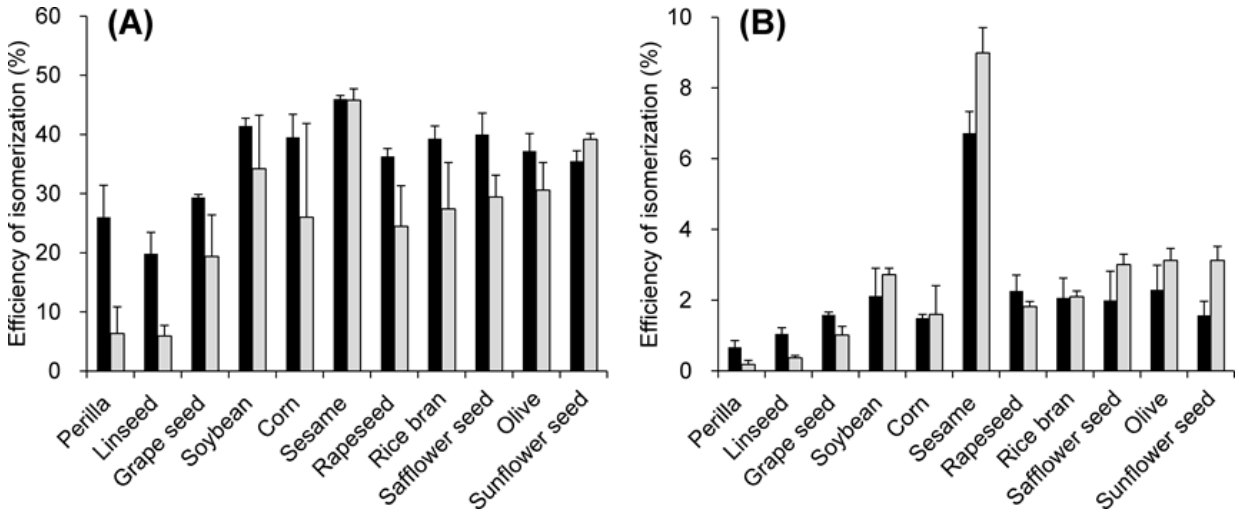

Figure 5. Efficiency of *E*-to-*Z* isomerization of lycopene in various vegetable oils. (all-*E*)-Lycopene was heated at 100 °C for 1 h (solid bars) and 3 h (shaded bars) in each oil. The efficiencies of isomerization to (A) *Z*-isomers of lycopene in total amount and (B) (5*Z*)-lycopene were calculated by multiplying the percentage content of *Z*-isomers by remaining ratio of total amount of lycopene isomers without decomposition and by one-hundredth. Error bars indicate the SD from triplicate samples.

7.5. Reference

[1] Takehara, M., Nishimura, M., Kuwa, T., Inoue, Y., Kitamura, C., Kumagai, T., Honda, M. Characterization and thermal isomerization of (*all-E*)-lycopene. *J. Agric. Food Chem.* **2014**, *62*, 264–269.

[2] Honda, M., Igami, H., Kawana, T., Hayashi, K., Takehara, M., Inoue, Y., Kitamura, C. Photosensitized *E*/*Z* isomerization of (*all-E*)-lycopene aiming at practical applications. *J. Agric. Food Chem.* **2014**, *62*, 11353–11356.

[3] Honda, M., Kawana, T., Takehara, M., Inoue, Y. Enhanced *E*/*Z* isomerization of (all-*E*)-lycopene by employing iron(III) chloride as a catalyst. *J. Food Sci.* **2015**, *80*, C1453–C1459.

[4] Honda, M., Takahashi, N., Kuwa, T., Takehara, M., Inoue, Y., Kumagai, T. Spectral characterization of *Z*-isomers of lycopene formed during heat treatment and solvent effects on the *E*/*Z* isomerization process. *Food Chem.* **2015**, *171*, 323–329.

[5] Yuan, J.-P., Chen, F. Isomerization of *trans*-astaxanthin to *cis* isomers in organic solvents. *J. Agric. Food Chem.* **1999**, *47*, 3656–3660.

[6] Yuan, J.-P., Chen, F. Kinetics for the reversible isomerization reaction of *trans*-astaxanthin. *Food Chem.* **2001**, *73*, 131–137.

[7] Knothe, G. Structure indices in FA chemistry. How relevant is the iodine value? *J.*

Am. Oil Chem. Soc. **2002**, *79*, 847–854.

[8] Karak, N. Vegetable oils and their derivatives. In *Vegetable oil-based polymers: properties, processing and applications*, Woodhead Publishing: Cambridge, U.K., **2012**, pp. 54–93.

[9] Codex Alimentarius, Codex standards for fats and oils from vegetable sources. http://www.fao.org/docrep/004/y2774e/y2774e04.htm.

[10] Gunstone, F. D. *Vegetable oils in food technology: composition, properties and uses*, 2nd ed., Blackwell Publishing: Oxford, U.K., **2011**.

[11] Fröhlich, K., Conrad, J., Schmid, A., Breithaupt, D. E., Böhm, V. Isolation and structural elucidation of different geometrical isomers of lycopene. *Int. J. Vitam. Nutr. Res.* **2007**, *77*, 369−375.

[12] Schierle, J., Bretzel, W., Bühler, I., Faccin, N., Hess, D., Steiner, K., Schüep, W. Content and isomeric ratio of lycopene in food and human blood plasma. *Food Chem.* **1997**, *59*, 459–465.

[13] Schieber, A., Carle, R. Occurrence of carotenoid *cis*-isomers in food: technological, analytical, and nutritional implications. *Trends Food Sci. Technol.* **2005**, *16*, 416–422.

[14] Guo, W.-H., Tu, C.-Y., Hu, C.-H. *Cis–trans* isomerizations of *β*-carotene and

lycopene: a theoretical study. *J. Phys. Chem. B* **2008**, *112*, 12158–12167.

[15] Colle, I. J. P., Lemmens, L., Van Buggenhout, S., Van Loey, A. M., Hendrickx, M. E. Modeling lycopene degradation and isomerization in the presence of lipids. *Food Bioprocess Technol.* **2013**, *6*, 909–918.

[16] Takehara, M., Kuwa, T., Inoue, Y., Kitamura, C., Honda, M., Isolation and characterization of (15Z)-lycopene thermally generated from a natural source. Biochem. Biophys. Res. Commun. **2015**, *467*, 58–62.

[17] HP information of Takemoto oil & fat Co., Ltd.: http://www.gomaabura.jp/faq.html

[18] Richelle, M., Lambelet, P., Rytz, A., Tavazzi, I., Mermoud, A.-F., Juhel, C., Borel, P., Bortlik, K. The proportion of lycopene isomers in human plasma is modulated by lycopene isomer profile in the meal but not by lycopene preparation. *Br. J. Nutr.* **2012**, *107*, 1482–1488.

[19] Müller, L., Goupy, P., Fröhlich, K., Dangles, O., Caris-Veyrat, C., Böhm, V. Comparative study on antioxidant activity of lycopene (*Z*)-isomers in different assays. *J. Agric. Food Chem.* **2011**, *59*, 4504–4511.

[20] Kang, S. S., Kim, J. S., Jung, J. H., Kim, Y. H. NMR assignments of two furofuran lignans from sesame seeds. *Arch. Pharm. Res.* **1995**, *18*, 361–363.

Chapter 8

Overall conclusion

In this study, we demonstrated the fundamental data acquisition, and thermal-, photo- and catalystic isomerization of (all-*E*)-lycopene, and characterization of an unidentified *Z*-isomer of lycopene; (15*Z*)-lycopene.

In Chapter 2, the chemical and physical properties such as the melting point, UV−vis spectra, IR spectra and NMR spectra of (all-*E*)-lycopene were obtained using an extremely purified extract from tomato paste. These results provided a new insight into the spectroscopic and geometrical properties of lycopene.

In Chapter 3, (15*Z*)-lycopene was thermally generated and purified from a natural source, and mainly identified by an NMR technique for the first time as a natural origin. Moreover, the occurrence and availability of the 15*Z*-isomer were also discussed on the basis of the calculation method, which provided a rational explanation for the experimental results obtained.

In Chapter 4, the elaborate UV–vis and NMR investigation of lycopene isomers, by which the molar extinction coefficients of (9*Z*)- and (13*Z*)-lycopene were determined for the first time, facilitated an accurate quantification of the concentrations of *Z*-isomers formed during heat treatment. The isomerization rates of the purified (all-*E*)-lycopene were examined in seven different solvents (acetone, hexane, benzene, CH_2Cl_2, $CHCl_3$, CCl_4, and CH_2Br_2) at 4 °C and 50 °C. Promoted *Z*-isomerization of

(all-*E*)-lycopene has been first demonstrated in CH_2Br_2 as well as CH_2Cl_2 and $CHCl_3$ at both temperatures. In CH_2Cl_2 and CH_2Br_2, (5*Z*)-lycopene was generated as the predominant isomer within the processing time, independent of the heating temperature; on the other hand, the 13*Z*-isomer was preferentially formed in the other solvents.

In Chapter 5, the photoisomerization of (all-*E*)-lycopene to *Z*-isomers with sensitizer and filtered light has proven to be more effective than thermal isomerization. In particular, the reaction condition with erythrosine in hexane under 60 min of irradiation at wavelengths between 480 and 600 nm was the best method to enrich the content of *Z*-isomers and suppress the decomposition of lycopene. As for the individual *Z*-isomers generated, (5*Z*)-lycopene which has higher bioavailability, antioxidant capacity, and greater storage stability among the *Z*-isomers was increased significantly by the photosensitized *E*/*Z* isomerization.

In Chapter 6, (all-*E*)-lycopene was isomerized to *Z*-isomers efficiently and largely without decomposition by employing an appropriate solvent and concentration of iron(III) chloride as catalyst under optimized temperature: the isomerization ratio of (all-*E*)-lycopene (0.1 mg/mL) to *Z*-isomers and the total amounts of the remaining lycopene were attained at 79.9% and 96.5%, respectively, with 1.0×10^{-3} mg/mL iron(III) chloride in acetone for 3 h at 60 °C.

In Chapter 7, the thermal isomerization of (all-*E*)-lycopene in edible vegetable oils was investigated for individual *Z*-isomers of lycopene quantitatively, and has demonstrated to be highly effective to obtain the isomers with ease for food processing. Especially in sesame oil, highly functional (5*Z*)-lycopene was increased significantly.

These findings will contribute to the fundamental chemistry of lycopene, and the development of facile isomerization of (all-*E*)-lycopene to *Z*-isomers in the fields of food, drink, and dietary supplement manufacturing.

Acknowledgements

First of all, I wish to express my sincere gratitude to Professor Chitoshi Kitamura of The University of Shiga Prefecture for his cordial guidance, advice, discussion and encouragement. I sincerely thank his helpful support.

I am grateful to Emeritus Professor Tsutomu Kumagai and Associate Professor Yoshinori Inoue of The University of Shiga Prefecture for their suggestions, supports, discussions, and encouragement throughout this work.

I would like to express my gratitude to Assistant Professor Munenori Takehara of The University of Shiga Prefecture for his helpful guidance, suggestion, advice and encouragement. My research is deeply influenced by his insights into chemistry.

I also thank Mr. Takahiro Kuwa, Mr. Kento Hayashi, Mr. Tatsuya Kudo, Mr. Masatoshi Nishimura, Mr. Ikumi Horiuchi, Mr. Hayato Hiramatsu, Mr. Tomoya Nishikawa, and Miss. Tomoko Kawarasaki of The University of Shiga Prefecture for the support on the experiments, the high purity lycopene preparation, and helpful discussion.

I also wish to express my thanks to all staff of The University of Shiga Prefecture.

I am grateful to Dr. Tetsuya Fukaya, Mr. Naoto Takahashi, Mr. Hiroyuki Ueda, Mr.

Yasuhiro Takeuchi, Mr. Takuma Higashiura, Mr. Motoki Sugiura, and Mr. Hiroki Hayashi of Kagome Co., Ltd. for valuable discussions and having given the opportunity of this research. I also thank to my colleagues of Kagome Co., Ltd. for their supports and encouragement.

Finally, I really appreciate powerful supports of all my family members, especially my parents and my wife, for their endless support and encouragement. I could not have completed this thesis without them.

Publications

[1] Honda, M., Higashiura, T., Fukaya, T. Safety assessment of a natural tomato oleoresin containing high amounts of *Z*-isomers of lycopene prepared with supercritical carbon dioxide. *J. Sci. Food Agric*. **2016**, *In press*.

[2] Honda, M., Horiuchi, I., Hiramatsu, H., Inoue, Y., Kitamura, C., Fukaya, T., Takehara, M. Vegetable oil-mediated thermal isomerization of (all-*E*)-lycopene: Facile and efficient production of *Z*-isomers. *Eur. J. Lipid Sci. Technol*. **2016**, *In press*.

[3] Takehara, M., Kuwa, T., Inoue, Y., Kitamura, C., Honda, M. Isolation and characterization of (15*Z*)-lycopene thermally generated from a natural source. *Biochem. Biophys. Res. Commun.* **2015**, *467*, 58–62.

[4] Honda, M., Kawana, T., Takehara, M., Inoue, Y. Enhanced *E*/*Z* isomerization of (all-*E*)-lycopene by employing iron(III) chloride as a catalyst. *J. Food Sci.* **2015**, *80*, C1453–C1459.

[5] Honda, M., Takahashi, N., Kuwa, T., Takehara, M., Inoue, Y., Kumagai, T. Spectral characterization of *Z*-isomers of lycopene formed during heat treatment and solvent effects on the *E*/*Z* isomerization process. *Food Chem.* **2015**, *171*, 323–329.

[6] Honda, M., Igami, H., Kawana, T., Hayashi, K., Takehara, M., Inoue, Y., Kitamura,

C. Photosensitized *E*/*Z* isomerization of (*all-E*)-lycopene aiming at practical applications. *J. Agric. Food Chem.* **2014**, *62*, 11353–11356.

[7] Takehara, M., Nishimura, M., Kuwa, T., Inoue, Y., Kitamura, C., Kumagai, T., Honda, M. Characterization and thermal isomerization of (*all-E*)-lycopene. *J. Agric. Food Chem.* **2014**, *62*, 264–269.